RÉPUBLIQUE ALGÉRIENNE DÉMOCRATIQUE ET POPULAIRE
MINISTÈRE DE L'ENSEIGNEMENT SUPÉRIEUR ET DE LA RECHERCHE SCIENTIFIQUE
UNIVERSITÉ MOHAMED BOUDIAF - M'SILA
FACULTÉ DE MATHÉMATIQUES ET DE L'INFORMATIQUE
DÉPARTEMENT DE MATHÉMATIQUES

N° d'ordre : .....

T H È S E

Présentée pour l'obtention du diplôme
de Doctorat de Troisième Cycle (LMD)

Domaine

Mathématiques et Informatique

Spécialité

Analyse numérique, EDPs et applications

Par

May Manal Bounif

Thème

Etude analytique et numérique d'un problème d'écoulement bidimensionnel à surface libre

Soutenue le 20/02/2022 devant le jury composé de :

Benyattou BENABDERRAHMANE	**Prof.**	**Université de M'sila**	**Président**
Abdelkader GASMI	**Prof.**	**Université de M'sila**	**Directeur**
Bachir GAGUI	**MCA**	**Université de M'sila**	**Examinateur**
Brahim NOUIRI	**MCA**	**Université de M'sila**	**Examinateur**
Abdelkader AMARA	**MCA**	**Université de Ouargla**	**Examinateur**
Brahim TELLAB	**MCA**	**Université de Ouargla**	**Examinateur**

Année Universitaire : 2021/2022

Msila University
Faculty of Mathematics and Informatics

"Analytical and numerical study of two-dimensional free surface flow problem"

BOUNIF May Manal

Thesis submitted in fulfillment of the requirements
for the degree of
doctorate in mathematics

Academic year 2021-2022

Acknowledgements

I acknowledge the presence of God who created me and gave me this rare privilege to achieve my dream of attaining the highest qualification, all praises are due to Almighty God Allah, Who provided me with the strength and willingness to undertake this work and the opportunity to contribute a drop in the sea of knowledge.

Firstly, I would like to express my sincere gratitude to my advisor Prof.Gasmi Abdelkader for the continuous support of my Ph.D study and related research, for his patience, motivation, and immense knowledge. His guidance helped me in all the time of research and writing of this thesis. I could not have imagined having a better advisor and mentor for my Ph.D study, it has been a great pleasure working with him.

I sincerely thank the chairman of the jury committee, Prof.Benyattou Benabderrahmane, and the other jury members, Dr.Gagui Bachir, Dr.Nouiri Brahim, Dr.Abdelkader Amara and Dr.Tellab Brahim for agreeing to read the manuscript.

I extend my sincere thanks to all members of the Department of Mathematics.

I would like to express my appreciation and sincerest words of thanks to Prof.Elhadj Dahia for his encouragement, motivation, advice and guidance.

Last but not the least, I would like to thank my family: my parents and to my brothers and sister for supporting me spiritually throughout writing this thesis and my my life in general.

M.M.Bounif

Dedication

This thesis is dedicated to:
The sake of Allah, my Creator and my Master,
My great teacher and messenger, Mohammed (May Allah bless and grant him), who taught us the purpose of life.
My homeland Algeria, the warmest womb.
To my dear grandfather; Bouzidi, May God prolong his life, protect him.
To my dear grandmother, may God have mercy on her.
My great parents, who never stop giving of themselves in countless ways.
My dearest mather, who leads me through the valley of darkness with light of hope and support .
My sister and brothers; Djoumana, Aymen and Abd nour, particularly my dearest brother, Elmahdi Ibrahim, who stands by me when things look bleak.
To all my family, the symbol of love and giving.
My friends who encourage and support me.
I dedicate this research.

M.M.Bounif

Abstract

In this thesis, we are interested to finding the analytical and the approximate solution to a two dimensional problem of a fluid flow under a gate, as well as a fluid flow over any obstacle, we consider that the fluid is incompressible and inviscid, and the effects of gravity are neglected. This problem is characterized by the nonlinear condition given by Bernoulli's equation on the free surface as well as the unknown shape of this flow. When the surface tension effect is neglected, the exact solution can be obtained using the Hodograph method's. But if we introduce the effect of surface tension, it becomes difficult to find the exact solution to this problem, so we resort to using an approximate method to find the approximate solution, and both methods based on the conformal transformations theory, these two methods demonstrate that there are easily implemented give very important simplifications to this type of problem. In the two cases the problem difficulty is reduced, and transformed it from a two-dimensional problem to a one-dimensional problem.

Contents

List of Figures

List of Tables

List of Symbols

$\arg(z)$	Argument of complex coordinate z.
A_i	Constant, power series j cofficient.
g	Gravity.
h_1	Fluid depth at upstream infinity.
h_2	Fluid depth at downstream infinity.
$H(t)$	Solution of the homogenous Hilbert problem in the upper half-plan.
$Im(z)$	Imaginary part of complex coordinate z.
$Re(z)$	Real part of complex coordinate z.
L	Length of inclined plane.
We	Weber number.
p	Pressure.
q	Magnitude of velocity.
$\chi(t)$	Solution of Hilbert problem.
t	Auxiliary half-plane.
t_i	Real t-plane coordinate.
u	x-component of vector velocity.
v	y-component of vector velocity.
U_1	Fluid speed at upstream infity.
U_2	Fluid speed at downstream infity.
$U(t)$	Real part of $\chi(t)$.
$V(t)$	Imaginary part of $\chi(t)$.
f	Complex velocity potential.
z	Complex coordinate in the physical plane $= x + iy$.
α	Inclination angle.
η	Normalized conjugate complex velocity.
θ	Argument of complex velocity.
ρ	Constant density of fluid.
ϕ	Velocity potential.
ψ	Stream function.
ω	The logarithmic hodograph variable$= \ln \eta$.
div$V$	$\frac{\partial u_1}{\partial x_1} + \frac{\partial u_2}{\partial x_2} + \frac{\partial u_3}{\partial x_3}$.
curl$V$	$\text{rot}V = \bigtriangledown \wedge u \begin{bmatrix} \frac{\partial}{\partial x_1} \\ \frac{\partial}{\partial x_2} \\ \frac{\partial}{\partial x_3} \end{bmatrix} \wedge \begin{bmatrix} u_1 \\ u_2 \\ u_3 \end{bmatrix} = \begin{bmatrix} \frac{\partial u_3}{\partial x_2} - \frac{\partial u_2}{\partial x_3} \\ \frac{\partial u_1}{\partial x_3} - \frac{\partial u_3}{\partial x_1} \\ \frac{\partial u_2}{\partial x_1} - \frac{\partial u_1}{\partial x_2} \end{bmatrix}$.

***Note**:Variables with stars (*) are variable physical dimensions and variables without stars(*) are non-dimensional variables.*

List of papers

chapter 2

- M.M, Bounif and A, Gasmi. *The Application of the Hodograph method to free surface flow problem.* Article submitted for publication in the journal of theoretical and applied mechanics (JTAM).

chapter 3

- M.M, Bounif and A, Gasmi. *First order perturbation approach for the free surface flow over a step with large Weber number*, INCAS Bulletin, 13(2), 11–19, 2021.

chapter 4

- M.M, Bounif and A, Gasmi. *An approximate solution technique for the flow past an obstacle with a large Weber number*. International journal of applied and computational mathematics, 8(1), 1–12, 2022.

chapter 5

- M.M, Bounif and A, Gasmi. *Perturbation approach for a flow over a trapezoidal obstacle*. Article accepted for publication.

chapter 6

- M.M, Bounif and A, Gasmi. *Two dimensional free surface flow over a round obstacle with surface tension effect*. Article submitted for publication.
- A, Gasmi and M.M, Bounif . *An approximate solution for the flow over a sinusoidal bottom with large Weber number effect*. Article submitted for publication.

General introduction

Two-dimensional flows of fluid with free surface intersecting straight wall or fluid over an obstacle placed in bottom can be and often observed in many natural or physical phenomena that occur in the industrial field. Thus of its major importance, this type of flow is the subject of several scientific research works, for example that of aerodynamics, river flow and jet or hydraulic engineering etc...

It is well known that his interest in the field of continuum media is very essential. These flows are based on the main aspects of fluid mechanics such as the law of momentum of continuous media and surface tensions which are capillarity forces acting on any interface between two different media (fluid and air), these forces come from the pressure variation between the two media and they are governed by Laplace's law, this law linking the local curvature of the interface separating these two media to the pressure difference (also called Laplace pressure) between these two environments.

Our research work falls within the general framework of an analytical and numerical study of a two-dimensional flow in intersecting straight wall and flow over obstacle of any shape. It continues previous studies already carried out within our MANUCAF research team of the LMPA laboratory laboratory, by Gasmi (2003) [22] on a jet coming from an opening, by Gasmi & mekias (2007) [23] on the flow past of a vertical plate placed in channel and by Gasmi & Amara (2018) [24] on the jet flow in U-shaped channel. In this study the fluid is considered to be incompressible, non-viscous and the effects of gravity are neglected. With these assumptions, we obtain simplifications on the Bernoulli's equation, which govern this problem. Thus we can apply the theory of functions of the complex variable such as the properties of analytical functions and conformal transformations.

This problems belongs to the class of flows for which there are intersections between the free surface and a solid, for more details related on this subject see for example Birkhoff & Zarantonello [9], Batchelor [8] Bhimsen & Shivamoggi [40], Milne-Thomson [34], Vander-Broeck et al [7,47–50] and Rutherford [36].
Several previous research have been published by several authors for this kind of problem, in particular Forbes and Schwartz [21], determine the nonlinear solutions of subcritical and supercritical flows over a semi-circular obstacle Gasmi and Mekias [22], Gasmi and Amara [24] and Vanden-Broeck [46], studied the problems of flow over an obstruction in a channel, whilst Dias, Killer and Vanden-Broeck [19], obtained solutions to both subcritical and supercritical free-surface flows past a triangular obstacle, Wiryanto [51] take the problem of the flow under a sluice gate, all these authors formulated the problem as an integrodifferential equation which they solved numerically. M.B. Abd-el-Malek and S.Z. Masoud [1] obtains the linear solution of the flow over a ramp, by representing the bottom in integral form using Fourier's double-integral theorem. M.B. Abd-el-Malek and S.N. Hanna [2] solved numerically the problem of the flow

over a ramp with gravity effect by the Hilbert Method and the perturbation technique. M. B. Abd-el-Malek, S. N. Hanna and M.T. Kamel [3] investigated the flow over triangular bottom. Other authors who studied similar problems include Cooker [17] Hureau & Weber [28], Klokov & Sergeev [29], Pengp & Parker [35], Semenov & Wu [37], Semenov et al [38, 39], Gasmi et al [6, 25, 26] and Bouderah et al [10, 11].

The problem considered in this work is characterized by the nonlinear condition given by the Bernoulli equation on the free surface on the one hand and on the other hand by the unknown form of this surface. In the case where the effect of surface tension is neglected, we apply the hodograph method to solve this problem analytically. But if we consider the surface tension effects this condition make the problem very difficult to solve it analytically, so it is necessary to look for an approximate solution to it.

The method that we employ in this thesis to approximate a solution of the considered problem follows three steps. Initially, we map the flow field of the physical plane onto the upper half plane using the Schwartz-Christoffel transformation. Accordingly, the Hilbert method helps us identify a system of nonlinear equation when applied to the new upper half plane's mixed-boundary value problem. Finally, the perturbation technique is utilized to provide a solution to the system for some large values of the Weber number and varied obstacle configurations. The employability of our method will then be clear given the acquired results, as it provides approximate solutions to the selected kind of problems.

This document is organized into six chapters:

- We started in the first chapter with a bibliographical analysis in which we exposed the preliminary notions which relate to the study of a potential and two-dimensional free surface flow, the second section of the chapter is devoted to the the theory of functions of a complex variable and precisely conformal transformations.
- The second chapter begins with the presentation of the jet flow issued from an opening, after that we present its mathematical modeling. The second section of this chapter is devoted to the analytical solution of the problem considered in the case where the effects of gravity and tension of surface are neglected, using the the hodograph method, which bases on the conformal transformations to determine the shape of the jet. The results found are submitted for publication in the journal of theoretical and applied mechanics (JTAM) Bounif and Gasmi Bounif and Gasmi [12].
- In the third chapter we present the problem of two-dimensional free surface flow of inviscid and incompressible fluid over a step in the case where the surface tension effect is taken into consideration, as well as the mathematical formulation of the problem using the Hilbert method and the perturbation technique; the results are calculated for a large values of the Weber number and small inclination angle of the step values. These results demonstrate that the used method is easily implemented. As well as the results obtained is the subject of an article in an internationally renowned journal Bounif and Gasmi [13].

- ☞ Chapter four models the nonlinear problem of a fluid's two dimensional free surface flow over a triangular obstacle . We assume the incompressible and inviscid nature of the fluid, and consider the flow to be stationary and irrotational. Supplementarily, while the superficial tension's effects are taken into account, the effects of gravity are disregarded. A characteristic of the given problem is its nonlinear condition on an undefined shape's free surface which we essentially define using the Bernoulli equation. The difficulty in solving this problem analytically necessitates the identification of an approximate solution. The obtained results are also a subject of an article in an internationally renowned journal Bounif and Gasmi [14].

- ☞ Chapter five deals with the steady two-dimensional and irrotational fluid flow over a trapezoidal obstacle. On the one hand, we assume the fluid is incompressible and inviscid. On the other hand, we consider the surface tension effect but neglect the effect of gravity. A major characteristic of the present problem is the nonlinear condition given through the Bernoulli equation on the free surface of an unknown shape. The latter can be identified aspart of the solution to the problem. The obtained results are also a subject of an article in an internationally renowned journal Bounif and Gasmi [15]

- ☞ In chapter six, we proposed two examples of the flow over a curved obstacle, the flow is assumed to be as steady and irrotational. The effect of the surface tension with smaller values is considered, but the gravity force is neglected. We apply the same steps as in the previous chapter for obtaining the free surface profiles for different Weber number. As well as the results obtained is the subject of two article in an internationally renowned journal [16], [27].

We end this thesis with a general conclusion in which we discuss the results of our contribution, and we open perspectives on our future works.

1

Two dimensional free surface flow: Some Preliminary Notions and equations

In this chapter we exposed the preliminary notions which relate to the study of a potential and two-dimensional free surface flow, the second section of the chapter is devoted to the theory of functions of a complex variable and precisely conformal transformations.

Contents in Brief

1.1 Equations of fluid mechanics and basic concepts

The mathematical equations that model fluid flow are governed by using the principles of fluid physics and in this thesis we will concentrate in our study on two-dimensional problems. Some of these fundamental principles of physics that are considered to study fluid flow are:

1.1.1 Conservation of mass (continuity equation)

The principle of conservation of mass states that the mass of a region occupied by fluid is constant during its motion(See [31]). The mass of fluid flowing in unit time through an element dF of the surface bounding this volume is $\rho V \cdot dF$. The total mass of fluid flowing out of the volume V_0 in unit time is therefore

$$\oint \rho V.dF, \tag{1.1}$$

where the integration is taken over the whole of the closed surface surrounding the volume in question, ρ is the fluid density and V is the fluid velocity.

Next, the decrease per unit time in the mass of fluid in the volume V_0 can be written

$$-\frac{\partial}{\partial t}\int \rho dV. \tag{1.2}$$

Equating the two expressions, we have

$$\frac{\partial}{\partial t}\int \rho dV = -\oint \rho V \cdot dF. \tag{1.3}$$

The surface integral can be transformed by **Green's formula** to a volume integral:

$$\oint \rho V.dF = \int \operatorname{div}(\rho V)\, dV. \tag{1.4}$$

Thus

$$\int \left[\frac{\partial \rho}{\partial t} + \operatorname{div}(\rho V)\right] dV = 0. \tag{1.5}$$

Since this equation must hold for any volume, the integrand must vanish, i.e.

$$\frac{\partial \rho}{\partial t} + \operatorname{div}(\rho V) = 0, \tag{1.6}$$

this is the equation of continuity. Expanding the expression $\operatorname{div}(\rho V)$, we can also write (1.6) as

$$\frac{\partial \rho}{\partial t} + \rho \operatorname{div}(V) + V \cdot \operatorname{grad} \rho = 0. \tag{1.7}$$

1.1.2 Conservation of Momentum (Euler equation)

Euler equation is given in [31] by:

$$\frac{\partial V}{\partial t} + (V.\operatorname{grad}) V = -\frac{1}{\rho} \operatorname{grad} p + F, \tag{1.8}$$

where p is the fluid pressure and F is the force per volume unit. This is the required equation of motion of the fluid; it was first obtained by L. EULER in 1755. It is one of the fundamental equations of fluid physics.

1.1.3 Bernoulli equation

Firstly we define the streamline as a line which is tangential at each of these points to the velocity vector along its path in the flow.

Bernoulli equation is derived from the Euler's equations, considering the flow along a streamline, and for an incompressible and steady flow ($\frac{\partial \rho}{\partial t} = 0$) where $V = (u, v)$ is the velocity along a streamline and $|V| = \sqrt{u^2 + v^2}$, the Euler's equations become:

$$\frac{1}{2} |V|^2 + gy + \frac{p}{\rho} = \text{Constant}, \tag{1.9}$$

which is the Bernoulli equation and is stated in [31].

1.1.4 Surface tension

In the chapter 3 at chapter 6, the effects of surface tension are included. The effects of gravity are neglected, and will be from this point. In this section, Laplace's capillarity equation is derived and such a derivation can be seen in many fluid mechanics texts, an example of which is Crapper [18]. For an element of free surface ds,

if $ds \to 0$ then the said element can be considered as an arc of a circle with a centre O and radius R. See Figure 1.1. The surface element is bisected by BO such that $\widehat{AOB} = \widehat{BOC} = d\theta'$.

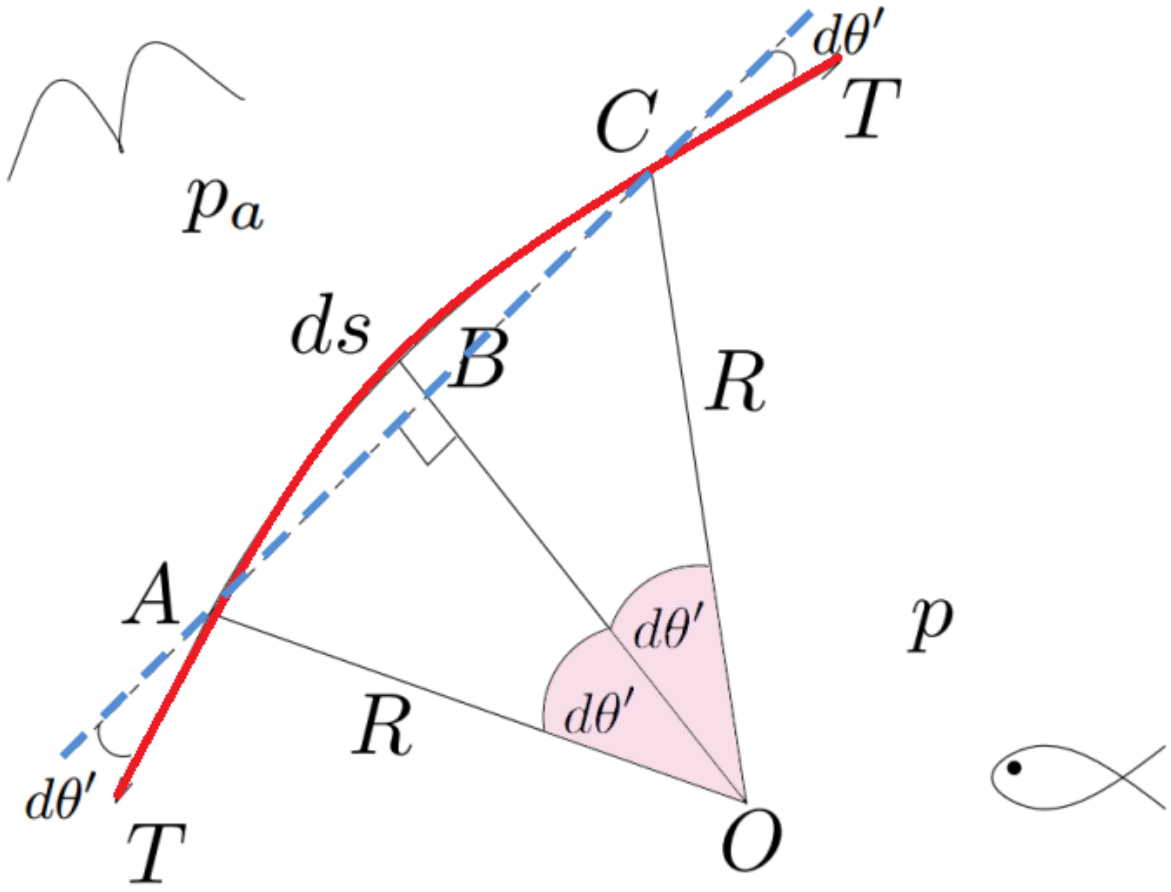

Figure 1.1: A section of a free surface.

The resultant force due to surface tension acting on this element ds, in the normal direction, is simply the sum of the forces at the two end points,

$$\text{Net force} = 2T \sin\left(d\theta'\right). \tag{1.10}$$

As $ds \to 0$, $d\theta^{'} \to 0$ and so there is a force

$$2T \sin\left(d\theta^{'}\right) \sim 2T d\theta^{'}. \tag{1.11}$$

directed along BO. This force must be balanced by a force due to the pressure difference across the free surface. This is because the forces are acting on an element of zero mass. Letting p be the fluid pressure, p_a be the atmospheric pressure, and equating force components along the normal OB gives

$$2T \sin\left(d\theta^{'}\right) = (p - p_a)\, ds. \tag{1.12}$$

Another consequence of considering $ds \to 0$ is that the surface element length can be expressed in terms of the radius R and the angle $d\theta^{'}$ by

$$ds = 2R d\theta^{'}. \tag{1.13}$$

Substituting (1.13) into (1.12) gives

$$(p - p_a)\, ds = \frac{T}{R} ds \Rightarrow (p - p_a) = \frac{T}{R}, \tag{1.14}$$

where $K^* = 1/R$ is the curvature, which is considered positive, if when viewed from the air side of B, the free surface is convex at B, as drawn in Figure 1.1. $K^* = 1/R$ is negative if B is concave.

1.1.5 Two-dimensional flow

It has been found experimentally that a large class of problems exists in which one of the velocity components, say w, is small when compared with the components u and v. Modelling such flows with the simplification obtained by setting $w = 0$ and allowing u and v to be functions of x and y, but not of z, leads to excellent agreement between theory and observation (see [8, 9, 32]). The flow is defined as being two dimensional.

For incompressible flow, i.e, the density of a parcel of fluid moving with the flow does not change, and for steady state flow $\frac{\partial \rho}{\partial t} = 0$, **the continuity equation** (1.6) take the form,

$$\operatorname{div} V = 0, \tag{1.15}$$

where $V = (u, v, 0)$, becomes

$$\frac{\partial u}{\partial x} + \frac{\partial v}{\partial y} = 0, \tag{1.16}$$

Consider the following first-order ordinary differential equation:

$$udy - vdx = 0. \tag{1.17}$$

From the theory of first order ordinary differential equations we know that eq (1.17) will be exact if the following condition is satisfied: $\frac{\partial u}{\partial x} + \frac{\partial v}{\partial y} = 0$, which is precisely the equation of continuity (1.16). Thus there exists a scalar function $\psi(x, y)$ such that

$$d\psi = udy - vdx = 0. \tag{1.18}$$

Integrating eq (1.18) gives

$$\psi(x, y) = constant. \tag{1.19}$$

Here $\psi(x, y)$ is a stream function, since by definition, the velocity is tangential to a streamline; therefore the differential equation of streamlines can be written as

$$\frac{dx}{u} = \frac{dy}{v}. \tag{1.20}$$

This equation can be derived from eq (1.18).

From eq (1.18) we have

$$\frac{\partial \psi}{\partial x}dx + \frac{\partial \psi}{\partial y}dy = udy - vdx. \tag{1.21}$$

Hence

$$u = \frac{\partial \psi}{\partial y}, \quad v = -\frac{\partial \psi}{\partial x}. \tag{1.22}$$

It is noted that $\psi(x, y)$ is related to u and v; and also that this stream function exists only in two dimensional flow. A good account of a velocity field and its streamlines can be found in Lighthill [30].

For the case where the motion is **irrotational** then we must have

$$\text{curl}V = 0, \tag{1.23}$$

that is

$$\frac{\partial v}{\partial x} - \frac{\partial u}{\partial y} = 0. \tag{1.24}$$

Equation (1.24) can be recognized as the condition for the differential equation:

$$udx + vdy = 0. \tag{1.25}$$

to be exact. Thus there exists a scalar function $\phi(x, y)$ such that

$$d\phi = udx + vdy. \tag{1.26}$$

such that

$$d\phi = 0, \tag{1.27}$$

and upon integration yields

$$\phi(x, y) = constant. \tag{1.28}$$

From eq (1.24), we have

$$\frac{\partial \phi}{\partial x}dx + \frac{\partial \phi}{\partial y}dy = udx + vdy. \tag{1.29}$$

Therefore by comparison it can be seen that

$$u = \frac{\partial \phi}{\partial x}, \quad v = \frac{\partial \phi}{\partial y}, \tag{1.30}$$

and the velocity vector V can be written as

$$V = \text{grad}\, \phi. \tag{1.31}$$

Here $\phi(x, y)$ is called the velocity potential. It is easily shown that both the stream function $\psi(x, y)$ and the velocity potential $\phi(x, y)$ satisfy Laplace's equation. Using eq (1.24) together with the irrotational flow condition (1.24) yields

$$\frac{\partial^2 \psi}{\partial x^2} + \frac{\partial^2 \psi}{\partial y^2} = 0. \tag{1.32}$$

Similarly, using eq (1.30) together with the continuity condition (1.16) yields

$$\frac{\partial^2 \phi}{\partial x^2} + \frac{\partial^2 \phi}{\partial y^2} = 0. \tag{1.33}$$

1.1.6 The velocity potential

In practice the velocity potential ϕ is defined as the value of the line integral of the velocity vector $v = (u, v, w)$ as

$$\phi = \int_C V \cdot dr = \int_C (udx + vdy + wdz). \tag{1.34}$$

where C is the contour of integration. The quantity $V \cdot dr$ is a measure of the fluid velocity in the direction of the contour at each point. Therefore ϕ is related to the product of the velocity and length along the path between two distinct points on C. For the value of ϕ to be independent of the path, i.e., for the flow rate between these two points to be the same no matter how the integration is carried out, the term in the integrand must be an exact differential $d\phi$, so that

$$d\phi = udx + vdy + wdz, \tag{1.35}$$

and therefore,

$$V = \text{grad}\, \phi. \tag{1.36}$$

To ensure that this scalar function ϕ exists, it is confirmed that curl of the velocity vector V must be zero, which indeed is so. Because the vector calculus identity confirms that

$$\text{curl} V = \text{curl grad} \phi = 0, \quad \text{always}. \tag{1.37}$$

1.1.7 The stream function

For the velocity potential, we defined ϕ in three-dimensions as the line integral of the velocity vector projected on the line element. Let us define in a similar manner the line integral composed of the velocity components perpendicular to the line element in two-dimensions as

$$\phi = \int_C V \cdot ndl, \tag{1.38}$$

where $dl = |dr|$.
The integrand here will physically imply that ψ represents the amount of fluid crossing the line C between two distinct points of C. The unit normal vector n is perpendicular to the path of integration C. This vector can be obtained from the relation that

$$n \cdot dr = 0, \tag{1.39}$$

such that the normal unit vector components can be obtained as

$$n_x = \frac{dy}{dl} \quad \text{and} \quad n_y = -\frac{dx}{dl}. \tag{1.40}$$

The integral then can be written as

$$\psi = \int_C (udy - vdx). \tag{1.41}$$

The value of this integral, i.e., the flow between these two distinct points will be independent of the path of integration provided the integrand becomes an exact differential, $d\psi$.

This requires that

$$u = \psi_y \quad \text{and} \quad v = -\psi_x, \tag{1.42}$$

from which we deduce that

$$u_x + v_y = 0, \tag{1.43}$$

which is precisely the continuity equation in two-dimensions.

The ψ is defined as the stream function. It is to be noted from this mathematical analysis that there exists a stream function for two-dimensional incompressible flow

1.2 Complex analysis

1.2.1 Complex potential

We have seen that the velocity components in two-dimensional flow can be related to $\psi(x, y)$ and $\phi(x, y)$ by the following equations:

$$u = \frac{\partial \psi}{\partial y} = \frac{\partial \phi}{\partial x}, \quad v = \frac{\partial \phi}{\partial y} = -\frac{\partial \psi}{\partial x}. \tag{1.44}$$

The above equations are usually defined as **the Cauchy-Riemann** equations (which is stated in [8,9,30,31]).

Using the Cauchy-Riemann conditions it can be easily verified that the lines of constant stream function (ψ = const.) and the lines of constant velocity potential (ϕ = const.) are perpendicular.

Also these conditions provide the necessary condition for the function

$$f = \phi + i\psi, \tag{1.45}$$

to be an analytic function of z, where $z = x + iy$.

The complex function f , whose real and imaginary parts are **the velocity potential** and **stream function**, respectively, is called **the complex potential** of the flow.

f is an analytic function of z and, hence

$$\frac{df}{dz} = \frac{\partial \phi}{\partial x} + i\frac{\partial \psi}{\partial x} = u - iv = qe^{-i\theta}, \tag{1.46}$$

where q is the speed of the fluid, and is given by:

$$q = \left|\frac{df}{dz}\right| = \sqrt{u^2 + v^2}, \tag{1.47}$$

and θ is the velocity direction relative to the real axis:

$$\theta = tan^{-1}\frac{v}{u}, \tag{1.48}$$

1.2.2 Conformal Mapping

1.2.2.1 Hodograph Method

The Hodograph Method is used to solve the nonlinear free surface problems in this thesis, The principle idea of this method is based on the transformation of the domain occupied by the fluid in the physical plane on to a part of unit disk. This simplifies the problem such that it becomes one-dimensional instead of two-dimensional. (Used in chapter 2: When the effects of the superficial tension and gravity are neglected)(see [40]).

This affords an alternate approach to solution of problems of free streamline flows.

First, from the hodograph variable (1.46) and (1.45), we obtain:

$$dz = \frac{e^{i\theta}}{q}df. \tag{1.49}$$

Next, the stream function ψ satisfied the Laplace's equation (1.32) in polar Coordinates:

$$\frac{\partial^2\psi}{\partial q^2}+\frac{1}{q}\frac{\partial\psi}{\partial q}+\frac{1}{q^2}\frac{\partial^2\psi}{\partial\theta^2}=0. \tag{1.50}$$

Then, if it is possible to specify the boundary conditions in terms of q and θ, equation (1.50), enables one to solve for $\psi(q,\theta)$.

After then, using the Cauchy-Riemann conditions (1.44) in new plane (Hodograph)

$$\frac{\partial\phi}{\partial q}=-\frac{1}{q}\frac{\partial\psi}{\partial\theta},\qquad \frac{\partial\psi}{\partial q}=\frac{1}{q}\frac{\partial\phi}{\partial\theta}, \tag{1.51}$$

we can determine the potential velocity ϕ as a function of the two variable q and θ.
(The Laplace's equation and the Cauchy-Riemann conditions in polar Coordinates are stated in [40]).

Finally, using (1.45) and (1.49) one then determines $z=z(q,\theta)$, and next $x=x(q,\theta)$ and $y=y(q,\theta)$.

1.2.2.2 The Schwartz–Christoffel Transformation

Consider a polygon Fig. 1.2 in the w plane having vertices at $w_1,w_2,\ldots,w_n$ with corresponding interior angles $\alpha_1,\alpha_1,\ldots,\alpha_n$ respectively. Let the points $w_1,w_2,\ldots,w_n$ be the images, respectively, of the points $x_1,x_2,\ldots,x_n$ on the real axis of the z plane Fig 1.3 (see [45]).

A transformation that maps the upper half $\mathcal{R}$ of the z plane onto the interior $\mathcal{R}'$ of the polygon of the w plane and the real axis onto the boundary of the polygon is given by

$$\frac{dw}{dz}=A\left(z-x_1\right)^{\frac{\alpha_1}{\pi}-1}\left(z-x_2\right)^{\frac{\alpha_2}{\pi}-1}\ldots\left(z-x_n\right)^{\frac{\alpha_n}{\pi}-1}, \tag{1.52}$$

or

$$w=A\int\left(z-x_1\right)^{\frac{\alpha_1}{\pi}-1}\left(z-x_2\right)^{\frac{\alpha_2}{\pi}-1}\ldots\left(z-x_n\right)^{\frac{\alpha_n}{\pi}-1}dz+B, \tag{1.53}$$

where A and B are complex constants.

The following facts should be noted:

- Any three of the points $x_1,x_2,\ldots,x_n$ can be chosen at will.
- The constants A and B determine the size, orientation, and position of the polygon.

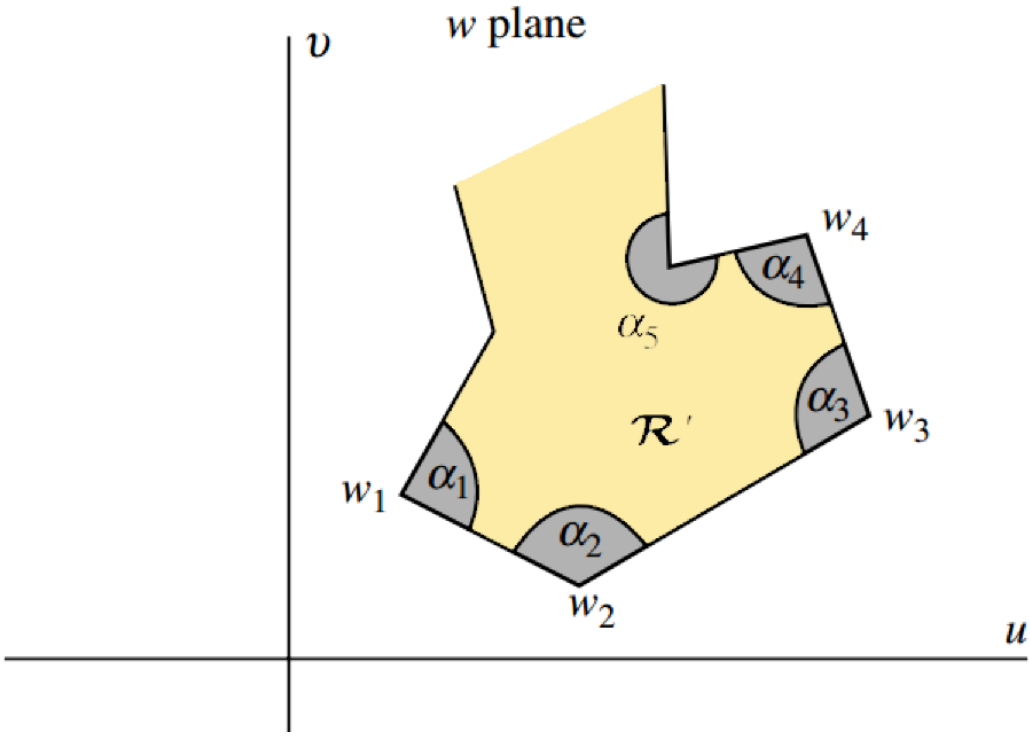

Figure 1.2: w-plane.

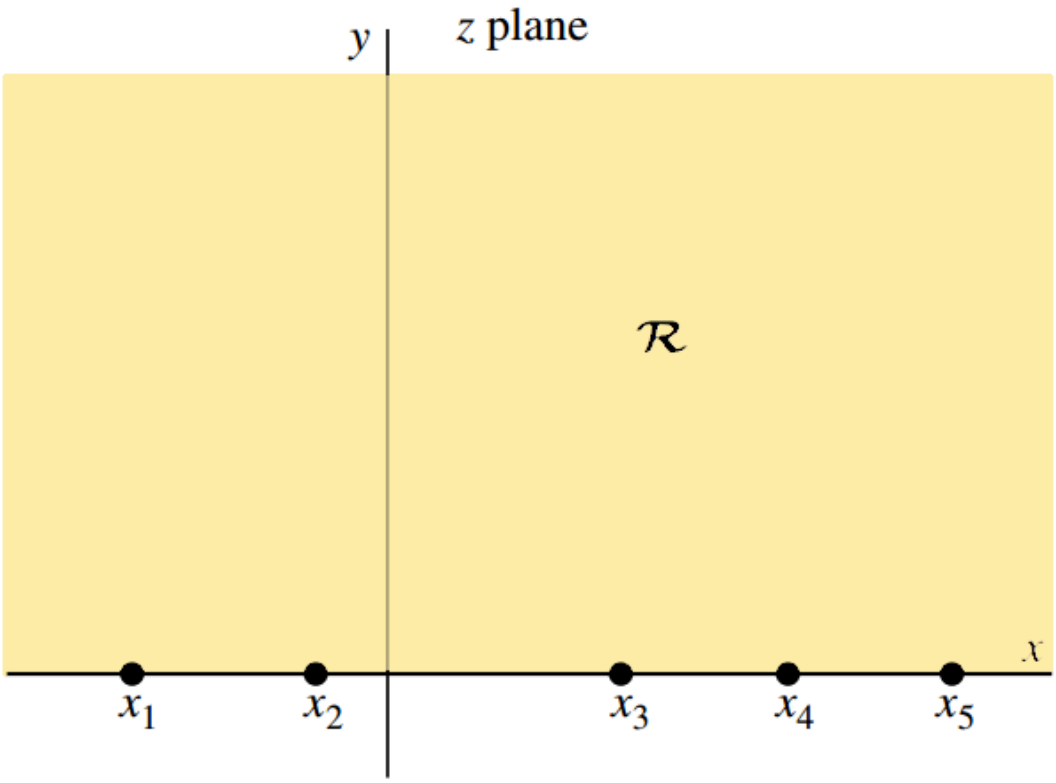

Figure 1.3: z-plane.

- It is convenient to choose one point, say x_n, at infinity in which case the last factor of (1.52)

and (1.53) involving x_n is not present.

- Infinite open polygons can be considered as limiting cases of closed polygons.

1.2.3 Hilbert Method

The general solution of the Hilbert method for a mixed boundary-value problen in the upper half plane is well known, for example, see Lim [41]. If the imaginary part of an analytic function $\chi(t)$ is known along $\mathrm{Im}(t) = 0$, the reat axis of the t-plane, then the value of $\chi(t)$ in the upper half-plane is given by

$$\chi(t) = \frac{1}{\pi} p.v. \int_{-\infty}^{+\infty} \frac{Im\left[\chi(s)\right]}{s-t} ds + \sum_{j=0}^{\infty} B_j t^j, \tag{1.54}$$

where B_j are real constants.

Note that we know either the imaginary or real part of the logarithmic hodograph variable $\omega(t)$ defined by (3.9), along the real-axis of the t-plane.

This boundary informtation can be converted into information about a related function $\chi(t)$ so that $\mathrm{Im}[\chi(t)]$ is known on the entire reat axis.

In the conversion process from $\omega(t)$ to $\chi(t)$ we need an auxiliary function $H(t)$, anatytic for $\mathrm{Im}(t) > 0$, which, on $\mathrm{Im}(t) = 0$, is purely real where the imaginary part of $\omega(t)$ is known and purely imaginary where the real part of $\omega(t)$ is known. Then the imaginary part of the quotient $\chi(t) = \frac{\omega(t)}{H(t)}$ known on the entire real axis.

The general solution for $\mathrm{H}(t)$ is

$$H(t) = a_i \left(t - b_i\right)^{\pm\frac{1}{2}}. \tag{1.55}$$

Where b_i are real constants, $a = \pm\sqrt{\pm 1}$.

Song [43] has shown that the final solution is independent of a particular choice for $H(t)$. A branch cut is selected on the real axis to ensure that $\mathrm{H}(t)$ is a single-valued functton. Hence $\omega(t)$ can be constructed explicitly by means of Hilbert's solution, where $\omega(t) = H(t)\chi(t)$.

In our problem, (the flow over a step Fig. 3.1, the flow over a trapezoidal obstacle Fig. 5.1); we choose $b_1 = 1, a = -i$ in (1.55) The coeffictents $A_j, j = 0, 1, 2, \ldots, n$ in (1.54) are al1 zero when the upstream boundary condition is applied. Hence in this case we find

$$H(t) = -i\sqrt{t-1}, \tag{1.56}$$

and

$$\chi(t) = \frac{1}{\pi} p.v. \int_{-\infty}^{+\infty} \frac{Im\left[\chi(s)\right]}{s-t} ds. \tag{1.57}$$

Therefore

$$\frac{\omega(t)}{H(t)} = \frac{1}{\pi} p.v. \int_{-\infty}^{+\infty} \frac{Im\left[\frac{\omega(s)}{H(s)}\right]}{s-t} ds = U(t) + iV(t). \tag{1.58}$$

Smith and Lim [41] used an equivalent form for (1.58),

$$U(t) = \frac{1}{\pi} p.v. \int_{-\infty}^{+\infty} \frac{V(s)}{s-t} ds. \tag{1.59}$$

$$V(t) = -\frac{1}{\pi} p.v. \int_{-\infty}^{+\infty} \frac{U(s)}{s-t} ds. \tag{1.60}$$

1.2.4 The Buckingham Pi Theorem in Dimensional Analysis

Theorem 1.1. *Let $q_1, q_2, q_3 ... q_n$ be n dimensional variables that are physically relevant in a given problem and that are inter-related by an (unknown) dimensionally homogeneous set of equations. These can be expressed via a functional relationship of the form:*

$$F(q_1, q_2, q_3 ... q_n) = 0 \quad \textit{or equivalently} \quad q_1 = f(q_2, q_3 ... q_n). \tag{1.61}$$

If k is the number of fundamental dimensions required to describe the n variables, then there will be k primary variables and the remaining $j = (n-k)$ variables can be expressed as $(n-k)$ dimensionless and independent quantities or 'Pi groups', $\Pi_1, \Pi_2, \Pi_3 ... \Pi_{n-k}$. The functional relationship can thus be reduced to the much more compact form:

$$F(\Pi_1, \Pi_2, \Pi_3 ... \Pi_{n-k}) = 0, \tag{1.62}$$

or equivalently

$$\Pi_1 = f(\Pi_2, \Pi_3 ... \Pi_{n-k}). \tag{1.63}$$

$\Rightarrow$ Note that this set of non-dimensional parameters is not unique. They are however independent and form a complete set.

1.2.5 Cauchy's Integral Formula

Theorem 1.2. *[44] Let $f(z)$ be analytic inside and on a simple closed curve C and let a be any point inside C Fig. 1.4. Then*

$$f(a) = \frac{1}{2\pi i}\int_C \frac{f(z)}{z-a}dz. \tag{1.64}$$

where C is traversed in the positive (counterclockwise) sense.

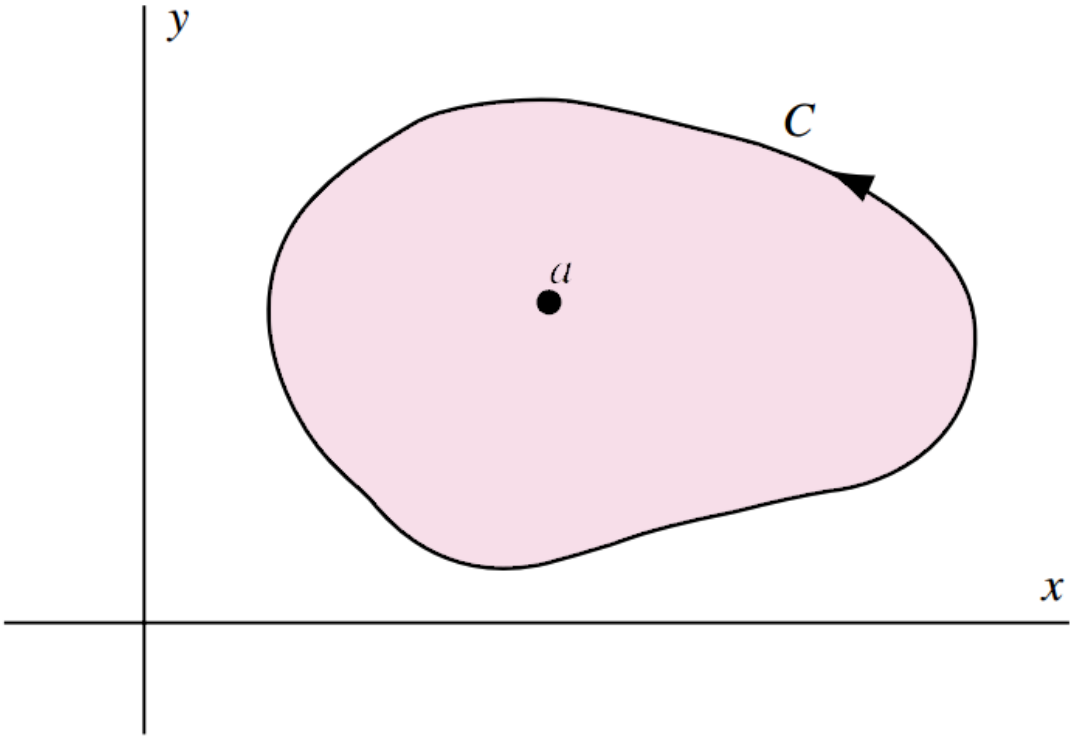

Figure 1.4: A simple closed curve C.

2

Analytical solution of flow under gate

An analytical method is considered to solve the problem of steady two-dimensional free-surface flow of a fluid issued under a gate. Hodograph transformation is used to map the domain occupied by the flow in the physical plane onto a part of unit disk, the hodograph method is used to solve this problem for various inclination angle of the gate wall, all the obtained results are agree with the experimental and numerical results given respectively by Birkhoff & Zarantonello and Gasmi & Mekias, some free streamline shapes are illustrated for several values of the inclination angle.

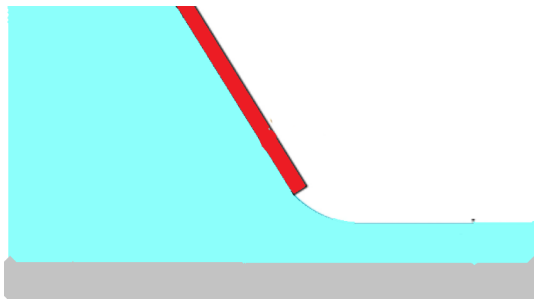

Contents in Brief

2.1 Formulation of Problem

Let us consider the motion of a two-dimensional flow of a fluid under a gate with inclined edge, we denote the inclination angle between the edge of the gate and the horizontal by α, the opening of the gate is of width d see Fig 2.1. The flow is considered to be incompressible, inviscid and steady. The effects of gravity and the surface tension are neglected.

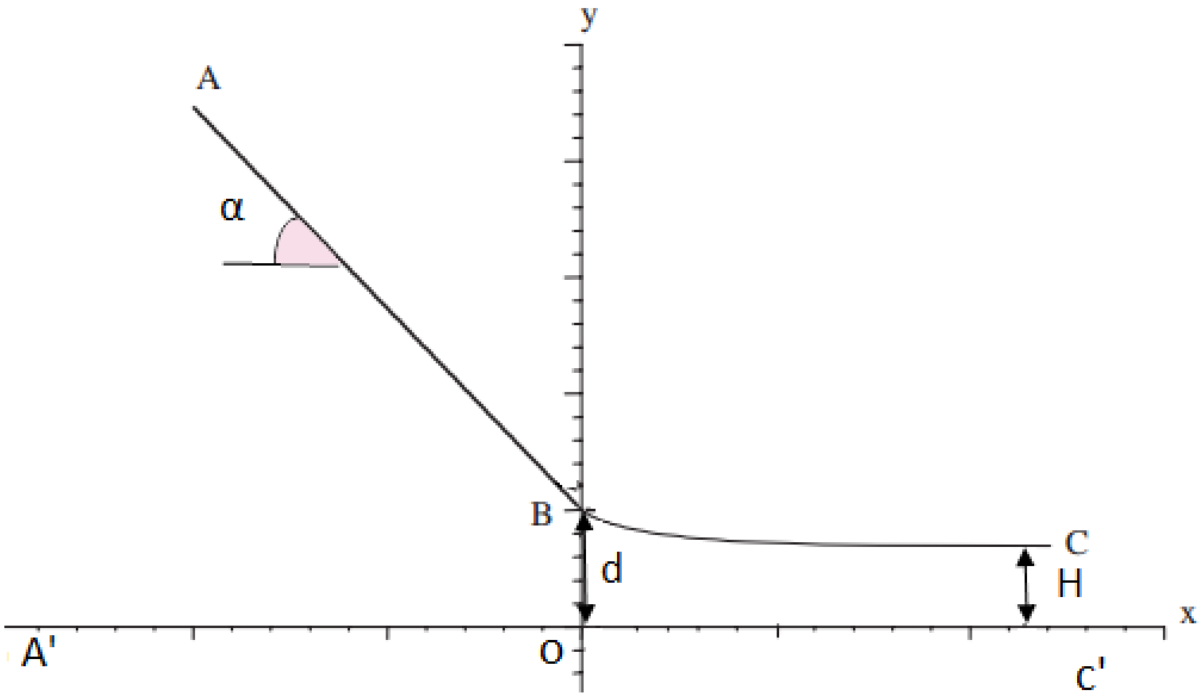

Figure 2.1: Sketch of the flow and of the coordinates. The width of the opening is d, the depth of the flow at ininity is H and the inclination angle of the gate is α.

Under the assumption of irrotationnality, the flow of incompressible fluids governed by Laplace's equation for the velocity potential ϕ^*

$$\Delta\phi^* = 0, \tag{2.1}$$

We introduce the cartesian coordinates with the Bottom $A'OC'$ on the x axis and the y axis is vertically through the point B. Far upstream the fluid in rest, and far downstream, we assume that the velocity approaches a constant U and the depth of the fluid tends to a constant H.

Due to the inviscid nature of the fluid, and since it has been assumed that the fluid is incompressible and the flow is steady and irrotational, the conditions on the free-surface BC take the

form:

$$\frac{1}{2}q^{*2} + \frac{p^*}{\rho} + gy^* = \text{constant}, \tag{2.2}$$

everywhere in the fluid. This result is known as Bernoulli's equation.

Here,

- $q^* = \sqrt{u^{*2} + v^{*2}}$ is the flow speed and u^*, v^* are the velocity components, the velocity components are given by:

$$\begin{cases} u^* = \dfrac{\partial \phi^*}{\partial x^*} = \dfrac{\partial \psi^*}{\partial y^*}, \\ v^* = \dfrac{\partial \phi^*}{\partial y^*} = -\dfrac{\partial \psi^*}{\partial x^*}. \end{cases} \tag{2.3}$$

- p^* is the fluid pressure,
- ρ is the constant fluid density,
- g is the constant acceleration due to gravity.

2.1.1 Dimensionless variables

Before the problem can be solved, it is necessary to non-dimensionalise the variables so as to reduce the number of free parameters. The dimensionless variables are defined by choosing U as the unit velocity and d as the unit length. The new dimensionless variables are:

$$x = \frac{x^*}{d}, \quad y = \frac{y^*}{d}, \quad u = \frac{u^*}{U}, \quad v = \frac{v^*}{U}, \phi = \frac{\phi^*}{CUd} = \frac{\phi^*}{UH} \text{ and } \psi = \frac{\psi^*}{CUd} = \frac{\psi^*}{UH}. \tag{2.4}$$

Here $C = \frac{H}{d}$ is the contraction coefficient.

We introduce the potential function ϕ and the stream function ψ. Without loss of generality we choose $\phi = 0$ at $(x, y) = (0, 1)$ and $\psi = 1$ on the streamline ABC. It follows from the choice of the dimensionless variables that $\psi = 0$ on the streamline $A'OC'$.

In order to use the conformal mapping techniques, we consider the flow in the complex plane $z = x + iy$ and the complex potential function

$$f(z) = \phi(z) + i\psi(z). \tag{2.5}$$

By this the mathematical problem is to determine the variable ψ which verifies the following conditions:

$$\Delta\psi = 0, \tag{2.6}$$

in the interior of the flow filed.

The condition on the free-surface BC, where The effects of gravity are neglected, is obtained from Bernoulli's equation (2.2) take the form:

$$\frac{1}{2}q^{*2} + \frac{p^*}{\rho} = \frac{1}{2}U_1^2 + \frac{p_a}{\rho}, \tag{2.7}$$

which implies that

$$\frac{1}{2}q^{*2} + \frac{p^* - p_a}{\rho} = \frac{1}{2}U_1^2. \tag{2.8}$$

Using (1.14), eq (2.8) take the form:

$$\frac{1}{2}\frac{q^{*2}}{U_1^2} + \frac{TK^*}{U_1^2\rho} = \frac{1}{2}, \tag{2.9}$$

where The effect of the surface tension is neglected ($T = 0$), and from (2.4) the Bernoulli's equation in the dimensionless variables take the form:

$$q^2 = 1, \tag{2.10}$$

which implies that

$$\left(\frac{\partial\psi}{\partial x}\right)^2 + \left(\frac{\partial\psi}{\partial y}\right)^2 = 1. \tag{2.11}$$

On the horizontal wall $A'OC'$:

$$\frac{\partial\psi}{\partial x} = 0. \tag{2.12}$$

On the inclined wall AB:

$$\frac{\partial\psi}{\partial x} = \frac{\partial\psi}{\partial y}\tan\alpha. \tag{2.13}$$

Next we introduce the complex velocity

$$\eta(z) = C\frac{df}{dz} = u - iv = qe^{-i\theta}. \tag{2.14}$$

Here $C = \frac{H}{d}$ is the contraction coefficient which is defined as the ratio of the thickness H of the flow as $x \to \infty$ to length of the opening of the gate d, $q = \sqrt{u^2 + v^2}$ is the flow speed, θ is the velocity direction relative to the real axis.

2.2 Solution of the problem by using the Hodograph method

The transformation (2.14) maps the flow field of z plane to a sector of the disk such as the free surface is mapped into a part of the circumference of the circle in the hodograph plane see Fig2.2

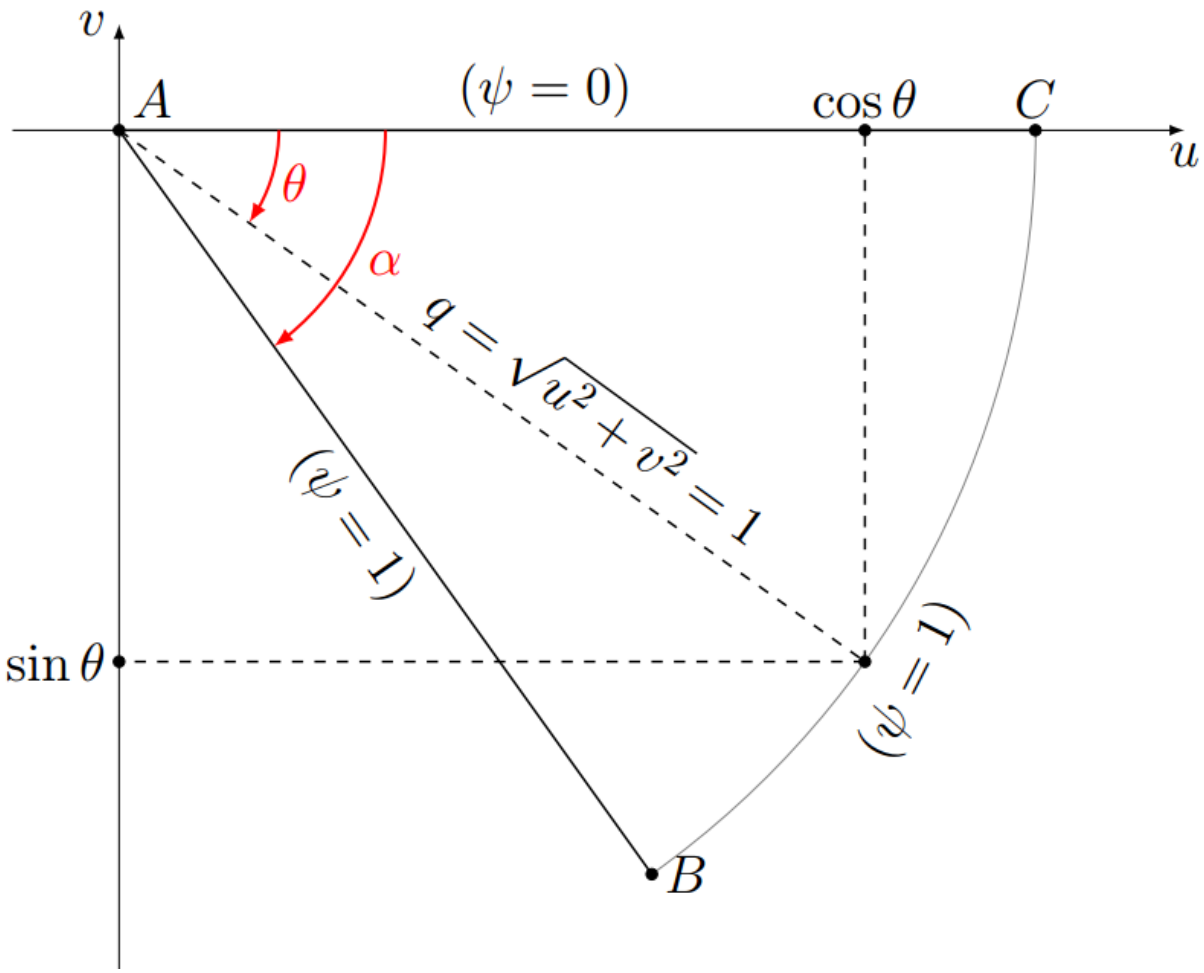

Figure 2.2: Hodograph plane (u, v)

Then the mathematical problem is to determine the stream function ψ as a function of the two

variables q and θ which verifies the following equation (see [40]):

$$\frac{\partial^2\psi}{\partial q^2}+\frac{1}{q}\frac{\partial\psi}{\partial q}+\frac{1}{q^2}\frac{\partial^2\psi}{\partial\theta^2}=0, \tag{2.15}$$

in the interior of the flow filed.

The two components of the potential function (the potential velocity and the stream function) satisfies the Cauchy-Riemann conditions, then

$$\frac{\partial\phi}{\partial q}=-\frac{1}{q}\frac{\partial\psi}{\partial\theta},\qquad \frac{\partial\psi}{\partial q}=\frac{1}{q}\frac{\partial\phi}{\partial\theta}, \tag{2.16}$$

which is stated in [40].

In the hodograph plane the conditions (2.11), (2.12) and (2.13) are easily transformed into the conditions

$$\begin{aligned}&\psi(1,\theta)=1;\quad -\alpha\leq\theta\leq 0,\ \text{ on }\ BC,\\ &\psi(q,-\alpha)=1;\quad 0<q<1,\ \text{ on }\ AB,\end{aligned} \tag{2.17}$$

and

$$\psi(q,0)=0;\quad 0\leq q\leq 1,\quad \text{on}\quad A'OC'. \tag{2.18}$$

Then to solve the above considered problem defined by Eq (2.15) and the conditions (2.17) and (2.18), we using the separation variable method. Firstly, we pose that:

$$\psi(q,\theta)=\xi(q,\theta)-\frac{\theta}{\alpha}. \tag{2.19}$$

As ξ satisfies the following problem :

$$\begin{cases}\dfrac{\partial^2\xi}{\partial q^2}+\dfrac{1}{q}\dfrac{\partial\xi}{\partial q}+\dfrac{1}{q^2}\dfrac{\partial^2\xi}{\partial\theta^2}=0,\quad 0\leq q\leq 1,\quad -\alpha\leq\theta\leq 0. & (2.20)\\ \xi(q,0)=\xi(q,-\alpha)=0,\quad 0\leq q\leq 1, & (2.21)\\ \xi(1,\theta)=\left(1+\dfrac{\theta}{\alpha}\right),\quad -\alpha\leq\theta\leq 0. & (2.22)\end{cases}$$

To solve this problem by the method of separation of variables, we begin by addressing equation (2.20). We propose that it has solutions of the form

$$\xi(q,\theta)=h(q)g(\theta), \tag{2.23}$$

where h is a function of q alone and g is a function of θ alone. To determine h and g, we first

compute the partial derivatives of ξ to obtain

$$\frac{\partial^2 \xi}{\partial q^2} = h^{''}(q)g(\theta), \quad \frac{\partial \xi}{\partial q} = h^{'}(q)g(\theta) \quad \text{and} \quad \frac{\partial^2 \xi}{\partial \theta^2} = h(q)g^{''}(\theta). \tag{2.24}$$

Substituting these expressions (2.24) into (2.20) gives

$$h^{''}(q)g(\theta) + \frac{1}{q}h^{'}(q)g(\theta) + \frac{1}{q^2}h(q)g^{''}(\theta) = 0, \tag{2.25}$$

and separating variables yields

$$\frac{-q^2 h^{''}(q) - qh^{'}(q)}{h(q)} = \frac{g^{''}(\theta)}{g(\theta)}. \tag{2.26}$$

We now observe that the functions on the left-hand side of (2.26) depend only on q, while those on the right-hand side depend only on θ. If we fix q and vary θ, the ratio on the right cannot change; it must be constant c_0,

$$\begin{cases} \dfrac{-q^2 h^{''}(q) - qh^{'}(q)}{h(q)} = c_0, & (2.27) \\ \dfrac{g^{''}(\theta)}{g(\theta)} = c_0, & (2.28) \end{cases}$$

where can be any constant. Thus

$$\begin{cases} q^2 h^{''}(q) + qh^{'}(q) + c_0 h(q) = 0, & (2.29) \\ g^{''}(\theta) - c_0 g(\theta) = 0. & (2.30) \end{cases}$$

Consequently, for separable solutions, we have reduced the problem of solving the partial differential quation (2.20) to solving the two ordinary differential equations in (2.29) and (2.30).

Next we consider the boundary conditions in (2.21). Since $\xi(q, \theta) = h(q)g(\theta)$ these conditions are

$$h(q)g(0) = 0 \quad \text{and} \quad h(q)g(-\alpha) = 0; \quad 0 \leq q \leq 1. \tag{2.31}$$

Hence, either $h(q) = 0$ for $0 \leq q \leq 1$ which implies that $\xi(q, \theta) = 0$ or

$$g(0) = 0 \quad \text{and} \quad g(-\alpha) = 0, \tag{2.32}$$

we combine the boundary conditions in (2.32) with the differential equation for g in (2.30) and obtain the boundary value problem

$$\begin{cases} g^{''}(\theta) - c_0 g(\theta) = 0, & (2.33) \\ g(0) = g(-\alpha) = 0. & (2.34) \end{cases}$$

We look for values of c_0 which gives us nontrivial solutions. We consider three possible cases:

$$c_0 > 0, \quad c_0 = 0 \quad \text{and} \quad c_0 = -\lambda^2 < 0.$$

- *Case 1.* $c_0 > 0$. The general solution in this case is of the form

$$g(\theta) = Ae^{-\sqrt{c_0}\theta} + Be^{\sqrt{c_0}\theta}, \tag{2.35}$$

where A and B are arbitrary constants. To satisfy the boundary conditions (2.34), we must have

$$\begin{cases} A + B = 0, & (2.36) \\ Ae^{\sqrt{c_0}\alpha} + Be^{-\sqrt{c_0}\alpha} = 0. & (2.37) \end{cases}$$

We see that the determinant of the system (2.36), (2.37) is different from zero. Consequently, A and B must both be zero, and hence, the general solution $g(\theta)$ is identically zero. The solution is trivial and hence, is no interest.

- *Case 2.* $c_0 = 0$. Here, the general solution is

$$g(\theta) = A + B\theta. \tag{2.38}$$

Applying the boundary conditions (2.34), we have

$$A = 0, \quad A - \alpha B = 0. \tag{2.39}$$

Hence $A = B = 0$. The solution is thus identically zero.

- *Case 3.* $c_0 = -\lambda^2 < 0$. In this case, the general solution of (2.33) assumes the form

$$g(\theta) = A\cos(\lambda\theta) + B\sin(\lambda\theta), \tag{2.40}$$

From the condition $g(0) = 0$, we obtain $A = 0$. The condition $g(-\alpha) = 0$ gives

$$B\sin(-\lambda\alpha) = 0. \tag{2.41}$$

If $B = 0$, the solution is trivial. For nontrivial solutions ($B \neq 0$), hence,

$$\sin(\lambda\alpha) = 0. \tag{2.42}$$

This equation is satisfied when

$$\lambda\alpha = n\pi, \quad \text{for} \quad n = 1, 2, 3, \cdots \tag{2.43}$$

or

$$\lambda_n = \frac{n\pi}{\alpha}; \quad \text{for} \quad n = 1, 2 \ldots . \tag{2.44}$$

For this infinite set of discrete values of λ, the problem has a nontrivial solution. These values of $c_0 = -\lambda_n^2$ are called the eigenvalues of the problem, and the functions

$$\sin\left(\frac{n\pi}{\alpha}\theta\right) \quad \text{for} \quad n = 1, 2 \ldots , \tag{2.45}$$

are the corresponding eigenfunctions.

The equation (2.40) is given as:

$$g_n(\theta) = B_n \sin\left(\frac{n\pi}{\alpha}\theta\right), \qquad n = 1, 2 \ldots , \tag{2.46}$$

where the B_n are arbitrary nonzero constants.

Then, the solution of the problem (2.20) is given by

$$\xi(q, \theta) = B_n\,(q) \sin\left(\frac{n\pi}{\alpha}\theta\right), \qquad n = 1, 2 \ldots . \tag{2.47}$$

The general solution of the problem can be obtained by the superposition of solution of the homogeneous problem (2.20) of the form

$$\xi(q, \theta) = \sum_{n=1}^{\infty} B_n\,(q) \sin\left(\frac{n\pi}{\alpha}\theta\right). \tag{2.48}$$

Having determined that $\lambda_n = \frac{n\pi}{\alpha}$ for any positive integer n and by replacing (2.48) in (2.20), we get the equation of the second-order homogeneous Cauchy-Euler:

$$q^2 B_n''(q) + q B_n'(q) - \left(\frac{n\pi}{\alpha}\right)^2 B_n(q) = 0. \tag{2.49}$$

Conseqently, The solution of (2.49) is given in the form:

$$B_n(q) = a q^{\frac{n\pi}{\alpha}} + b q^{-\frac{n\pi}{\alpha}}, \tag{2.50}$$

where a and b are constants.

Consequently,

$$\xi(q, \theta) = \sum_{n=1} a q^{\frac{n\pi}{\alpha}} \sin\left(\frac{n\pi}{\alpha}\theta\right). \tag{2.51}$$

Then, after using the condition of (2.22), we get :

$$\begin{aligned} a &= \frac{2}{\alpha}\int_{-\alpha}^{0}\left(1+\frac{t}{\alpha}\right)\sin\left(\frac{n\pi}{\alpha}t\right)dt, \\ &= -\frac{2}{\alpha}\left(\frac{\alpha}{n\pi}\right). \end{aligned} \tag{2.52}$$

Consequently, the solution of the problem (2.20)-(2.22) is given by:

$$\xi(q,\theta) = -\frac{2}{\alpha}\sum_{n=1}\frac{\alpha}{n\pi}q^{\frac{n\pi}{\alpha}}\sin\left(\frac{n\pi}{\alpha}\theta\right). \tag{2.53}$$

On the other hand, from (2.19) and the result (2.53) we can obtain the stream function ψ as follows:

$$\psi(q,\theta) = -\frac{2}{\alpha}\sum_{n=1}\frac{\alpha}{n\pi}q^{\frac{n\pi}{\alpha}}\sin(\frac{n\pi}{\alpha}\theta) - \frac{1}{\alpha}\theta, \tag{2.54}$$

from the Cauchy-Riemann condition (2.16) and the relation of the stream function (2.54), we have

$$\begin{aligned} \frac{\partial\phi}{\partial q} &= -\frac{1}{q}\frac{\partial}{\partial\theta}\left[-\frac{2}{\alpha}\sum_{n=1}\frac{\alpha}{n\pi}q^{\frac{n\pi}{\alpha}}\sin(\frac{n\pi}{\alpha}\theta) - \frac{1}{\alpha}\theta\right] \\ &= \frac{2}{\alpha}\sum_{n=1}q^{\frac{n\pi}{\alpha}-1}\cos(\frac{n\pi}{\alpha}\theta) + \frac{1}{\alpha q}. \end{aligned} \tag{2.55}$$

By integration, we obtains the velocity potential ϕ:

$$\phi(q,\theta) = \frac{2}{\alpha}\sum_{n=1}\frac{\alpha}{n\pi}q^{\frac{n\pi}{\alpha}}\cos(\frac{n\pi}{\alpha}\theta) + \frac{1}{\alpha}\ln(q). \tag{2.56}$$

Thus,

$$\begin{aligned} f(q,\theta) &= \phi(q,\theta) + i\psi(q,\theta) \\ &= \frac{2}{\alpha}\sum_{n=1}\frac{\alpha}{n\pi}q^{\frac{n\pi}{\alpha}}\left[\cos(\frac{n\pi}{\alpha}\theta) - i\sin(\frac{n\pi}{\alpha}\theta)\right] + \frac{1}{\alpha}\left(\ln(q) - i\theta\right) \\ &= \frac{2}{\alpha}\sum_{n=1}\frac{\alpha}{n\pi}q^{\frac{n\pi}{\alpha}}e^{-i\frac{n\pi}{\alpha}} + \frac{1}{\alpha}\ln(qe^{-i\theta}). \end{aligned} \tag{2.57}$$

From the complex velocity (2.14) we have $\eta = qe^{-i\theta}$. Therefore, the potential function (2.57) take the form:

$$f(\eta) = \frac{2}{\alpha}\sum_{n=1}\frac{\alpha}{n\pi}\eta^{\frac{n\pi}{\alpha}} + \frac{1}{\alpha}\ln(\eta). \tag{2.58}$$

Using the relation of the complex velocity (2.14), we have:

$$\begin{aligned} dz &= C\frac{df(\eta)}{\eta} \\ &= C\left(\frac{2}{\alpha}\sum_{n=1}\eta^{\frac{n\pi}{\alpha}-2}+\frac{1}{\alpha\eta^2}\right)d\eta. \end{aligned} \tag{2.59}$$

Then, we pose $R=\sum_{n=1}\eta^{\frac{n\pi}{\alpha}}$, therefore $R-\eta^{\frac{\pi}{\alpha}}R=\eta^{\frac{\pi}{\alpha}}$. Which yield,

$$\sum_{n=1}\eta^{\frac{n\pi}{\alpha}-2}=\frac{\eta^{\frac{\pi}{\alpha}-2}}{1-\eta^{\frac{\pi}{\alpha}}}. \tag{2.60}$$

Consequently, by substituting (2.60) into (2.59) we get:

$$dz=\frac{2C}{\alpha}\left(\frac{\eta^{\frac{\pi}{\alpha}-2}}{1-\eta^{\frac{\pi}{\alpha}}}\right)d\eta+\frac{C}{\alpha\eta^2}d\eta. \tag{2.61}$$

2.3 Free streamline forms for various value of α

2.3.1 The free streamline for $\alpha=\frac{\pi}{4}$

substitute this value in equation (2.61) we get:

$$dz=\frac{8C}{\pi}\left(\frac{\eta^2}{1-\eta^4}\right)d\eta+\frac{4C}{\pi\eta^2}d\eta, \tag{2.62}$$

by integrating both sides of this equation, we get:

$$\begin{aligned} z=&\frac{4C}{\pi}\int\left(\frac{2\eta^2}{1-\eta^4}+\frac{1}{\eta^2}\right)d\eta+c_1, \\ =&\frac{4C}{\pi}\int\left(\frac{2\eta^2}{1-\eta^4}d\eta+\int\frac{1}{\eta^2}\right)d\eta+c_1, \\ =&\frac{4C}{\pi}\left(\int\left(\frac{1}{1-\eta^2}-\frac{1}{1+\eta^2}\right)d\eta-\frac{1}{\eta}\right)+c_1, \\ =&\frac{4C}{\pi}\left(\operatorname{arctanh}(\eta)-\arctan(\eta)-\frac{1}{\eta}\right)+c_1, \\ =&\frac{4C}{\pi}\left(\frac{1}{2}\ln\left(\frac{\eta+1}{1-\eta}\right)+\frac{i}{2}\ln\left(\frac{1+i\eta}{1-i\eta}\right)-\frac{1}{\eta}\right)+c_1. \end{aligned} \tag{2.63}$$

On the free streamline we have:

$$\eta = e^{-i\theta}, \quad \text{with} \quad -\frac{\pi}{4} \leq \theta \leq 0. \tag{2.64}$$

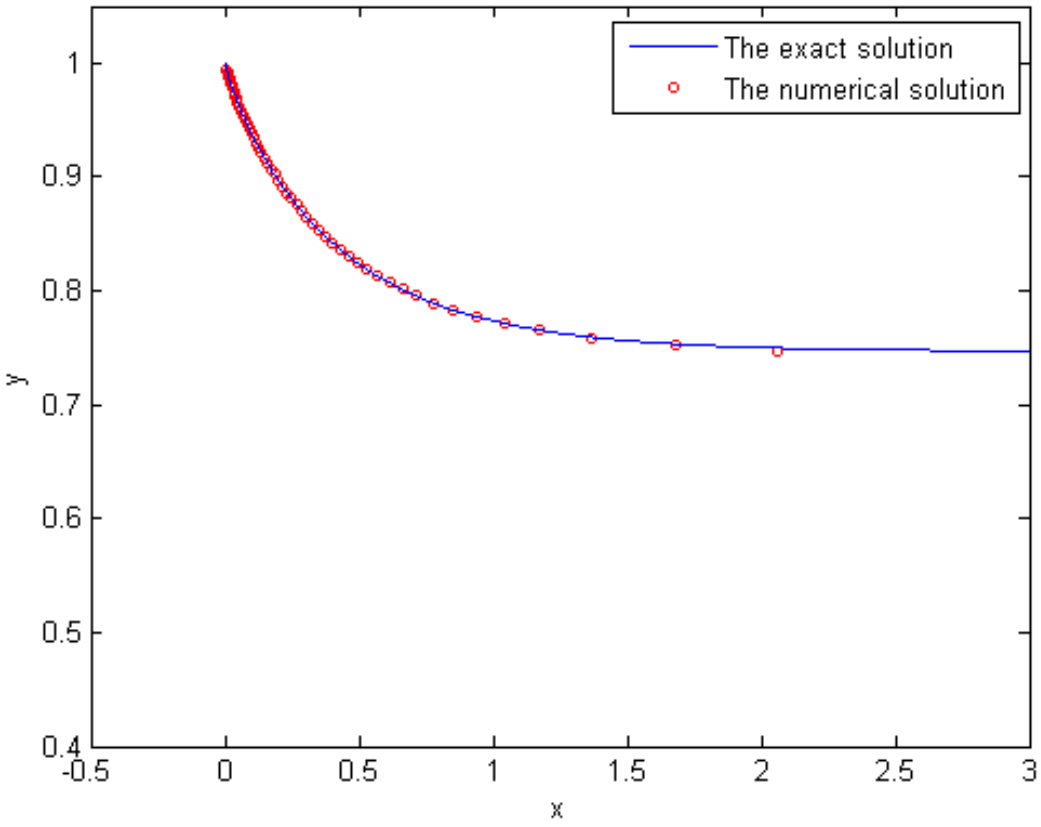

Figure 2.3: Comparison of the analytical solution and the numerical solutions for $\alpha = \frac{\pi}{4}$

Separate (2.63) into real and imaginary parts:

$$\begin{aligned} \ln\left(\frac{\eta+1}{1-\eta}\right) &= \ln\left(\frac{e^{-i\theta}+1}{1-e^{-i\theta}}\right) \\ &= \ln\left(\frac{2\cos(\theta/2)}{2i\sin(\theta/2)}\right) \\ &= -\frac{\pi}{2}i - \ln(\tan(\theta/2)) \\ &= -\frac{\pi}{2}i + \tanh^{-1}(\cos(\theta)), \end{aligned} \tag{2.65}$$

$$\begin{aligned}
\arctan(\eta) &= -\frac{i}{2}\ln\left(\frac{1+i\eta}{1-i\eta}\right)\\
&= -\frac{i}{2}\ln\left(\frac{1-e^{-i(\pi/2+\theta)}}{1+e^{-i(\pi/2+\theta)}}\right)\\
&= -\frac{i}{2}\ln\left(\frac{e^{i(\pi/4+\theta/2)}-e^{-i(\pi/4+\theta/2)}}{e^{i(\pi/4+\theta/2)}+e^{-i(\pi/2+\theta/2)}}\right)\\
&= -\frac{i}{2}\ln\left(\frac{2i\sin(\pi/4+\theta/2)}{2\cos(\pi/4+\theta/2)}\right)\\
&= -\frac{i}{2}\ln(i)-\frac{i}{2}\ln(\tan(\pi/4+\theta/2))\\
&= \frac{\pi}{4}-\frac{i}{2}\ln(\tan(\pi/4+\theta/2))\\
&= \frac{\pi}{4}-\frac{i}{2}\ln\left(\sqrt{\frac{1-\cos(\theta+\pi/2)}{1+\cos(\theta+\pi/2)}}\right)\\
&= \frac{\pi}{4}+\frac{i}{4}\ln\left(\frac{1+\cos(\theta+\pi/2)}{1-\cos(\theta+\pi/2)}\right)\\
&= \frac{\pi}{4}+\frac{i}{2}\tanh^{-1}(\cos(\theta+\pi/2)).
\end{aligned} \tag{2.66}$$

Consequently, substituting (2.65) and (2.66) into (2.63) we get:

$$\begin{aligned}
z &= \frac{2C}{\pi}\left(\operatorname{arctanh}(\cos(\theta))-\frac{\pi}{2}i-\frac{\pi}{2}-i\operatorname{arctanh}\left(\cos\left(\theta+\frac{\pi}{2}\right)\right)\right)\\
&- \frac{4C}{\pi}(\cos(\theta)+i\sin(\theta))+c_1.
\end{aligned} \tag{2.67}$$

On the other hand, at the point B, we have $\theta=-\pi/4$ and $z=i$, wich yields

$$c_1 = -\frac{2C}{\pi}\left(\operatorname{arctanh}\left(\frac{\sqrt{2}}{2}\right)-\sqrt{2}-\frac{\pi}{2}\right)+i\left(1-\frac{2C}{\pi}\left(-\operatorname{arctanh}\left(\frac{\sqrt{2}}{2}\right)-\sqrt{2}+\frac{\pi}{2}\right)\right). \tag{2.68}$$

By separating the real parts and the imaginary parts, we obtain:

$$\begin{cases}
x=\frac{2C}{\pi}\left(\operatorname{arctanh}(\cos\theta)-\operatorname{arctanh}\left(\frac{\sqrt{2}}{2}\right)-2\cos\theta+\sqrt{2}\right),\\
y=1-\frac{2C}{\pi}\left(\operatorname{arctanh}\left(\cos\left(\theta+\frac{\pi}{2}\right)\right)-\operatorname{arctanh}\left(\frac{\sqrt{2}}{2}\right)+2\sin(\theta)+\sqrt{2}\right).
\end{cases} \tag{2.69}$$

The amplitude of the flow at the infinity is calculated as:

$$\begin{aligned}
C=\frac{H}{d}=\lim_{\theta\longrightarrow 0}y(\theta)&=1-\frac{2C}{\pi}\left(-\operatorname{arctanh}\left(\frac{\sqrt{2}}{2}\right)+\sqrt{2}\right).\\
\Rightarrow C&=\frac{\pi}{\left(\pi-2\operatorname{arctanh}\left(\frac{\sqrt{2}}{2}\right)+2\sqrt{2}\right)}.
\end{aligned} \tag{2.70}$$

Figure 2.3 presents the comparison of the exact form of the free streamlines with the numerical solution calculated by the series truncation method for $\alpha=\frac{\pi}{4}$.

2.3.2 The free streamline for $\alpha = \frac{\pi}{2}$

For $\alpha = \frac{\pi}{2}$, it becomes that the values of the angle θ are given by $-\frac{\pi}{2} \leq \theta \leq 0$, and from the equation (2.61) we get:

$$dz = \frac{4C}{\pi}\left(\frac{1}{1-\eta^2}\right)d\eta + \frac{2C}{\pi\eta^2}d\eta, \tag{2.71}$$

by integrating both sides of this equation, we get:

$$\begin{aligned} z &= \frac{4C}{\pi}\int\left(\frac{1}{1-\eta^2}\right)d\eta + \int\frac{2C}{\pi\eta^2}d\eta + c_2, \\ &= \frac{2C}{\pi}\left(\operatorname{arctanh}(\eta) - \frac{1}{\eta}\right) + c_2, \\ &= \frac{2C}{\pi}\left(\ln\left(\frac{\eta+1}{1-\eta}\right) - \frac{1}{\eta}\right) + c_2, \end{aligned} \tag{2.72}$$

On the free streamline we have :

$$\eta = e^{-i\theta}, \quad \text{with} \quad -\frac{\pi}{2} \leq \theta \leq 0. \tag{2.73}$$

Separate (2.63) into real and imaginary parts, we get:

$$\begin{aligned} z &= \frac{2C}{\pi}\left(\ln\left(\frac{e^{-i\theta}+1}{1-e^{-i\theta}}\right) - \frac{1}{e^{-i\theta}}\right) + c_2, \\ &= \frac{2C}{\pi}\left(\ln\left(-\frac{i}{\tan(\theta/2)}\right) - e^{i\theta}\right) + c_2, \\ &= \frac{2C}{\pi}\left(\operatorname{arctanh}(\cos\theta) - \cos\theta\right) - i\frac{2C}{\pi}\left(\sin\theta + \frac{\pi}{2}\right) + c_2. \end{aligned} \tag{2.74}$$

On the other hand, by using the conditions at point B ($\theta = -\pi/2$ and $z = i$) we find the free streamlines:

$$\begin{cases} x = \frac{2C}{\pi}\left(\operatorname{arctanh}(\cos\theta) - \cos\theta\right). \\ y = 1 - \frac{2C}{\pi}\left(\sin\theta + 1\right). \end{cases} \tag{2.75}$$

The amplitude of the flow at the infinity is calculated as:

$$\begin{aligned} C = \frac{H}{d} = \lim_{\theta \longrightarrow 0} y(\theta) = 1 - \frac{2C}{\pi}, \\ \Rightarrow C = \frac{\pi}{(\pi+2)}. \end{aligned} \tag{2.76}$$

This solution is also obtained in [8] by the free streamline theory methods and the comparison of this result with the numerical solution obtained by [22] is shown in Fig 2.4.

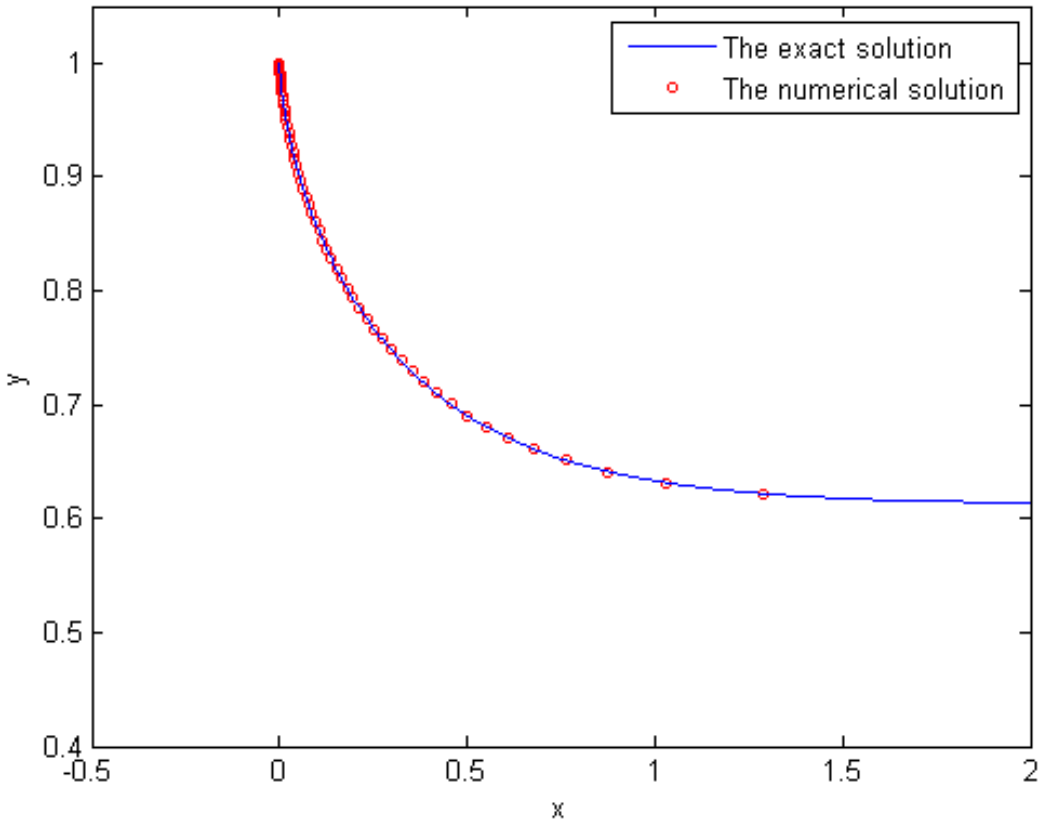

Figure 2.4: Comparison of the analytical solution and the numerical solutions for $\alpha = \frac{\pi}{2}$

2.3.3 The free streamline for $\alpha = \frac{3\pi}{4}$

For $\alpha = \dfrac{3\pi}{4}$, substitute this value in equation (2.61) we get:

$$dz = \frac{8C}{3\pi}\left(\frac{\eta^{-2/3}}{1-\eta^{4/3}}\right)d\eta + \frac{4C}{3\pi\eta^2}d\eta, \tag{2.77}$$

by integrating both sides of this equation, we get:

$$\begin{aligned} z &= \frac{8C}{3\pi}\int\left(\frac{\eta^{-2/3}}{1-\eta^{4/3}}\right)d\eta + \int\frac{4C}{3\pi\eta^2}d\eta + c_3, \\ &= \frac{2C}{\pi}\left(2\arctan\left(\eta^{1/3}\right) + \ln\left(\frac{\eta^{1/3}+1}{\eta^{1/3}-1}\right)\right) - \frac{4C}{3\pi\eta} + c_3, \\ &= \frac{2C}{\pi}\left(-i\ln\left(\frac{1+i\eta^{1/3}}{1-i\eta^{1/3}}\right) + \ln\left(\frac{\eta^{1/3}+1}{\eta^{1/3}-1}\right)\right) - \frac{4C}{3\pi\eta} + c_3. \end{aligned} \tag{2.78}$$

On the free streamline we have:

$$\eta = e^{-i\theta}, \quad \text{with} \quad -3\pi/4 \leq \theta \leq 0, \tag{2.79}$$

on the other, we have:

$$\begin{aligned}
\arctan\left(\eta^{1/3}\right) &= \frac{1}{2i}\ln\left(\frac{1+ie^{-i\theta/3}}{1-ie^{-i\theta/3}}\right) \\
&= \frac{1}{2i}\ln\left(\frac{e^{i(\pi/4+\theta/6)}-e^{-i(\pi/4+\theta/6)}}{e^{i(\pi/4+\theta/6)}+e^{-i(\pi/4+\theta/6)}}\right) \\
&= \frac{1}{2i}\ln\left(\frac{2i\sin\left(\pi/4+\theta/6\right)}{2\cos\left(\pi/4+\theta/6\right)}\right) \\
&= \frac{1}{2i}\left(\ln\left(i\right)+\ln\left(\tan\left(\pi/4+\theta/6\right)\right)\right) \\
&= \frac{\pi}{4}-\frac{i}{2}\ln\left(\tan\left(\pi/4+\theta/6\right)\right),
\end{aligned} \tag{2.80}$$

and

$$\begin{aligned}
\ln\left(\frac{\eta^{1/3}+1}{\eta^{1/3}-1}\right) &= \ln\left(\frac{e^{-i\theta/3}+1}{e^{-i\theta/3}-1}\right) \\
&= \ln\left(\frac{e^{-i\theta/6}+e^{i\theta/6}}{e^{-i\theta/6}-e^{i\theta/6}}\right) \\
&= \ln\left(\frac{2\cos\left(\theta/6\right)}{2i\sin\left(\theta/6\right)}\right) \\
&= \ln\left(i\right)-\ln\left(\tan\left(\theta/6\right)\right) \\
&= \frac{3\pi}{2}-\ln\left(\tan\left(-\theta/6\right)\right)
\end{aligned} \tag{2.81}$$

Consequently, substituting (2.80), (2.81) into (2.78) we get:

$$\begin{aligned}
z &= \frac{2C}{\pi}\left(\frac{\pi}{2}-i\ln\left(\tan\left(\pi/4+\theta/6\right)\right)+\frac{3\pi}{2}-\ln\left(\tan\left(-\theta/6\right)\right)\right) \\
&\quad -\frac{4C}{3\pi}\left(\cos\left(\theta\right)+i\sin\left(\theta\right)\right)+c_3.
\end{aligned} \tag{2.82}$$

By separating the real parts and the imaginary parts, and using the conditions at point B ($\theta = -3\pi/4$ and $z = i$), we get the free streamlines:

$$\begin{cases}
x = \frac{2C}{\pi}\left(-\ln\left(\tan\left(-\frac{\theta}{6}\right)\right)-\frac{2}{3}\cos\left(\theta\right)+\ln\left(\sqrt{2}-1\right)-\frac{\sqrt{2}}{3}\right). \\
y = 1-\frac{2C}{\pi}\left(\ln\left(\tan\left(\frac{\pi}{4}+\frac{\theta}{6}\right)\right)+\frac{2}{3}\sin\left(\theta\right)-\ln\left(\sqrt{2}-1\right)+\frac{\sqrt{2}}{3}\right).
\end{cases} \tag{2.83}$$

The amplitude of the flow at the infinity is calculated as:

$$\begin{aligned}
C = \frac{H}{d} = \lim_{\theta\longrightarrow 0} y\left(\theta\right) &= 1-\frac{2C}{\pi}\left(-\ln\left(\sqrt{2}-1\right)+\frac{\sqrt{2}}{3}\right), \\
\Rightarrow C &= \frac{1}{\left(1+\frac{2}{\pi}\left(\frac{\sqrt{2}}{3}-\ln\left(\sqrt{2}-1\right)\right)\right)}.
\end{aligned} \tag{2.84}$$

Figure 2.5 presents the comparison of the exact form of the free streamlines with the numerical solution calculated by the series truncation method for $\alpha = \frac{3\pi}{4}$.

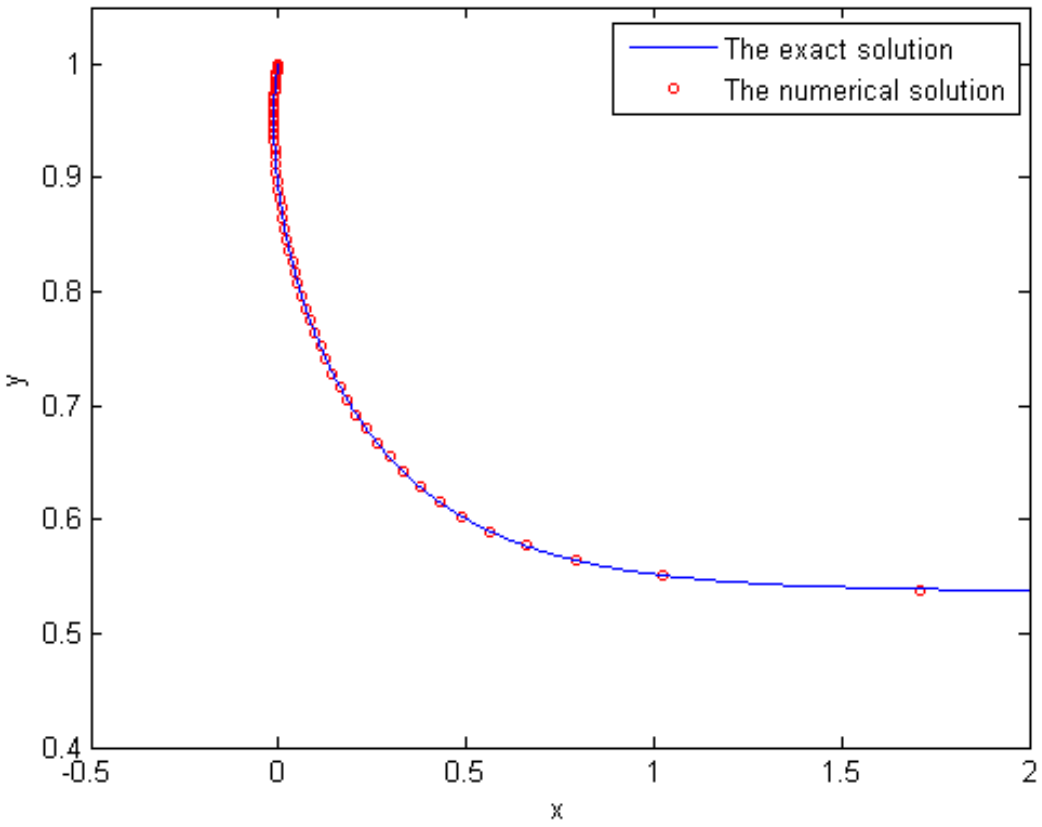

Figure 2.5: Comparison of the analytical solution and the numerical solutions for $\alpha = \frac{3\pi}{4}$

2.3.4 The free streamline for $\alpha = \pi$

For $\alpha = \pi$, substitute this value in equation (2.61), we get:

$$dz = \frac{2C}{\pi}\left(\frac{\eta^{-1}}{1-\eta}\right)d\eta + \frac{C}{\pi\eta^2}d\eta, \tag{2.85}$$

by integrating both sides of this equation, we get:

$$\begin{aligned} z &= \frac{2C}{\pi}\int\left(\frac{\eta^{-1}}{1-\eta}\right)d\eta + \int\frac{C}{\pi\eta^2}d\eta + c_4, \\ &= \frac{2C}{\pi}\int\left(\frac{1}{\eta} - \frac{1}{1-\eta}\right)d\eta + \int\frac{C}{\pi\eta^2}d\eta + c_4, \\ &= \frac{2C}{\pi}\left(\ln(\eta) - \ln(\eta-1)\right) - \frac{C}{\pi\eta} + c_4, \end{aligned} \tag{2.86}$$

on the free streamline we have :

$$\eta = e^{-i\theta}, \quad \text{with} \quad -\pi \leq \theta \leq 0, \tag{2.87}$$

on the other hand, we have:

$$\begin{aligned} \ln(\eta - 1) &= \ln\left(e^{-i\theta} - 1\right) \\ &= \ln\left(e^{-i\theta/2}\left(e^{-i\theta/2} - e^{i\theta/2}\right)\right) \\ &= \ln\left(e^{-i\theta/2}\right) + \ln\left(e^{-i\theta/2} - e^{i\theta/2}\right) \\ &= -i\theta/2 + \ln\left(-2i\sin\left(\frac{\theta}{2}\right)\right) \\ &= i\left(\frac{\pi - \theta}{2}\right) + \ln\left(-2\sin\left(\frac{\theta}{2}\right)\right). \end{aligned} \tag{2.88}$$

$$\begin{aligned} z &= \frac{2C}{\pi}\left(-\ln\left(-2\sin\left(\frac{\theta}{2}\right)\right) - \frac{1}{2}\cos(\theta)\right) \\ &\quad -i\frac{2C}{\pi}\left(\frac{1}{2}\sin(\theta) + \frac{\theta + \pi}{2}\right) + c_4. \end{aligned} \tag{2.89}$$

On the other hand, at the point B, we have $\theta = -\pi$ and $z = i$, wich yields

$$c_4 = i - \frac{2C}{\pi}\left(\frac{1}{2} - \ln(2)\right). \tag{2.90}$$

By separating the real parts and the imaginary parts, we obtain:

$$\begin{cases} x = \frac{2C}{\pi}\left(\ln(2) - \ln\left(-2\sin\left(\frac{\theta}{2}\right)\right) - \frac{1}{2}\cos((\theta)) - \frac{1}{2}\right), \\ y = 1 - \frac{2C}{\pi}\left(\frac{1}{2}\sin(\theta) + \frac{\theta}{2} + \frac{\pi}{2}\right). \end{cases} \tag{2.91}$$

The amplitude of the flow at the infinity is calculated as:

$$\begin{aligned} C = \frac{H}{d} = \lim_{\theta \longrightarrow 0} y(\theta) = 1 - \frac{2C}{\pi}\left(\frac{\pi}{2}\right) \\ \Rightarrow C = \frac{1}{2}. \end{aligned} \tag{2.92}$$

Figure 2.6 presents the comparison of the exact form of the free streamlines with the numerical solution calculated by the series truncation method for $\alpha = \pi$. The free surface shapes for different values of the inclination angle α is presented in Fig 2.7

The comparison of the calculated coefficient of contraction of the flow for different values of the inclination angle α with the experimental results given in [9] and the numerical solutions given in [22] is shown in Table 2.1 and Fig 2.8.

Finally through all the presented results we observe that the obtained results using the hodograph method agree with those calculated numerically by series truncation method [22].

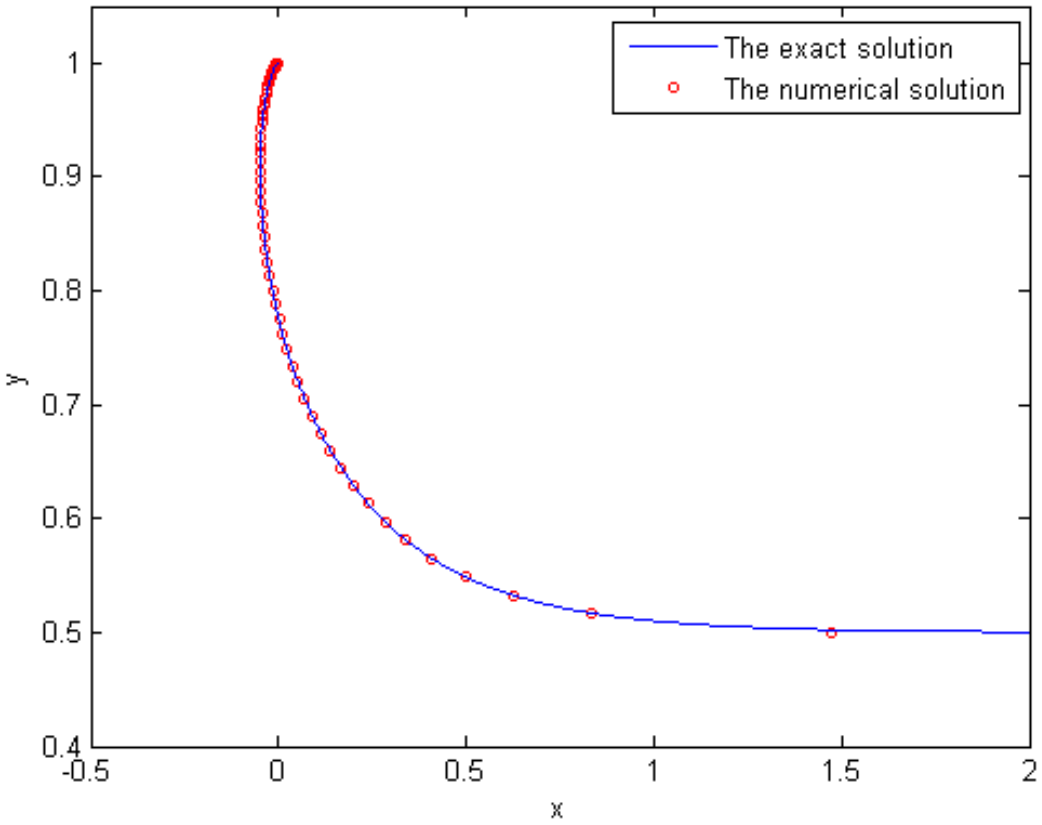

Figure 2.6: Comparison of the analytical solution and the numerical solutions for $\alpha = \pi$

Table 2.1: Comparision of the theory, numerical and experimental values of the contraction Coefficient C for several value of the inclination angle α

α	$\pi/4$	$\pi/2$	$3\pi/4$	π
The Contraction Coefficient C(numerical)	0.746	0.611	0.537	0.5
The Contraction Coefficient C(exper)	0.753	0.632	0.577	0.541
The Contraction Coefficient C(theory)	0.7467	0.611	0.5373	0.5

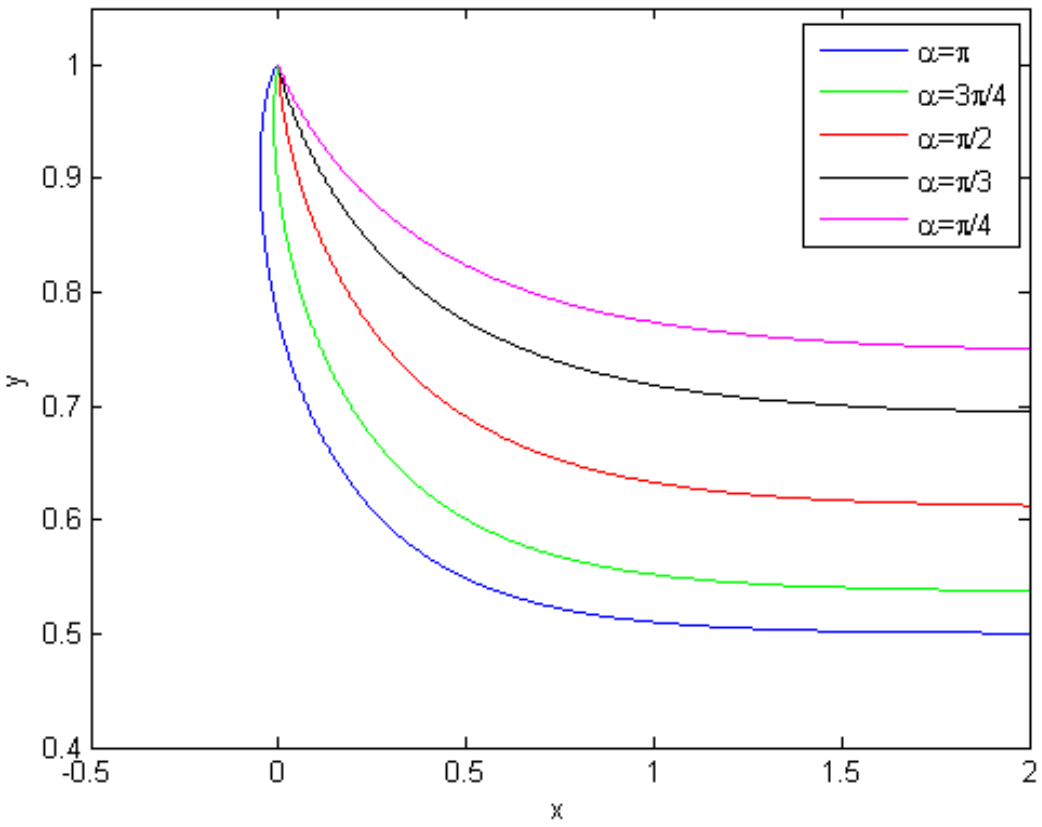

Figure 2.7: The variation of the free surface with respect to α

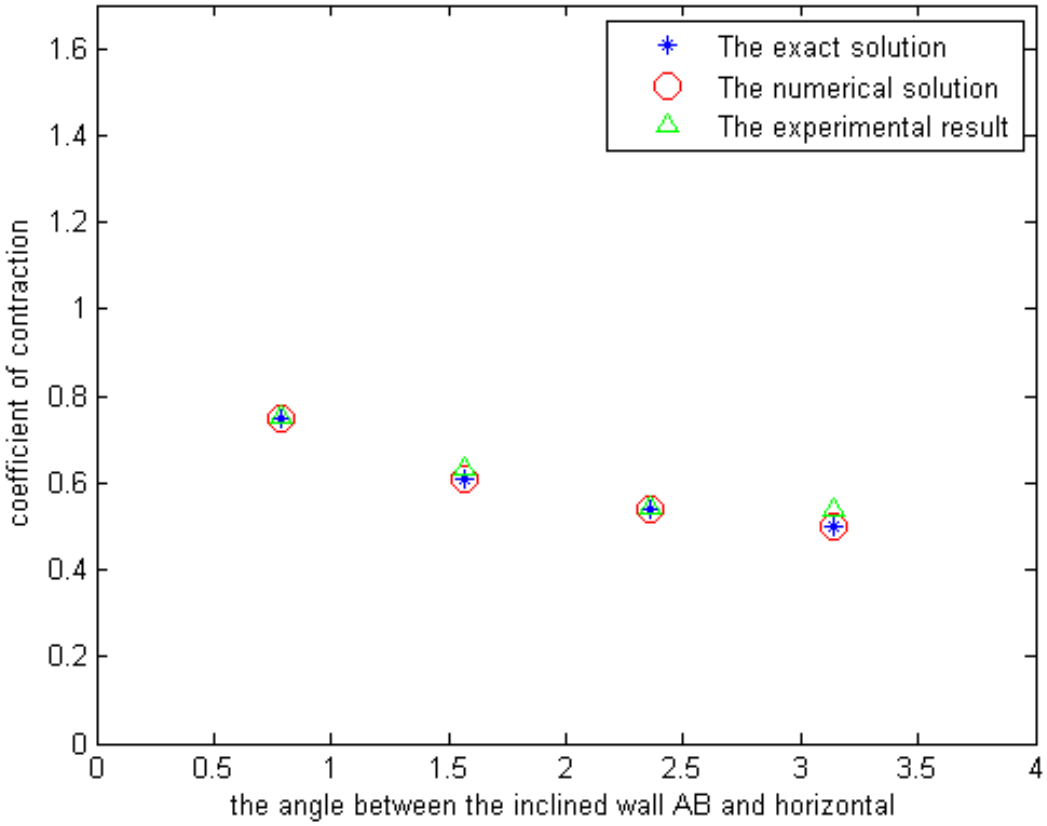

Figure 2.8: Comparision of the analytical values, experimental data and the numerical results of the contraction coefficient C for several value of the inclination angle α

3

Two dimensional free surface flow over a step

The problem of two-dimensional free surface flow of inviscid and incompressible fluid over a step is considered in this chapter. The flow is assumed to be as steady and irrotational, the effect of the surface tension is considered, but the gravity force is neglected. This problem is characterized by the nonlinear condition given by Bernoulli's equation on the unknown free surface, which can be considered as part of the solution. The main purpose of this work is to give an approximate solution of this problem, by using the Hilbert transformation and the perturbation technique; the results are calculated for a large values of the Weber number and small inclination angle of the step values. These results demonstrate that the used method is easily implemented, and provides approximate solutions to these kinds of problems.

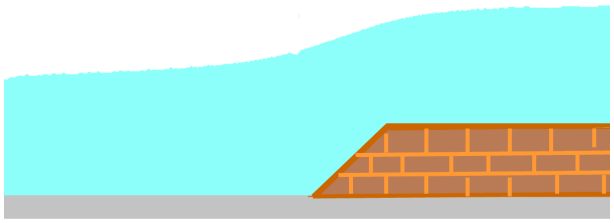

Contents in Brief

3.1 Problem formulation

Let us consider the motion of a two-dimensional flow of a fluid over a step placed in the bottom of a channel. The fluid is assumed to be incompressible, irrotational and inviscid. The effect of gravity is neglected but we take into account the superficial tension effect with small values.

Far upstream and downstream, the flow is proposed as uniform with a constant discharge $U_1h_1 = U_2h_2$, where $U_i, i = 1, 2$ design the velocities and $h_i, i = 1, 2$ the depths of the flow at upstream and downstream respectively, so that the bottom consists of a horizontal walls AB, CD and the inclined wall BC; we note by α and l the inclination angle and the length of the step inclined wall BC and as reference we choose the Cartesian coordinates with the origin placed in the stagnation point B, the x^* axis in the direction of the wall AB and y^* axis directed vertically upward (see Figure 3.1).

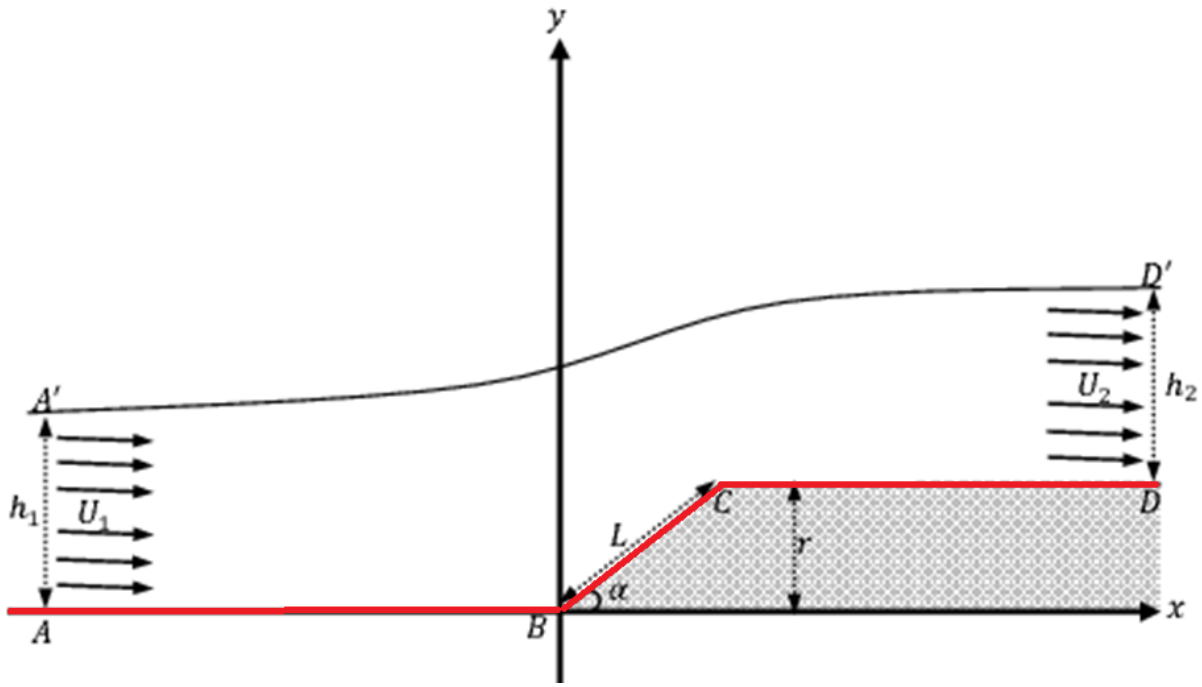

Figure 3.1: Sketch of the flow and of the coordinates. The length of the step is l and the angle between the inclined wall AB and the horizontal is α.

Since the flow is potential, its velocity η^* can be described as the gradient of a scalar function ϕ^* called a potential function, and we can write:

$$\begin{cases} u^* = \dfrac{\partial \phi^*}{\partial x^*}, \\ v^* = \dfrac{\partial \phi^*}{\partial y^*}. \end{cases} \tag{3.1}$$

Here u^* and v^* are the real and imaginary parts, respectively, of a complex velocity η^*.

Next, we introduce the complex analytic function f^* of the variable $z^* = x^* + iy^*$ defined by:

$$f^* = \phi^* + i\psi^*. \tag{3.2}$$

where ψ^* is the stream function which is the conjugate of the potential function.
From (3.1) and (3.2), we obtain:

$$\eta^* = \frac{df^*}{dz^*} = u^* - iv^* = q^* e^{-i\theta}. \tag{3.3}$$

3.1.1 Dimensionless variables

For simplicity, we use the dimensionless analysis, then we choose U_1 and h_1 as the unit velocity and the unit length respectively, and the new non-dimensional variables are:

$$x = \frac{x^*}{h_1},\ \ y = \frac{y^*}{h_1}, u = \frac{u^*}{U_1}, v = \frac{v^*}{U_1}, \phi = \frac{\phi^*}{U_1 h_1} \text{ and } \psi = \frac{\psi^*}{U_1 h_1}. \tag{3.4}$$

On the free-surface$A^{'}D^{'}$, where the pressure is uniform, the Bernoulli's equation (2.2) take the form:

$$\frac{1}{2}q^{*2} + \frac{p^*}{\rho} = \frac{1}{2}U_1^2 + \frac{p_a}{\rho}, \tag{3.5}$$

which implies that

$$\frac{1}{2}q^{*2} + \frac{p^* - p_a}{\rho} = \frac{1}{2}U_1^2. \tag{3.6}$$

Using (1.14), eq (3.6) take the form:

$$\frac{1}{2}\frac{q^{*2}}{U_1^2} + \frac{TK^*}{U_1^2\rho} = 1, \tag{3.7}$$

where K is the curvature in dimensionless ($K = h_1 K^*$), then from (3.4), we get:

$$q^2 + \frac{2TK}{U_1^2 h_1 \rho} = 1. \tag{3.8}$$

Let us introduce the variable ω as a function of two variables q and θ by the relation:

$$\omega = \ln \eta = \ln q - i\theta, \tag{3.9}$$

here ω is called the logarithmic hodograph variable.

From (3.3) and (3.9), we get

$$z = \int e^{-\omega} df. \tag{3.10}$$

Denote the dimensionless step height by r, where

$$r = L \sin \alpha. \tag{3.11}$$

3.1.2 Conformal mapping

Obstacle problem, like other free surface problems, often have complicated geometries in the Cartesian $(x; y)$ - plane (see Figure 3.1). It is shown now that the problem is considerably simplified, if the flow is viewed in the $(\phi; \psi)$ - plane, see Figure 3.2. This means that ϕ and ψ are used as the independent variables instead of x and y.

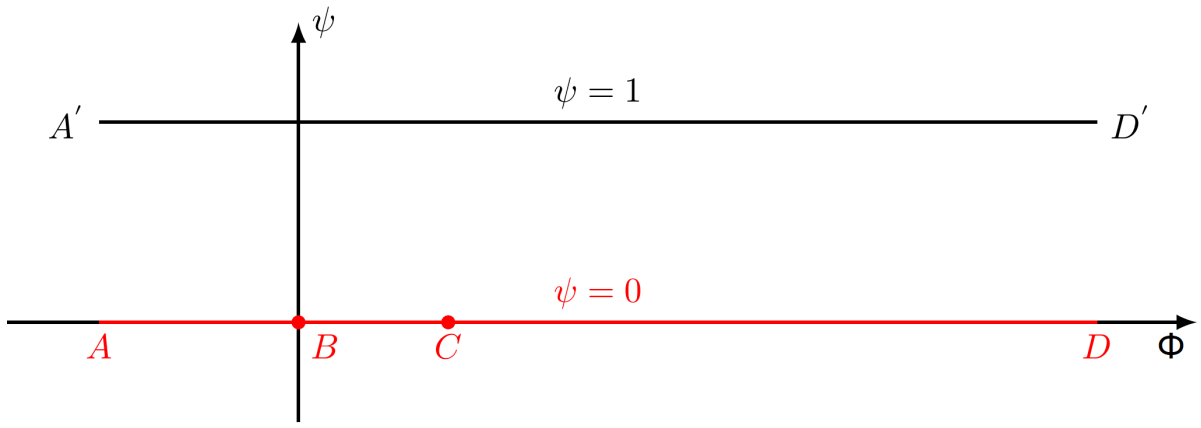

Figure 3.2: The potential f plane.

Table 3.1: Table to show the positioning of the major points of the container problem in the f - plane.

Cartesian plane	f-plane
A	$\psi = 0, \phi = \phi_A = -\infty$
B	$\psi = 0, \phi = \phi_B = 0$
C	$\psi = 0, \phi = \phi_C > 0$
D	$\psi = 0, \phi = \phi_D = \infty$
$A^{'}$	$\psi = 1, \phi = \phi_{A'} = -\infty$
$D^{'}$	$\psi = 1, \phi = \phi_{D'} = \infty$

Without loss of generality, we choose $\phi = 0$ at the point B, $\psi = 1$ on the streamline $A^{'}D^{'}$, and $\psi = 0$ on the streamline $ABCD$(see Figure 3.2).
By using the Schwartz-Christoffel transformation, the strip occupied by the fluid in the potential f-plane in Figure 3.2 is mapped onto the upper half of another auxiliary t-plane (see Figure 3.3). Table 3.1 can now be extended to include the image of the points of interest in the new t - plane. This gives the new table 3.2:

Table 3.2: A table to show the position of the major points of the container problem due to the conformal map.

Cartesian plane	f-plane	t-plane
A	$\psi = 0, \phi = \phi_A = -\infty$	$t = -\infty$
B	$\psi = 0, \phi = \phi_B = 0$	$t = 0$
C	$\psi = 0, \phi = \phi_C > 0$	$t = t_C$
D	$\psi = 0, \phi = \phi_D = \infty$	$t = 1$
$A^{'}$	$\psi = 1, \phi = \phi_{A'} = -\infty$	$t = \infty$
$D^{'}$	$\psi = 1, \phi = \phi_{D'} = \infty$	$t = 1$

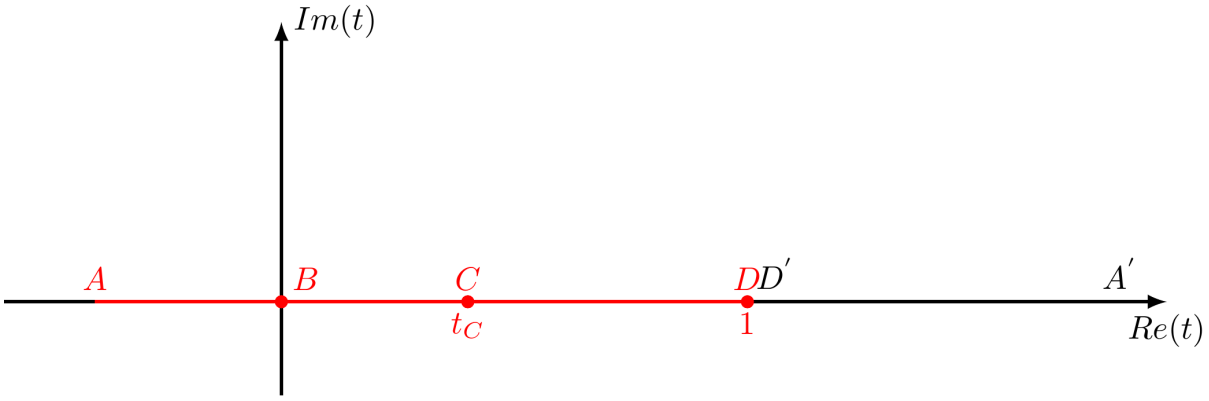

Figure 3.3: The auxiliary t-plane.

The transformation of Schwartz-Christoffel defined by:

$$\frac{df}{dt} = M\,(t-t_1)^{\frac{\alpha_1}{\pi}-1}\,(t-t_2)^{\frac{\alpha_2}{\pi}-1}\ldots(t-t_n)^{\frac{\alpha_n}{\pi}-1}\,. \tag{3.12}$$

where α_i is the interior angles of polygon in the plane f and M is complex constant.
From (3.12) and figures 3.2, 3.3, we get the transformation :

$$f(t) = -\frac{1}{\pi}\ln(1-t)\,. \tag{3.13}$$

On the other hand, we have

$$u^2 + v^2 = q^2\left(\cos^2\theta + \sin^2\theta\right) = q^2, \tag{3.14}$$

then, the curvature K of a streamline, in terms of θ is

$$K = \frac{1}{R} = \mp\left|\frac{\partial\theta}{\partial s}\right| = \mp\left|\frac{\partial\theta}{\partial\phi}\frac{\partial\phi}{\partial s} + \frac{\partial\theta}{\partial\psi}\frac{\partial\psi}{\partial s}\right|, \tag{3.15}$$

since ψ constant along a streamline, $\frac{\partial\psi}{\partial s} = 0$. Furthermore

$$\frac{\partial\phi}{\partial s} = q, \tag{3.16}$$

therefore (3.15) can be simplified to

$$K = \mp q \left| \frac{\partial \theta}{\partial \phi} \right|. \tag{3.17}$$

Substituting (3.14) and (3.17) into (3.8), gives the final form of Bernoulli$'$s equation

$$q^2 + \frac{2}{We} \left| \frac{\partial \theta}{\partial \phi} \right| q = 1, \quad \text{on } A'D', \tag{3.18}$$

where $We = \frac{\rho U_1^2 h_1}{T}$, is the Weber Number.

3.1.3 The Hilbert method

In order to express ω as the single variable t function, we need to use the Hilbert method for the obtained mixed problem of the new plane. Hence, the solution for an analytic function $\chi(t)$ in the upper half-plane (see [33, 42, 43]) is given by

$$\chi(t) = \frac{1}{\pi} p.v. \int_{-\infty}^{+\infty} \frac{Im\left[\chi(s)\right]}{s-t} ds + \sum_{j=0}^{\infty} B_j t^j. \tag{3.19}$$

Where B_j are real constants and $p.v.$ is the principal value of the integral.
The real and imaginary parts of $\omega(t)$ are given by

$$\begin{aligned} Im\left[\omega(t)\right] &= -\theta(t), \\ Re\left[\omega(t)\right] &= \ln q(t). \end{aligned} \tag{3.20}$$

Where

$$\theta(t) = \begin{cases} 0, & t < 0, \\ \alpha, & 0 < t < t_C, \\ 0, & t_C < t < 1, \\ \theta(t), & t > 1. \end{cases} \tag{3.21}$$

To switch the function $\omega(t)$ to $\chi(t)$, we use an auxiliary function $H(t)$

$$H(t) = \begin{cases} \sqrt{1-t}, & t < 1, \\ -i\sqrt{t-1}, & t > 1. \end{cases} \tag{3.22}$$

Using (3.20) and (3.22) , with $\chi(t) = \omega(t)/H(t)$, we get

$$\chi(t) = \left\{ \begin{array}{ll} \frac{\ln q(t) - i\theta(t)}{\sqrt{1-t}}, & t < 1, \\ \frac{\ln q(t) - i\theta(t)}{-i\sqrt{t-1}}, & t > 1. \end{array} \right\} = U(t) + iV(t). \tag{3.23}$$

Next, we examine upstream condition, as we approach point $A^{'}$ along the upper free surface, i.e,

$$\text{as} \quad t \longrightarrow \infty; \quad H(t) = -i\sqrt{t}, \tag{3.24}$$

and

$$\omega(t) \longrightarrow \ln 1 = 0, \tag{3.25}$$

therefore

$$\chi(t) = \frac{\omega(t)}{H(t)} \longrightarrow 0, \tag{3.26}$$

and from (3.19),

$$B_j = 0, j = 0, 1, 2, \ldots. \tag{3.27}$$

Thus, (3.19) take the form

$$\chi(t) = \frac{1}{\pi} p.v. \int_{-\infty}^{+\infty} \frac{Im\left[\chi(s)\right]}{s-t} ds. \tag{3.28}$$

Smith and Lim [41] used an equivalent form for (3.28),

$$U(t) = \frac{1}{\pi} p.v. \int_{-\infty}^{+\infty} \frac{V(s)}{s-t} ds. \tag{3.29}$$

$$V(t) = -\frac{1}{\pi} p.v. \int_{-\infty}^{+\infty} \frac{U(s)}{s-t} ds. \tag{3.30}$$

Along the real axis of the upper half-plane $Im(t) = 0$ (see fig 3.3), the distribution of both real and imaginary parts of $\chi(t)$ can be recapitulated; check Table 3.3. Therefore, $q_j(t), j = 1, 2, 3$, $q_1(t)$being the flow speed in $t < 0$, $q_2(t)$ being the flow speed in $0 < t < t_C$ and $q_3(t)$ being the flow speed in $t_C < t < 1$.

Table 3.3: Distribution of the flow quantities along $Im(t) = 0$

t	$U(t)$	$V(t)$
$t < 0$	$\frac{\ln q_1(t)}{\sqrt{1-t}}$	0
$0 < t < t_C$	$\frac{\ln q_2(t)}{\sqrt{1-t}}$	$\frac{-\alpha}{\sqrt{1-t}}$
$t_C < t < 1$	$\frac{\ln q_3(t)}{\sqrt{1-t}}$	0
$t > 1$	$\frac{\theta(t)}{\sqrt{t-1}}$	$\frac{\ln q(t)}{\sqrt{t-1}}$

Using (3.29), (3.30) and Table 3.3, we obtain the following systems of the nonlinear integral equations:

$$\frac{\theta(t)}{\sqrt{t-1}} = \frac{1}{\pi} p.v. \int_1^{+\infty} \frac{\ln q(s)}{(s-t)\sqrt{s-1}} ds - \frac{1}{\pi} p.v. \int_0^{t_C} \frac{\alpha}{(s-t)\sqrt{1-s}} ds, \qquad t > 1, \tag{3.31}$$

and

$$\frac{\ln(q_j(t))}{\sqrt{1-t}} = -\frac{1}{\pi}p.v.\int_1^{+\infty}\frac{\ln q(s)}{(s-t)\sqrt{s-1}}ds + \frac{1}{\pi}p.v.\int_0^{t_C}\frac{\alpha}{(s-t)\sqrt{1-s}}ds, \tag{3.32}$$

where $p.v.$ is the principal value of the integral and $q_j(t), j = 1, 2, 3$, $q_1(t)$ being the flow speed in $t < 0$, $q_2(t)$ being the flow speed in $0 < t < t_C$ and $q_3(t)$ being the flow speed in $t_C < t < 1$.
By integration, (3.32) take the form:

$$\theta(t) = \frac{\sqrt{t-1}}{\pi}p.v.\int_1^{+\infty}\frac{\ln q(s)}{(s-t)\sqrt{s-1}}ds + \frac{2\alpha}{\pi}\tan^{-1}\left(\frac{(1-\sqrt{1-t_C})\sqrt{t-1}}{t-1+\sqrt{1-t_C}}\right), \quad t > 1. \tag{3.33}$$

Using (3.10) and (3.13), the coordinates of a point on the free-surface can be obtained as follows:

$$z(t) = z_\infty + \int_{+\infty}^{t}\frac{e^{i\theta(s)}}{q(s)}\frac{1}{\pi(1-s)}ds = z_\infty - \frac{1}{\pi}\int_t^{+\infty}\frac{e^{i\theta(s)}}{(1-s)q(s)}ds, \quad t > 1, \tag{3.34}$$

by separating the real and imaginary parts, we get:

$$x(t) = x_\infty - \frac{1}{\pi}\int_t^{+\infty}\frac{\cos\theta(s)}{(1-s)q(s)}ds, \quad t > 1, \tag{3.35}$$

$$y(t) = 1 - \frac{1}{\pi}\int_t^{+\infty}\frac{\sin\theta(s)}{(1-s)q(s)}ds, \quad t > 1, \tag{3.36}$$

and the form of the bottom by:

$$z(t) = z_0 + \frac{1}{\pi}\int_{t_0}^{t}\frac{e^{i\theta(s)}}{(1-s)q(s)}ds, \quad t < 1. \tag{3.37}$$

Along BC we have $\theta = \alpha, q = q_2, t = 0$ and $t = t_C$, the langth L of the inclined plane BC can be obtained by using (3.37):

$$z(t) - z_0 = \frac{1}{\pi}\int_0^{t_C}\frac{e^{i\alpha}}{(1-s)q_2(s)}ds = Le^{i\alpha}. \tag{3.38}$$

Therefore,

$$L = \frac{1}{\pi}\int_0^{t_C}\frac{1}{(1-s)q_2(s)}ds. \tag{3.39}$$

3.2 The approximate equations

In this section, we approximate the nonlinear integral equations (3.18), (3.33), (3.35) and (3.36), when Weber number is large.

Using the first-order Taylor development with respect to $\frac{1}{We}\left|\frac{\partial\theta}{\partial\phi}\right|$, we can give the solution to the Bernoulli equation (3.18) as follows:

$$\begin{aligned} q(t) &= -\frac{1}{We}\left|\frac{\partial\theta}{\partial\phi}\right| + \sqrt{\frac{1}{(We)^2}\left|\frac{\partial\theta}{\partial\phi}\right|^2 + 1} \\ &\approx 1 - \frac{1}{We}\left|\frac{\partial\theta}{\partial\phi}\right| + \frac{1}{2(We)^2}\left|\frac{\partial\theta}{\partial\phi}\right|^2 \\ &\approx 1 - \frac{1}{We}\left|\frac{\partial\theta}{\partial\phi}\right|. \end{aligned} \tag{3.40}$$

On the other hand, we have:

$$\frac{\partial\theta}{\partial\phi} = \frac{\partial\theta}{\partial t}\frac{\partial t}{\partial\phi}, \tag{3.41}$$

then, using the relation of the transformation (3.13), we get:

$$\frac{\partial\theta}{\partial\phi} = \pi(t-1)\frac{\partial\theta}{\partial t}, \quad t > 1. \tag{3.42}$$

Consequently, for $t > 1$ the flow speed (3.40) is approximated by

$$q(t) \approx 1 - \frac{\pi}{We}(t-1)\frac{\partial\theta}{\partial t}(t). \tag{3.43}$$

Which yields

$$\begin{aligned} \ln q(t) &\approx \ln\left(1 - \frac{\pi}{We}(t-1)\frac{\partial\theta}{\partial t}(t)\right) \\ &\approx -\frac{\pi}{We}(t-1)\frac{\partial\theta}{\partial t}(t), \end{aligned} \tag{3.44}$$

and

$$\begin{aligned} \frac{1}{q(t)} &\approx \frac{1}{1 - \frac{\pi}{We}(t-1)\frac{\partial\theta}{\partial t}(t)} \\ &\approx 1 + \frac{\pi}{We}(t-1)\frac{\partial\theta}{\partial t}(t), \end{aligned} \tag{3.45}$$

For small angle α, the change in θ will be minor, thus, allowing us to approximate $\sin\theta$ by $\theta(t)$ and $\cos\theta$ by one.

Using (3.44), we can approximate the angle of the free surface with the horizontal (3.33) by

$$\theta(t) \approx -\frac{\sqrt{t-1}}{We} p.v. \int_1^{+\infty} \frac{(s-1)\frac{\partial\theta}{\partial s}(s)}{(s-t)\sqrt{s-1}} ds + \frac{2\alpha}{\pi}\tan^{-1}\left(\frac{\left(1-\sqrt{1-t_C}\right)\sqrt{t-1}}{t-1+\sqrt{1-t_C}}\right), \qquad t > 1, \tag{3.46}$$

substituting (3.45) into (3.35) and (3.36), and after simplification, the free surface equations take the

form:

$$\begin{aligned} x(t) &\approx x_\infty - \frac{1}{\pi}\int_t^{+\infty} \frac{1}{(1-s)}\left[1+\frac{\pi}{We}(s-1)\frac{\partial\theta}{\partial s}(s)\right]ds \\ &\approx x_\infty - \frac{1}{\pi}\int_t^{+\infty} \frac{1}{(1-s)}ds + \frac{1}{We}\left[\lim_{s\longrightarrow\infty}\theta(s)-\theta(t)\right] \\ &\approx x_\infty - \frac{1}{\pi}\int_t^{+\infty} \frac{1}{(1-s)}ds - \frac{1}{We}\theta(t), \end{aligned} \tag{3.47}$$

and

$$\begin{aligned} y(t) &\approx 1 - \frac{1}{\pi}\int_t^{+\infty} \frac{\theta(s)}{(1-s)}\left[1+\frac{\pi}{We}(s-1)\frac{\partial\theta}{\partial s}(s)\right]ds \\ &\approx 1 - \frac{1}{\pi}\int_t^{+\infty} \frac{\theta(s)}{(1-s)}ds + \frac{1}{2We}\left[\lim_{s\longrightarrow\infty}\theta^2(s)-\theta(t)^2\right] \\ &\approx 1 - \frac{1}{\pi}\int_t^{+\infty} \frac{\theta(s)}{(1-s)}ds - \frac{\theta^2(t)}{2We}. \end{aligned} \tag{3.48}$$

To solve the system of the nonlinear integral equations (3.43), (3.46)-(3.48), we use the Perturbation technique.

3.3 Perturbation technique

We expand $X(t)$ in terms of the small parameter α

$$X(t) = \sum_{k=0}^{\infty} \alpha^k X_k(t). \tag{3.49}$$

Where $X(t)$ stands for $q(t)$, $\theta(t)$, $\theta^{'}(t)$, $x(t)$ and $y(t)$.

3.3.1 Zero-order approximation

This case corresponds to the flow far upstream, which we consider as uniform. Then, the zero-order approximation of the nonlinear integral equations (3.43), (3.46)-(3.48) is presented by:

The velocity of the flow

$$q_0(t) \approx 1 - \frac{\pi}{We}(t-1)\theta_0'(t) \approx 1. \tag{3.50}$$

The velocity direction relative to the horizontal

$$\theta_0(t) \approx -\frac{\sqrt{t-1}}{We} p.v. \int_1^{+\infty} \frac{(s-1)\theta_0'(s)}{(s-t)\sqrt{s-1}} ds \approx 0, \tag{3.51}$$

The free streamline equations:

$$\begin{aligned} x_0(t) &\approx x_\infty - \frac{1}{\pi}\int_t^{+\infty} \frac{1}{(1-s)} ds - \frac{1}{We}\theta_0(t) \\ &\approx x_\infty - \frac{1}{\pi}\int_t^{+\infty} \frac{1}{(1-s)} ds. \end{aligned} \tag{3.52}$$

and

$$y_0(t) \approx 1 - \frac{1}{\pi}\int_t^{+\infty} \frac{\theta_0(s)}{(1-s)} ds - \frac{\theta_0^2(t)}{2We} \approx 1. \tag{3.53}$$

On the other hand, at point B when $x = 0, t = 0$ and from (3.37) we have the formula:

$$x(0) = 0 \approx x_\infty - \frac{1}{\pi} p.v. \int_0^{+\infty} \frac{1}{(1-s)} ds. \tag{3.54}$$

Therefore

$$x_\infty \approx \frac{1}{\pi} p.v. \int_0^{+\infty} \frac{1}{(1-s)} ds, \tag{3.55}$$

hence, equation (3.52) take the form:

$$\begin{aligned} x_0(t) &\approx \frac{1}{\pi} p.v. \int_0^{+\infty} \frac{1}{(1-s)} ds - \frac{1}{\pi} p.v. \int_t^{+\infty} \frac{1}{(1-s)} ds \\ &\approx \frac{1}{\pi} p.v. \int_0^{t} \frac{1}{(1-s)} ds \\ &\approx -\frac{1}{\pi}\ln(t-1). \end{aligned} \tag{3.56}$$

3.3.2 First-order approximation

Now, we find the first-order approximation of the nonlinear integral equations (3.43), (3.46)-(3.48) by using development (3.49) and the zero-order approximation of the system.

Using the development (3.49), we can write

$$X_1(t) \approx \frac{X(t) - X_0(t)}{\alpha}. \tag{3.57}$$

Substituting (3.43) and (3.50) into (3.57) yields

$$\begin{aligned} q_1(t) &\approx \frac{\frac{\pi}{We}(t-1)\theta^{'}(t)}{\alpha} \\ &\approx \frac{\pi}{\alpha We}(t-1)\left(\theta_0^{'}(t)+\alpha\theta_1^{'}(t)\right). \end{aligned} \tag{3.58}$$

But we know $\theta_0^{'}(t)=0$. Thus

$$q_1(t) \approx \frac{\pi}{We}(t-1)\theta_1^{'}(t). \tag{3.59}$$

Then, from (3.46), (3.51) and (3.57) we get:

$$\theta_1(t) \approx -\frac{\sqrt{t-1}}{\alpha We}\int_1^{+\infty}\frac{(s-1)\theta^{'}(s)}{(s-t)\sqrt{s-1}}ds+\frac{2}{\pi}\tan^{-1}\left(\frac{\left(1-\sqrt{1-t_C}\right)\sqrt{t-1}}{t-1+\sqrt{1-t_C}}\right), \tag{3.60}$$

using (3.39), equation (3.60) take the form:

$$\begin{aligned} \theta_1(t) &\approx -\frac{\sqrt{t-1}}{\alpha We}\int_1^{+\infty}\frac{(s-1)\left(\theta_0^{'}+\alpha\theta_1^{'}\right)(s)}{(s-t)\sqrt{s-1}}ds+\frac{2}{\pi}\tan^{-1}\left(\frac{\left(1-\sqrt{1-t_C}\right)\sqrt{t-1}}{t-1+\sqrt{1-t_C}}\right), \\ &\approx -\frac{\sqrt{t-1}}{We}\int_1^{+\infty}\frac{(s-1)\theta_1^{'}(s)}{(s-t)\sqrt{s-1}}ds+\frac{2}{\pi}\tan^{-1}\left(\frac{\left(1-\sqrt{1-t_C}\right)\sqrt{t-1}}{t-1+\sqrt{1-t_C}}\right). \end{aligned} \tag{3.61}$$

On the other hand, from (3.47), (3.54), (3.55) and (3.57), we find:

$$\begin{aligned} x_1(t) &\approx -\frac{1}{\alpha We}\theta(t) \\ &\approx -\frac{1}{\alpha We}\left(\theta_0(t)+\alpha\theta_1(t)\right) \\ &\approx -\frac{1}{We}\theta_1(t), \end{aligned} \tag{3.62}$$

and by using (3.48), (3.53) and (3.57), we get:

$$\begin{aligned} y_1(t) &\approx -\frac{1}{\pi}\int_t^{+\infty}\frac{\theta(s)}{(1-s)}ds-\frac{\theta^2(t)}{2We} \\ &\approx -\frac{1}{\alpha\pi}\int_t^{+\infty}\frac{\theta_0(s)+\alpha\theta_1(s)}{(1-s)}ds-\frac{1}{2\alpha We}\left(\theta_0^2(t)+\alpha^2\theta_1^2(t)+2\alpha\theta_0(t)\theta_1(t)\right) \\ &\approx -\frac{1}{\pi}\int_t^{+\infty}\frac{\theta_1(s)}{(1-s)}ds. \end{aligned} \tag{3.63}$$

From (3.60), and for a very large value of the Weber number We, we may neglect the first term with respect to the second one. Thus, we get the first-order approximation of the velocity direction relative to the horizontal axis:

$$\theta_1(t)=\frac{2}{\pi}\tan^{-1}\left(\frac{\left(1-\sqrt{1-t_C}\right)\sqrt{t-1}}{t-1+\sqrt{1-t_C}}\right). \tag{3.64}$$

Substituting (3.64) into (3.62) and (3.63) and carrying out the integration, one finds

$$x_1(t) \approx -\frac{2}{\pi We}\tan^{-1}\left(\frac{(1-\sqrt{1-t_C})\sqrt{t-1}}{t-1+\sqrt{1-t_C}}\right), \tag{3.65}$$

and

$$y_1(t) \approx \frac{4-4\sqrt{1-t_C}}{\pi^2\sqrt[4]{1-t_C}}\tan^{-1}\frac{\sqrt[4]{1-t_C}}{\sqrt{t-1}}. \tag{3.66}$$

Using results (3.53),(3.53), (3.65)-(3.66) and expanding (3.49) enables finding the approximate solutions of the free-surface flow:

$$x(t) \approx -\frac{1}{\pi}\ln(t-1) - \frac{2\alpha}{\pi We}\tan^{-1}\left(\frac{(1-\sqrt{1-t_C})\sqrt{t-1}}{t-1+\sqrt{1-t_C}}\right), \tag{3.67}$$

and

$$y(t) \approx 1+\alpha\frac{4-4\sqrt{1-t_C}}{\pi^2\sqrt[4]{1-t_C}}\tan^{-1}\frac{\sqrt[4]{1-t_C}}{\sqrt{t-1}}. \tag{3.68}$$

3.4 Results

The obtained approximate scheme is used to calculate the solutions and the free surface profiles for a fixed values of the inclination angle $\alpha = \pi/6$, the step height $r = 0.7$, the point $t = 0.9877$ and different values of Weber number.

Figure 3.4 presents the variation of the free surface shape with respect to the Weber number.
As shown in figure 3.4, if the Weber number decreases, the curvature of the free surface is decreased, because this is one of the most important characteristic property of the surface tension effects.

Figure 3.5 illustrates the free-surface profiles for different angles α, for a fixed values of the step height $r = 0.6$ and the Weber number $We = 10^4$. As we can see from Figure 3.5, if the angle value decreases, the elevation of the free surface at the downstream increases.
Table 3.4 presents some values of the positions of the point t_C and the length of the step L for different values of the angle.

For a fixed values of the angle $\alpha = \pi/8$ and the Weber number $We = 100$, the results of the position of

Table 3.4: Some t_C values for different values of the of the angle α

α	l	t_c
$\pi/6$	1.200	0.9769
$\pi/8$	1.5679	0.9927
$\pi/10$	1.9416	0.9978
$\pi/12$	2.3182	0.9993

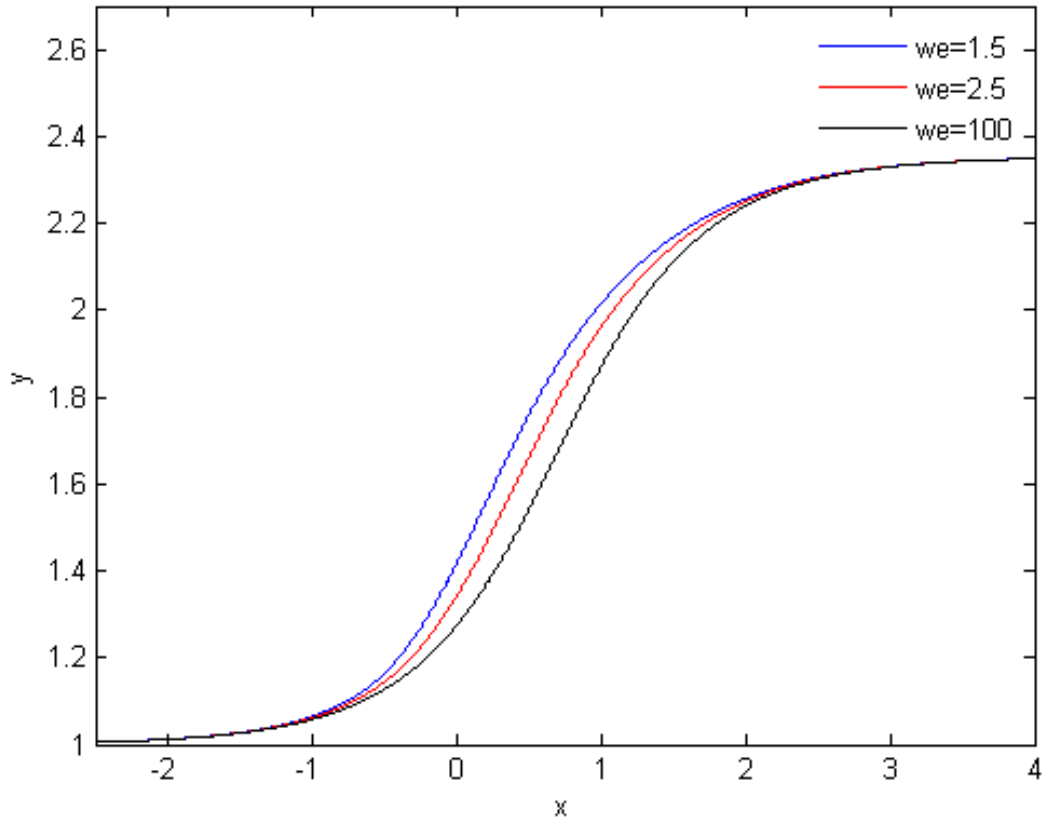

Figure 3.4: Effect of the weber number on the free-surface profile for the angle $\alpha = \pi/6$, and the step height $r = 0.7$

the point t_C for different values of the step height r are presented in table 3.5:

As the values of the step height increase, the flow velocity reduces, which leads to increasing also the elevation of the free surface at the downstream, as shown in Figure 3.6.

Finally, in this chapter, the first order approximate method is employed to solve the nonlinear problem of steady free-surface flow over a step bottom. The results show that the used method is easy to implement, and provides solutions to these kinds of problems.

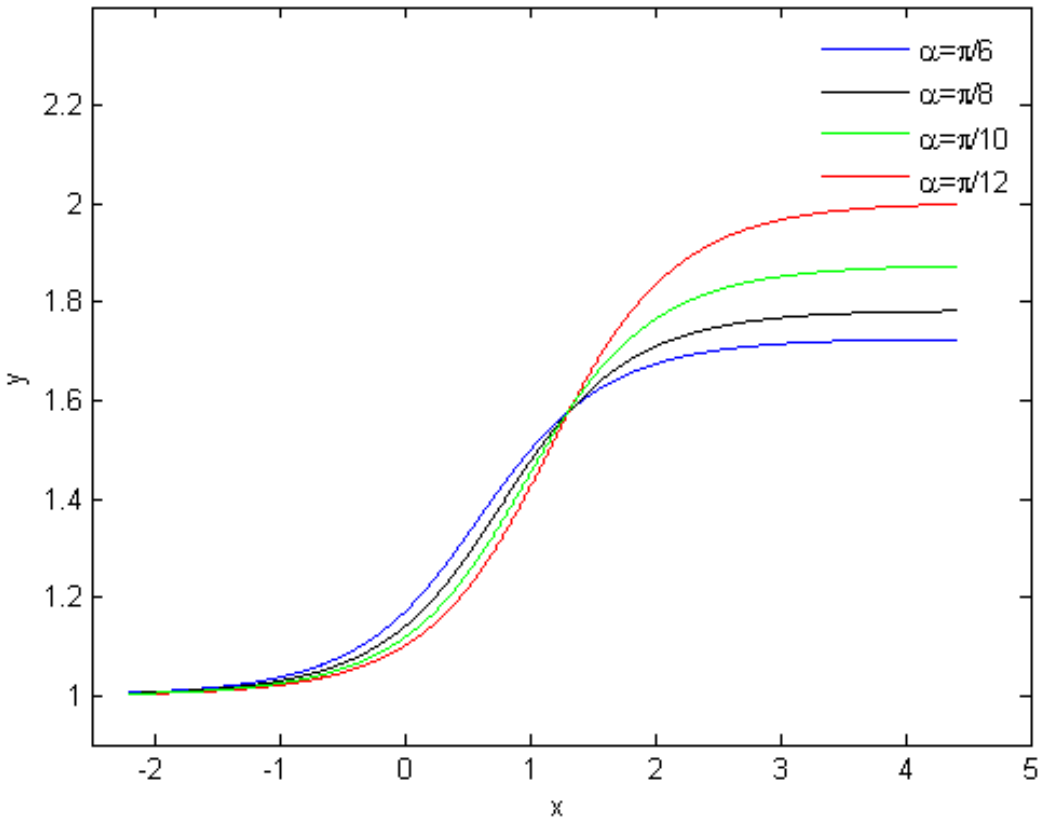

Figure 3.5: Effect of the inclination angle α on the free-surface profile for $We = 10^4$ and $r = 0.6$

Table 3.5: Some t_C values for different values of the ramp height r

r	l	t_C
0.2	0.5226	0.8064
0.3	0.7839	0.9148
0.4	1.0453	0.9625
0.5	1.3066	0.9835
0.7	1.8292	0.9968

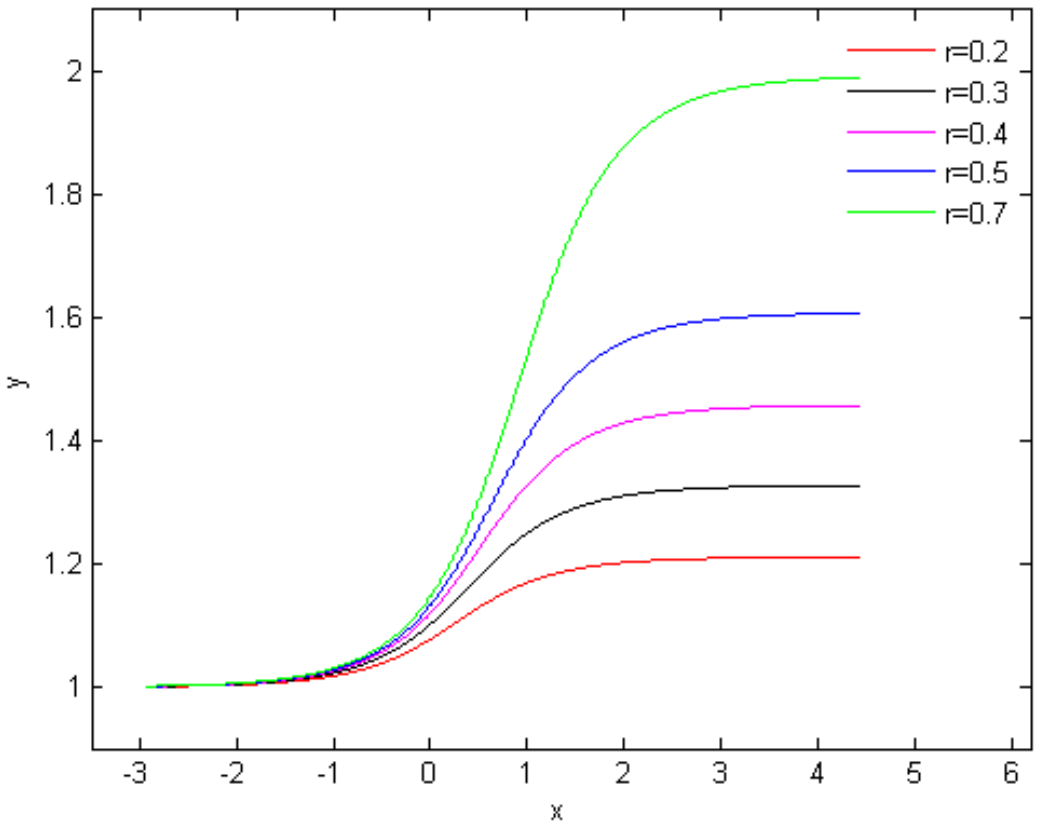

Figure 3.6: Effect of the step height$r$ on the free-surface profile for $We = 100$ and $\alpha = \pi/8$

4

Free surface flow over a triangular obstacle

The main objective of this work was to determine the shape of the two-dimensional free-surface flow over a triangular obstacle placed over a semi infinite channel's bottom. The fluid possesses an inviscid and an incompressible nature, while the flow is considered irrotational and steady. Furthermore, we considered the impact of the superficial tension while neglecting the gravity's. Employing the Hilbert transformation in tandem with the perturbation technique provides an approximate solution to the given problem with a large Weber number and slight variations of the triangle angle values. The unknown free-surface profiles are established for these variations of the triangle configuration and various Weber numbers. The obtained results reveal the simplicity of the used method and provide approximate solutions for problems of the same type.

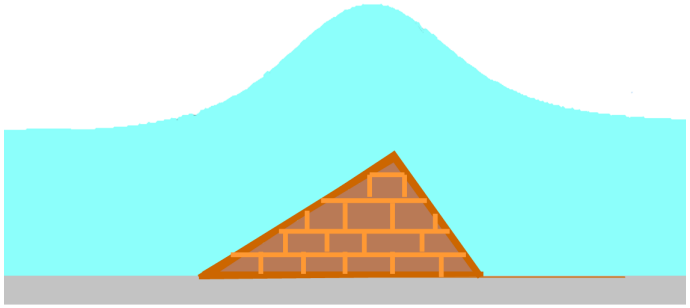

Contents in Brief

4.1 Formulation of the Problem

Initially, we consider the motion of a two-dimensional flow of a fluid crossing a triangular obstacle. α and β denote the two interior angles of the triangle on the horizontal axis, while l and d denote the length of the walls BC and CD respectively. We assume that the fluid is incompressible and inviscid in nature while its flow is irrotational. The effect of gravity is neglected, while the superficial tension effect is taken into consideration. Far upstream and downstream, we consider the flow to be uniform with velocities U_1, U_2 and the constant heights h_1 and h_2 respectively, so that the bottom consists of the horizontal walls AB and DE and the triangle BCD. Hence, we define the Cartesian coordinates with the origin in point B(see figure 4.1).

In order to define the dimensionless variables, we denote that U_1 is the unit of velocity and h_1 is the

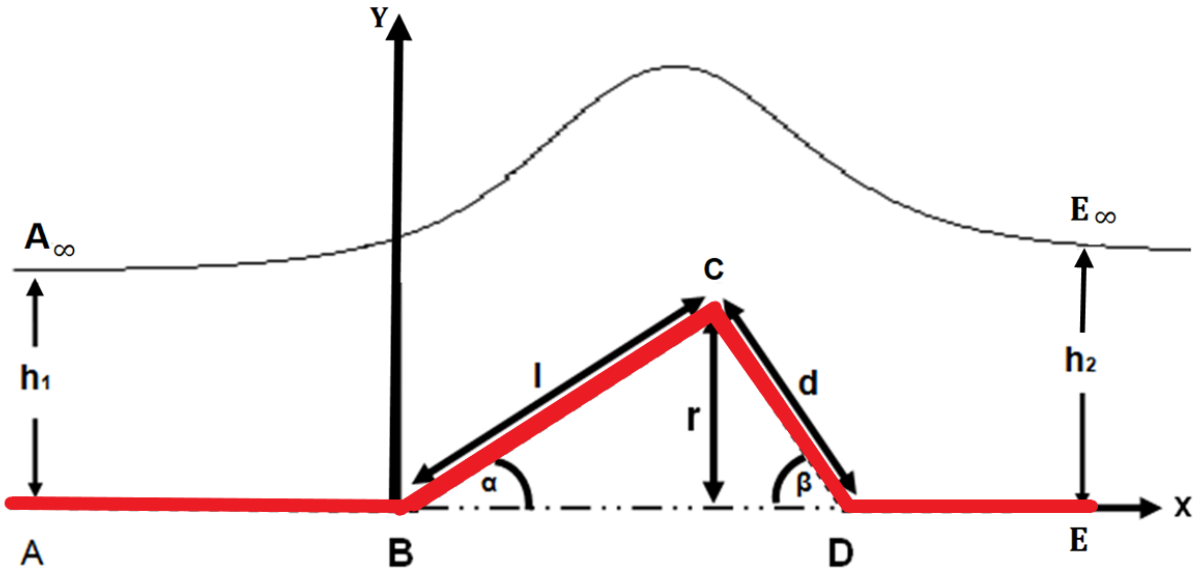

Figure 4.1: A sketch that illustrates the flow and the coordinates. The figure is an actual computed surface profile for $\alpha = \pi/8, \beta = \pi/6, We = 200$ and $r = 0.5$.

unit of length. We also have the complex potential $f(z) = \phi(z) + i\psi(z)$, where ϕ represents the potential function, ψ defines the stream function (wherein ϕ and ψ are Laplace equation's conjugate solutions), and $f(z)$ represents an analytic function of z within the region of flow, with the complex conjugate velocity

$$\eta = \frac{df(z)}{dz} = u - iv = qe^{-i\theta}. \tag{4.1}$$

Let

$$\omega = \ln \eta = \ln q - i\theta, \tag{4.2}$$

we call ω the variable of the logarithmic hodograph.

Then, from (4.1) and (4.2) we get

$$z = \int e^{-\omega} df. \tag{4.3}$$

Without a loss of generality, we take $\phi = 0$ at a point B, $\psi = 1$ on the streamline $A_\infty E_\infty$, and $\psi = 0$ on the streamline $ABCDE$ (see figure 4.2). We denote the dimensionless height of the triangle by r, where

$$r = l\sin(\alpha) = d\sin(\beta). \tag{4.4}$$

From (3.18), when the pressure is uniform on the free-surface, the dimensionless form of Bernoulli equation is given by:

$$q^2 + \frac{2}{We}\left|\frac{\partial\theta}{\partial\phi}\right| q = 1, \tag{4.5}$$

where We is the dimensional parameter, known as the Weber number, and which is defined by

$$We = \frac{\rho U_1^2 h_1}{T}, \tag{4.6}$$

T is the surface tension, and ρ is the density of the fluid.

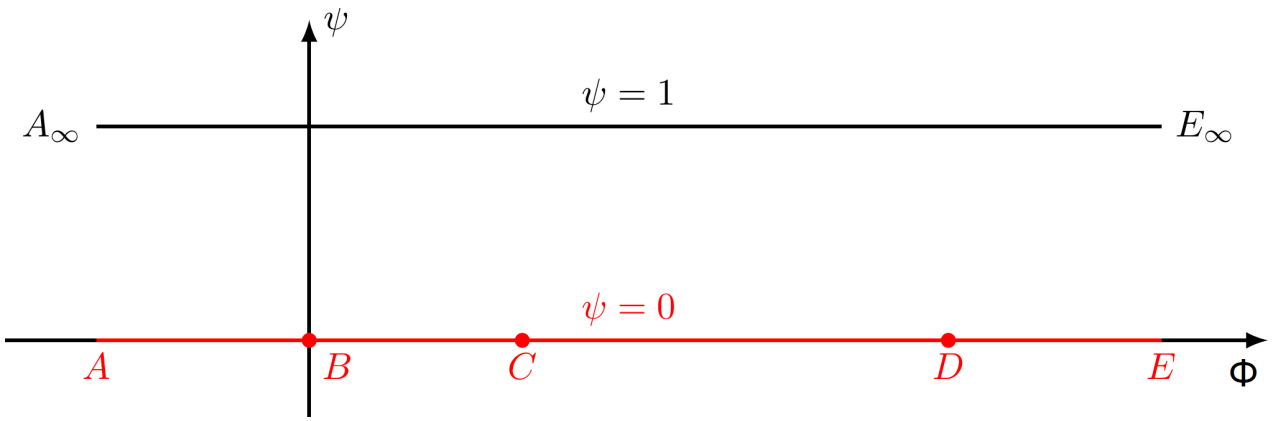

Figure 4.2: The potential f plane

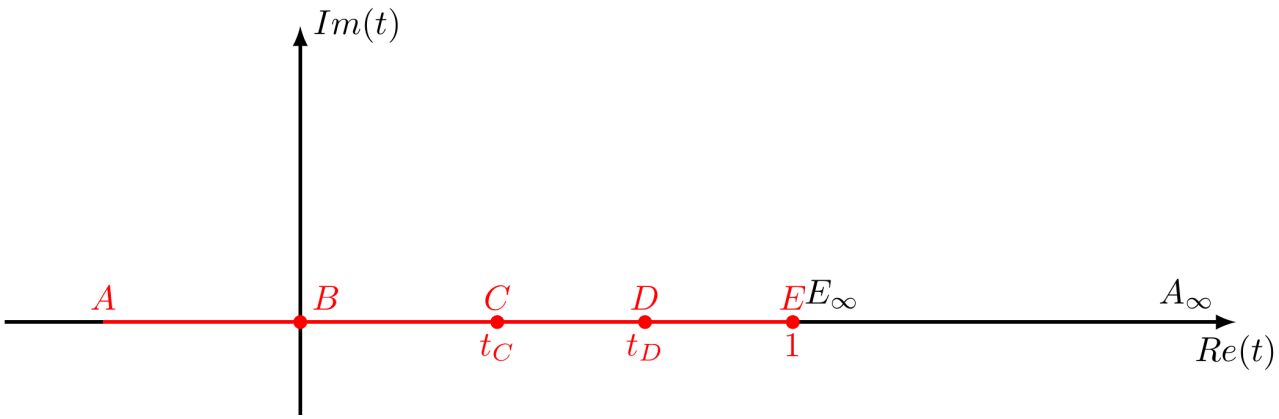

Figure 4.3: The auxiliary t plane

Mapping the potential plane f (in Figure 4.2) onto the upper half of the auxiliary t-plane is achieved through applying Schwartz-Christoffel transformation, see Figure 4.3.

The used transformation is:

$$f(t) = -\frac{1}{\pi}\ln(1-t). \tag{4.7}$$

Expressing ω as t function's single variable requires the use of the Hilbert method for the obtained mixed problem of the new plane. Hence, we give the analytic function X(t) solution in the upper half-plane (see [46]) by:

$$\chi(t) = \frac{1}{\pi} p.v. \int_{-\infty}^{+\infty} \frac{Im[\chi(s)]}{s-t} ds + \sum_{j=0}^{\infty} B_j t^j. \tag{4.8}$$

Where B_j denotes real constants and $p.v.$ is the principal value of the integral.
The real and imaginary parts of $\omega(t)$ are given by

$$\begin{aligned} Im[\omega(t)] &= -\theta(t). \\ Re[\omega(t)] &= \ln q(t). \end{aligned} \tag{4.9}$$

Where

$$\theta(t) = \begin{cases} 0, & t < 0, \\ \alpha, & 0 < t < t_C, \\ -\beta, & t_C < t < t_D, \\ 0, & t_D < t < 1, \\ \theta(t), & t > 1. \end{cases} \tag{4.10}$$

To switch the function $\omega(t)$ to $\chi(t)$, an auxiliary function $H(t)$ is used

$$H(t) = \begin{cases} \sqrt{1-t}, & t < 1, \\ -i\sqrt{t-1}, & t > 1. \end{cases} \tag{4.11}$$

Using (4.9) and (4.11) , with $\chi(t) = \omega(t)/H(t)$, we get

$$\chi(t) = \left\{ \begin{array}{ll} \frac{\ln q(t) - i\theta(t)}{\sqrt{1-t}}, & t < 1, \\ \frac{\ln q(t) - i\theta(t)}{-i\sqrt{t-1}}, & t > 1. \end{array} \right\} = U(t) + iV(t). \tag{4.12}$$

Examining upstream condition, we obtain the following:

$$B_j = 0, j = 0, 1, 2, \ldots.$$

Hence

$$\chi(t) = \frac{1}{\pi} p.v. \int_{-\infty}^{+\infty} \frac{Im[\chi(s)]}{s-t} ds. \tag{4.13}$$

Smith and Lim [41] used an equivalent form for (4.13), we obtain

$$U(t) = \frac{1}{\pi} p.v. \int_{-\infty}^{+\infty} \frac{V(s)}{s-t} ds. \tag{4.14}$$

$$V(t) = -\frac{1}{\pi} p.v. \int_{-\infty}^{+\infty} \frac{U(s)}{s-t} ds. \tag{4.15}$$

Throughout the upper half-plane's real axis $Im(t) = 0$ (see fig 4.3), the distribution of both real and imaginary parts of $\chi(t)$ can be recapitulated; check Table 4.1.

Table 4.1: Flow Quantities' distribution across $Im(t) = 0$

t	$U(t)$	$V(t)$
$t < 0$	$\frac{\ln q_1(t)}{\sqrt{1-t}}$	0
$0 < t < t_C$	$\frac{\ln q_2(t)}{\sqrt{1-t}}$	$\frac{-\alpha}{\sqrt{1-t}}$
$t_C < t < t_D$	$\frac{\ln q_3(t)}{\sqrt{1-t}}$	$\frac{\beta}{\sqrt{1-t}}$
$t_D < t < 1$	$\frac{\ln q_4(t)}{\sqrt{1-t}}$	0
$t > 1$	$\frac{\theta(t)}{\sqrt{t-1}}$	$\frac{\ln q(t)}{\sqrt{t-1}}$

Using (4.14), (4.15) and Table 4.1 , we obtain the following systems of the nonlinear integral equations:

$$\begin{aligned}\theta(t) &= \frac{\sqrt{t-1}}{\pi} p.v. \int_1^{+\infty} \frac{\ln q(s)}{(s-t)\sqrt{s-1}} ds + \frac{2\alpha}{\pi} \tan^{-1}\left(\frac{\left(1-\sqrt{1-t_C}\right)\sqrt{t-1}}{t-1+\sqrt{1-t_C}}\right) \\ &- \frac{2\beta}{\pi} \tan^{-1}\left(\frac{\left(\sqrt{1-t_C}-\sqrt{1-t_D}\right)\sqrt{t-1}}{t-1+\sqrt{(1-t_C)\,(1-t_D)}}\right), \quad t > 1, \end{aligned} \tag{4.16}$$

$$\begin{aligned}\ln(q_j(t)) &= \frac{\sqrt{1-t}}{\pi} p.v. \int_1^{+\infty} \frac{\ln(q(s))}{(s-t)\sqrt{s-1}} ds - \alpha \frac{\sqrt{1-t}}{\pi} \int_0^{t_C} \frac{ds}{(s-t)\sqrt{1-s}} \\ &+ \beta \frac{\sqrt{1-t}}{\pi} \int_{t_C}^{t_D} \frac{ds}{(s-t)\sqrt{1-s}}, \end{aligned} \tag{4.17}$$

where $j = 1, 2, 3, 4$, $q_1(t)$ is defined in $t < 0$, $q_2(t)$ in $0 < t < t_C$, $q_3(t)$ in $t_C < t < t_D$ and $q_4(t)$ in $t_D < t < 1$.
Using (4.3) and (4.7) and separating the real and imaginary parts, we get the free-surface shape:

$$x(t) = x_\infty - \frac{1}{\pi} \int_t^{+\infty} \frac{\cos\theta(s)}{(1-s)q(s)} ds, \quad t > 1, \tag{4.18}$$

and

$$y(t) = 1 - \frac{1}{\pi} \int_t^{+\infty} \frac{\sin\theta(s)}{(1-s)q(s)} ds, \quad t > 1. \tag{4.19}$$

The additional conditions along the solid boundaries include:

$$z(t_0) = z_0 + \frac{1}{\pi} \int_{t_0}^{t} \frac{e^{i\theta(s)}}{(1-s)q(s)} ds, \quad t < 1. \tag{4.20}$$

On BC, we have $\theta = \alpha$ and $q = q_2$, with $z = le^{i\alpha}$. Therefore

$$l = \frac{1}{\pi} \int_0^{t_C} \frac{1}{(1-s)q_2(s)} ds. \tag{4.21}$$

And on CD, we have $\theta = -\beta$ and $q = q_3$, with $z = de^{-i\beta}$. Therefore

$$d = \frac{1}{\pi}\int_{t_C}^{t_D} \frac{1}{(1-s)q_3(s)} ds. \tag{4.22}$$

4.2 Approach solution

4.2.1 Expression of the boundary-value problem in an approximate form

Firstly, for solved this problem, we approximate the nonlinear integral equations (4.5), (4.16), (4.18) and (4.19) with a large Weber number.

By using first-order Taylor development with respect to $\frac{1}{We}\left|\frac{\partial\theta}{\partial\phi}\right|$, the solution of Bernoulli equation (4.5) is given by

$$q(t) \approx 1 - \frac{1}{We}\left|\frac{\partial\theta}{\partial\phi}\right|. \tag{4.23}$$

Using relation (4.7), we obtain:

$$\frac{\partial\theta}{\partial\phi} = \frac{\partial\theta}{\partial t}\frac{\partial t}{\partial\phi} = \pi(t-1)\frac{\partial\theta}{\partial t}, \quad t > 1. \tag{4.24}$$

Consequently, for $t > 1$ we obtain:

$$q(t) \approx 1 - \frac{\pi}{We}(t-1)\frac{\partial\theta}{\partial t}(t), \tag{4.25}$$

which yields

$$\ln q(t) \approx -\frac{\pi}{We}(t-1)\frac{\partial\theta}{\partial t}(t), \quad \text{and} \quad \frac{1}{q(t)} \approx 1 + \frac{\pi}{We}(t-1)\frac{\partial\theta}{\partial t}(t). \tag{4.26}$$

For the small angles α and β, the change in θ will be insignificant. An approximate $\sin\theta$ is defined as $\theta(t)$ and $\cos\theta$ is approximated by one.
Using (4.26), we can approximate the free-surface's angle with the horizontal (4.16) by:

$$\begin{aligned}\theta(t) \approx & -\frac{\sqrt{t-1}}{We} p.v. \int_1^{+\infty} \frac{\sqrt{s-1}}{(s-t)}\frac{\partial\theta}{\partial s}(s)ds + \frac{2\alpha}{\pi}\tan^{-1}\left(\frac{\left(1-\sqrt{1-t_C}\right)\sqrt{t-1}}{t-1+\sqrt{1-t_C}}\right) \\ & - \frac{2\beta}{\pi}\tan^{-1}\left(\frac{\left(\sqrt{1-t_C}-\sqrt{1-t_D}\right)\sqrt{t-1}}{t-1+\sqrt{(1-t_C)(1-t_D)}}\right),\end{aligned} \tag{4.27}$$

with the substitution of (4.26) into (4.18) and (4.19), and after a simplification, the free surface equations take the following forms:

as for the real part:

$$x(t) \approx x_\infty - \frac{1}{\pi}\int_t^{+\infty} \frac{1}{(1-s)} ds - \frac{1}{We}\theta(t), \tag{4.28}$$

the imaginary is given by:

$$y(t) \approx 1 - \frac{1}{\pi}\int_t^{+\infty} \frac{\theta(s)}{(1-s)} ds - \frac{\theta^2(t)}{2We}. \tag{4.29}$$

Along the solid boundaries BC and CD, we can approximate q_j by one, (4.21) and (4.22) become

$$l \approx -\frac{1}{\pi}\ln(1-t_C), \tag{4.30}$$

$$d \approx -\frac{1}{\pi}\ln\left(\frac{1-t_D}{1-t_C}\right). \tag{4.31}$$

The system of the nonlinear integral equations (4.25), (4.27), (4.28) and (4.29) can be solved using the perturbation technique.

4.2.2 Perturbation method

$X(t)$ is expanded in terms of the small parameters α and β

$$X(t) = \sum_{k=0}^{\infty} \alpha^k X_{k,\alpha}(t) + \beta^k X_{k,\beta}(t). \tag{4.32}$$

Where $X(t)$ stands for $q(t)$, $\theta(t)$, $\theta^{'}(t)$, $x(t)$ and $y(t)$.

4.2.2.1 Zero-order approximation

This case corresponds to the flow far upstream, which we consider to be uniform. Thus, the zero-order approximation of the nonlinear integral equations (4.25),(4.27)- (4.29) is presented as follows:
The velocity of the flow

$$q_0(t) \approx 1 - \frac{\pi}{We}(t-1)\theta_0'(t) \approx 1. \tag{4.33}$$

Then, velocity's relative direction to the horizontal axis

$$\theta_0(t) \approx -\frac{\sqrt{t-1}}{We} p.v. \int_1^{+\infty} \frac{(s-1)\theta_0'(s)}{(s-t)\sqrt{s-1}} ds \approx 0. \tag{4.34}$$

And the free streamline equations are:

$$\begin{aligned} x_0(t) &\approx x_\infty - \frac{1}{\pi}\int_t^{+\infty} \frac{1}{(1-s)} ds - \frac{1}{We}\theta_0(t) \\ &\approx x_\infty - \frac{1}{\pi}\int_t^{+\infty} \frac{1}{(1-s)} ds. \end{aligned} \tag{4.35}$$

and

$$y_0(t) \approx 1 - \frac{1}{\pi}\int_t^{+\infty} \frac{\theta_0(s)}{(1-s)} ds - \frac{\theta_0^2(t)}{2We} \approx 1. \tag{4.36}$$

On the other hand, we have the formula:

$$x_\infty \approx \frac{1}{\pi} p.v. \int_0^{+\infty} \frac{1}{(1-s)} ds, \tag{4.37}$$

hence

$$x_0(t) \approx -\frac{1}{\pi}\ln(t-1). \tag{4.38}$$

4.2.2.2 First-order approximation

Now, we find the first-order approximation of the nonlinear integral equations (4.25),(4.27)-(4.29) by using development (4.32) and the zero-order approximation of the system.

Using the development (4.32), we can write

$$\begin{aligned} X_{1,\alpha}(t) &\approx \frac{X(t) - X_0(t)}{\alpha}, \\ X_{1,\beta}(t) &\approx \frac{X(t) - X_0(t)}{\beta}. \end{aligned} \tag{4.39}$$

Substituting (4.25) and (4.33) into (4.39) yields

$$\begin{aligned} q_{1,\alpha}(t) &\approx -\frac{\pi}{We}(t-1)\theta'_{1,\alpha}(t), \\ q_{1,\beta}(t) &\approx -\frac{\pi}{We}(t-1)\theta'_{1,\beta}(t). \end{aligned} \tag{4.40}$$

Using (4.27), (4.34) and (4.39), we obtain

$$\begin{aligned} \theta_{1,\alpha}(t) &\approx -\frac{\sqrt{t-1}}{We} p.v. \int_1^{+\infty} \frac{\sqrt{s-1}\theta'_{1,\alpha}(s)}{(s-t)} ds + \frac{2}{\pi}\tan^{-1}\left(\frac{\left(1-\sqrt{1-t_C}\right)\sqrt{t-1}}{t-1+\sqrt{1-t_C}}\right), \\ \theta_{1,\beta}(t) &\approx -\frac{\sqrt{t-1}}{We} p.v. \int_1^{+\infty} \frac{\sqrt{s-1}\theta'_{1,\beta}(s)}{(s-t)} ds - \frac{2}{\pi}\tan^{-1}\left(\frac{\left(\sqrt{1-t_C}-\sqrt{1-t_D}\right)\sqrt{t-1}}{t-1+\sqrt{(1-t_C)(1-t_D)}}\right). \end{aligned} \tag{4.41}$$

On the other hand, from (4.28), (4.38) and (4.39), we find

$$\begin{aligned} x_{1,\alpha}(t) &\approx -\frac{1}{We}\theta_{1,\alpha}(t), \\ x_{1,\beta}(t) &\approx -\frac{1}{We}\theta_{1,\beta}(t). \end{aligned} \tag{4.42}$$

Then, using (4.29), (4.36) and (4.39), we have

$$\begin{aligned} y_{1,\alpha}(t) &\approx -\frac{1}{\pi}\int_t^{+\infty}\frac{\theta_{1,\alpha}(s)}{(1-s)}ds, \\ y_{1,\beta}(t) &\approx -\frac{1}{\pi}\int_t^{+\infty}\frac{\theta_{1,\beta}(s)}{(1-s)}ds. \end{aligned} \tag{4.43}$$

4.2.3 Solution of the boundary-value problem

From (4.41), and for a very large value of the Weber number We, the first term may be neglected with respect to the second one so that we get:

$$\begin{aligned} \theta_{1,\alpha}(t) &\approx \frac{2}{\pi}\tan^{-1}\left(\frac{\left(1-\sqrt{1-t_C}\right)\sqrt{t-1}}{t-1+\sqrt{1-t_C}}\right), \\ \theta_{1,\beta}(t) &\approx -\frac{2}{\pi}\tan^{-1}\left(\frac{\left(\sqrt{1-t_C}-\sqrt{1-t_D}\right)\sqrt{t-1}}{t-1+\sqrt{(1-t_C)(1-t_D)}}\right). \end{aligned} \tag{4.44}$$

Substituting (4.44) into (4.42) and (4.43) and carrying out the integration, we find

$$\begin{aligned} x_{1,\alpha}(t) &\approx -\frac{2}{\pi We}\tan^{-1}\left(\frac{\left(1-\sqrt{1-t_C}\right)\sqrt{t-1}}{t-1+\sqrt{1-t_C}}\right), \\ x_{1,\beta}(t) &\approx \frac{2}{\pi We}\tan^{-1}\left(\frac{\left(\sqrt{1-t_C}-\sqrt{1-t_D}\right)\sqrt{t-1}}{t-1+\sqrt{(1-t_C)(1-t_D)}}\right), \end{aligned} \tag{4.45}$$

and

$$\begin{aligned} y_{1,\alpha}(t) &\approx \frac{4-4\sqrt{1-t_C}}{\pi^2\sqrt[4]{1-t_C}}\tan^{-1}\frac{\sqrt[4]{1-t_C}}{\sqrt{t-1}}, \\ y_{1,\beta}(t) &\approx -\frac{4\sqrt{1-t_C}-4\sqrt{1-t_D}}{\pi^2\sqrt[4]{(1-t_C)(1-t_D)}}\tan^{-1}\frac{\sqrt[4]{(1-t_C)(1-t_D)}}{\sqrt{t-1}}. \end{aligned} \tag{4.46}$$

Finally, using results (4.36), (4.38), (4.45), (4.46) and the development (4.32), we find the free streamlines:

$$\begin{aligned} x(t) &\approx -\frac{1}{\pi}\ln(t-1) - \frac{2\alpha}{\pi We}\tan^{-1}\left(\frac{\left(1-\sqrt{1-t_C}\right)\sqrt{t-1}}{t-1+\sqrt{1-t_C}}\right) \\ &+ \frac{2\beta}{\pi We}\tan^{-1}\left(\frac{\left(\sqrt{1-t_C}-\sqrt{1-t_D}\right)\sqrt{t-1}}{t-1+\sqrt{(1-t_C)(1-t_D)}}\right), \end{aligned} \tag{4.47}$$

and

$$y(t) \approx 1+\alpha\frac{4-4\sqrt{1-t_C}}{\pi^2\sqrt[4]{1-t_C}}\tan^{-1}\frac{\sqrt[4]{1-t_C}}{\sqrt{t-1}} - \beta\frac{4\sqrt{1-t_C}-4\sqrt{1-t_D}}{\pi^2\sqrt[4]{(1-t_C)(1-t_D)}}\tan^{-1}\frac{\sqrt[4]{(1-t_C)(1-t_D)}}{\sqrt{t-1}}. \quad (4.48)$$

4.3 Numerical results and discussion

The free-surface profiles of four different Weber numbers We are plotted in Figure 4.4 at a fixed height of the triangle, $r = 0.9$ and the angles $\alpha = \beta = \pi/8$. The free-surface profiles for different heights of the triangle r at a fixed $\alpha = \beta = \pi/6$ and $We = 200$, are given in Figure 4.5.
Figures 4.6, 4.7 and 4.8 illustrate the free-surface profiles for different angles α, β, at a fixed $r = 0.5$ and at a fixed Weber number $We = 200$.
As shown in figure 4.4, if there is a decrease in the Weber number, the free-surface curvature declines,

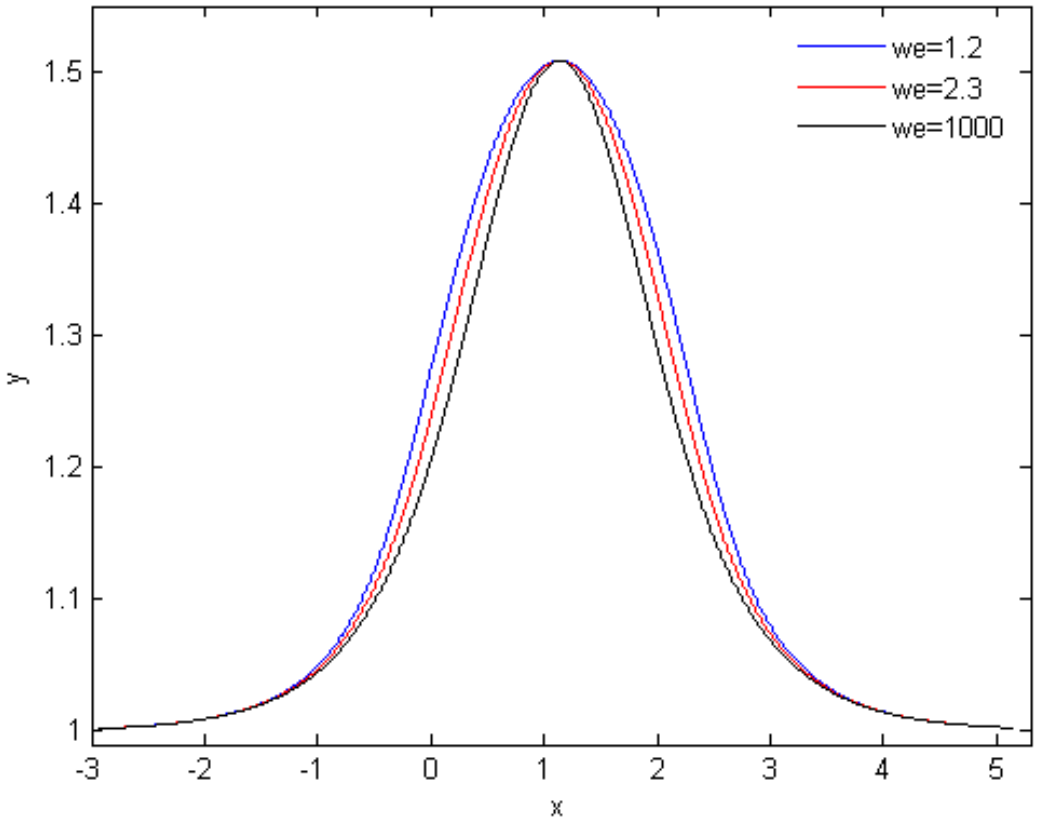

Figure 4.4: Effect of the Weber number on the free-surface profile for the angles $\alpha = \beta = \pi/8$ and the height of the triangle $r = 0.7$.

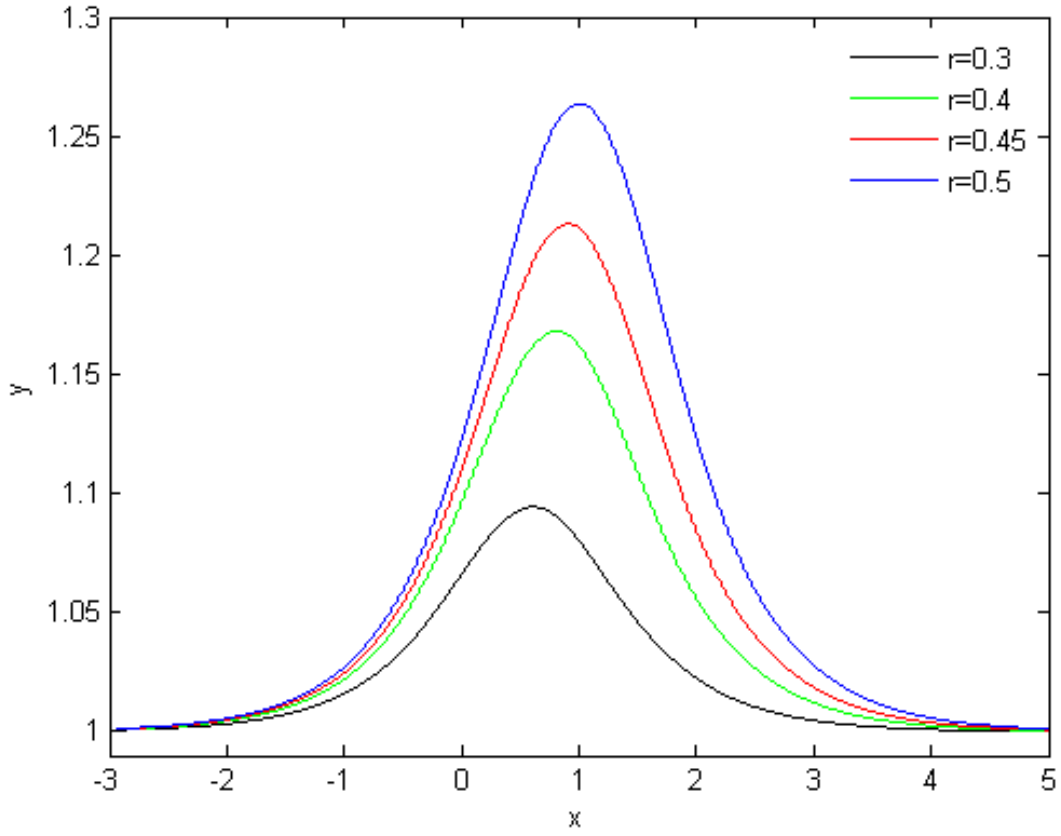

Figure 4.5: Effect of the height of the triangle r on the free-surface profile Weber number $We = 200$ and the angles $\alpha = \beta = \pi/6$.

because this is an important property of the surface tension effects. As the values of the triangle height increase, the flow of velocity decreases, which leads to the elevation of the free surface downstream as shown in Figure 4.5. The effect of the angles is evident from Figures 4.6, 4.7 and 4.8 what we notice, then, is that a change in the angles affects the deviation of the free surfaces.

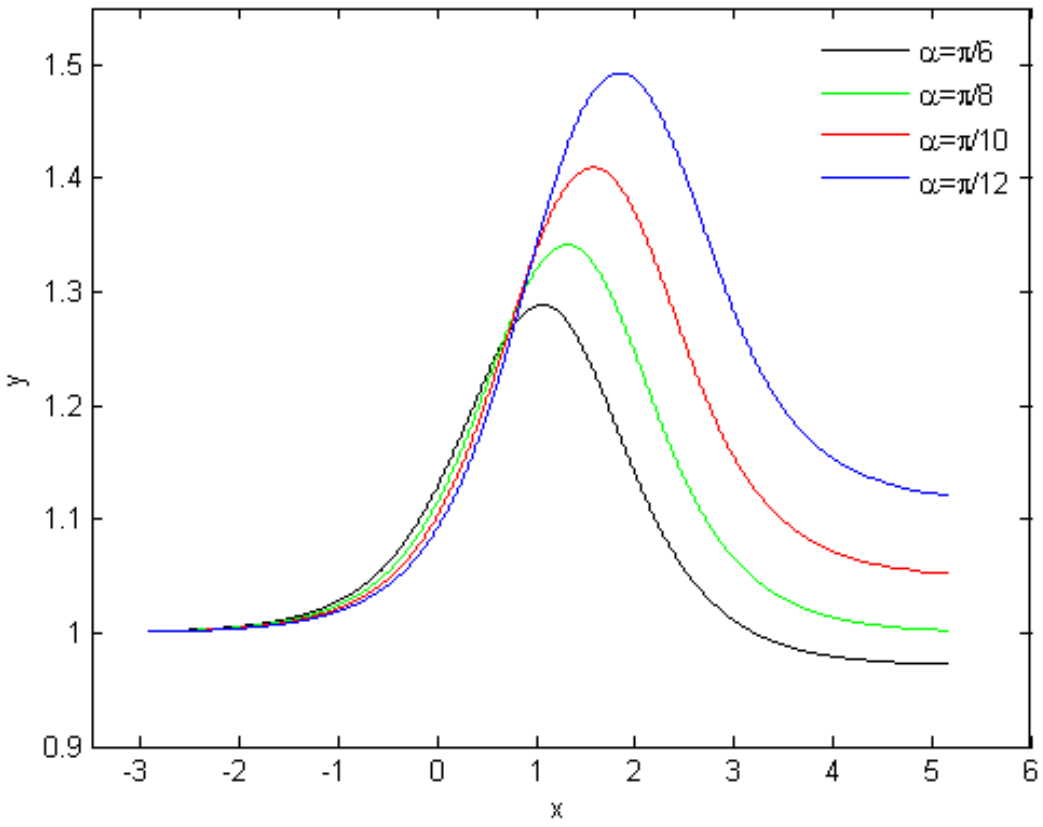

Figure 4.6: Effect of the angle α on the free-surface profile Weber number $We = 200$, $r = 0.5$ and $\beta = \pi/8$

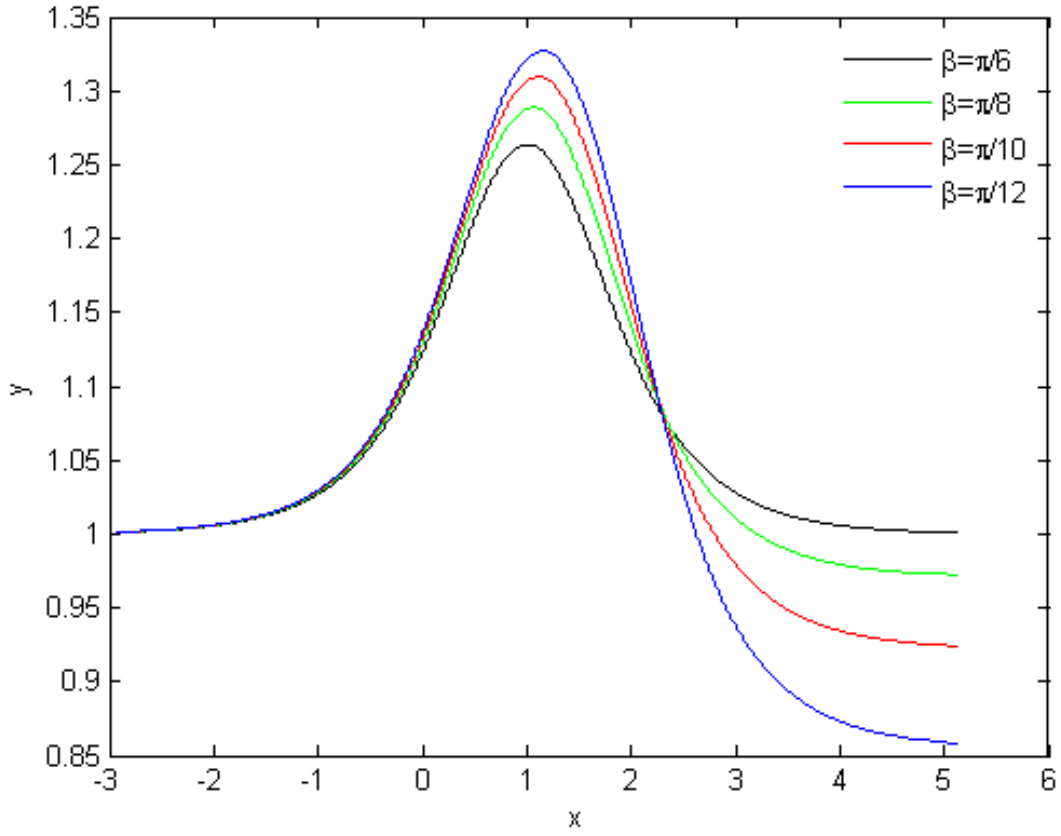

Figure 4.7: Effect of the angle β on the free-surface profile Weber number $We = 200$, $r = 0.5$ and $\alpha = \pi/6$

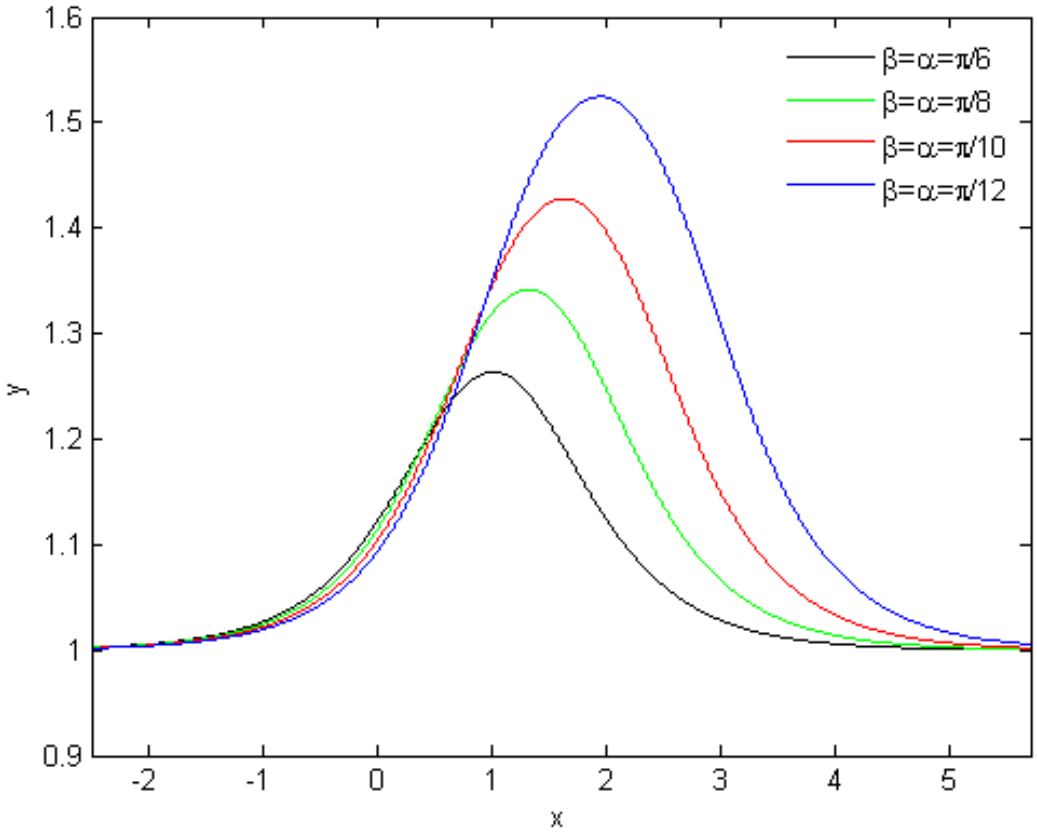

Figure 4.8: Effect of the angle α, β on the free-surface profile Weber number $We = 200$ and $r = 0.5$

5

Free-surface flow over a trapezoidal obstacle

In this chapter, we tackle the two-dimensional and irrotational flow of inviscid and incompressible fluid over a trapezoidal obstacle. The free surface of the flow which is governed by the Bernoulli condition is determined as a part of solution of the problem. This condition renders difficult an analytical solution of the problem. Hence, our work's objective is utilize the Hilbert transformation and the perturbation technique to provide an approximate solution to this problem for large Weber numbers and various configurations of the obstacle. The obtained results demonstrate that the used method is easily applicable, and provides approximate solutions to these kinds of problems.

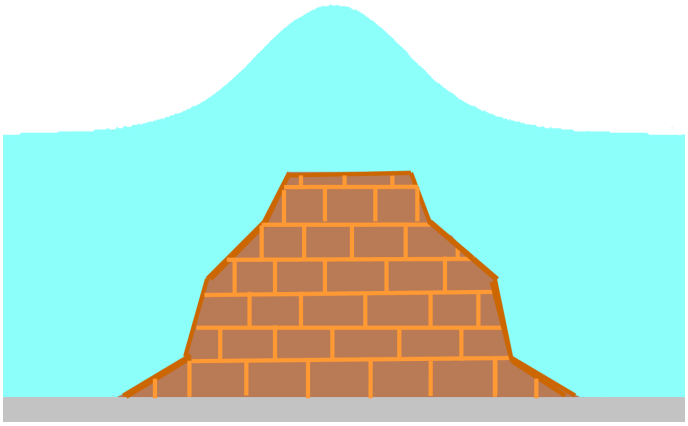

Contents in Brief

5.1 Formulation of Problem

Let us consider the motion of a two-dimensional flow of a fluid over a trapezoidal obstacle. The fluid is assumed to be incompressible, irrotational and inviscid. The effect of gravity is neglected but we take into account the superficial tension effect. The flow we propose is uniform and has a constant discharge $U_1h_1 = U_2h_2$, where $U_i, i = 1, 2$ designates the velocities and $h_i, i = 1, 2$ are the depths of the flow upstream and downstream respectively. Hence, the bottom consists of the horizontal walls A_0A_{-1} and $A_1A^{'}$ and the asymmetric polygon $A_{-1}A_{-2}...A_{-N}A_N...A_2A_1$ of $2N$ angles α_i and $(2N-1)$ straight-line segments. Furthermore, we choose Cartesian coordinates with the origin in the point (see Fig.5.1).

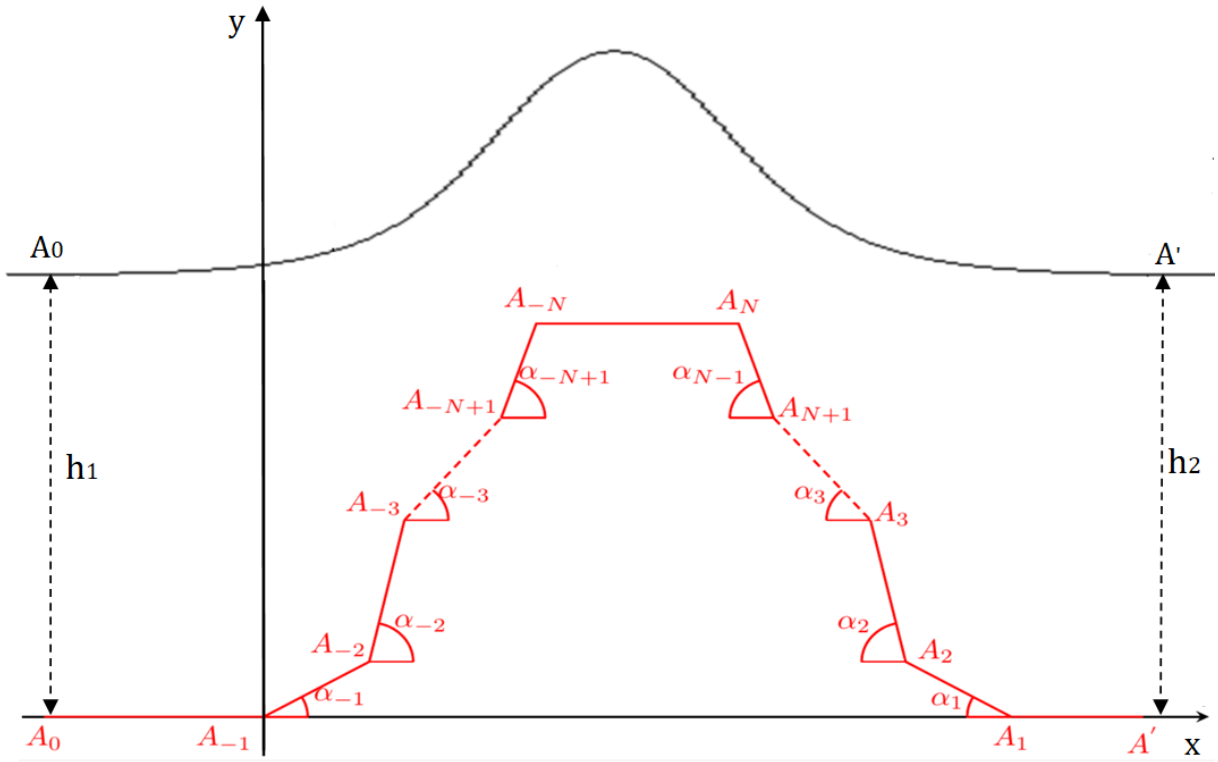

Figure 5.1: Sketch of the flow and of the coordinates.

The dimensionless variables are defined by choosing U_1 as the unit velocity and h_1 as the unit length. We introduce the complex potential $f(z) = \phi(z) + i\psi(z)$, where ϕ is the potential function, ψ the stream function (ϕ and ψ are conjugate solutions of Laplace's equation) and $f(z)$ is an analytic function of z within the region of flow with complex conjugate velocity

$$\eta = \frac{df(z)}{dz} = u - iv = qe^{-i\theta}. \tag{5.1}$$

Let

$$\kappa = \ln \eta = \ln q - i\theta, \tag{5.2}$$

where κ is called the logarithmic hodograph variable. Then, from (5.1) and (5.2) we get

$$z = \int e^{-\kappa} df. \tag{5.3}$$

Without loss of generality, we choose $\phi = 0$ at a point A_{-1} , $\psi = 1$ on the streamline $A_0A^{'}$, and $\psi = 0$ on the streamline $A_0A_{-1}A_{-2}...\ A_{-N}A_N...A_1A^{'}$ (see Fig. 5.2). We denote the dimensionless trapezoid depth by r_i, where

$$r_i = l_i \sin(\alpha_i). \tag{5.4}$$

Where

$$l_i = \begin{cases} |A_iA_{i-1}|, & i = -1, ..., -N+1; \\ |A_iA_{i+1}|, & i = 1, ..., N-1. \end{cases} \tag{5.5}$$

On the free-surface, where the pressure is uniform, the dimensionless form of the Bernoulli equation is given by:

$$q^2 + \frac{2}{We}\left|\frac{\partial\theta}{\partial\phi}\right| q = 1, \tag{5.6}$$

where We is the adimensional parameter, known as the Weber number and defined by:

$$We = \frac{\rho U_1^2 h_1}{T}, \tag{5.7}$$

T is the surface tension, and ρ is the density of the fluid.

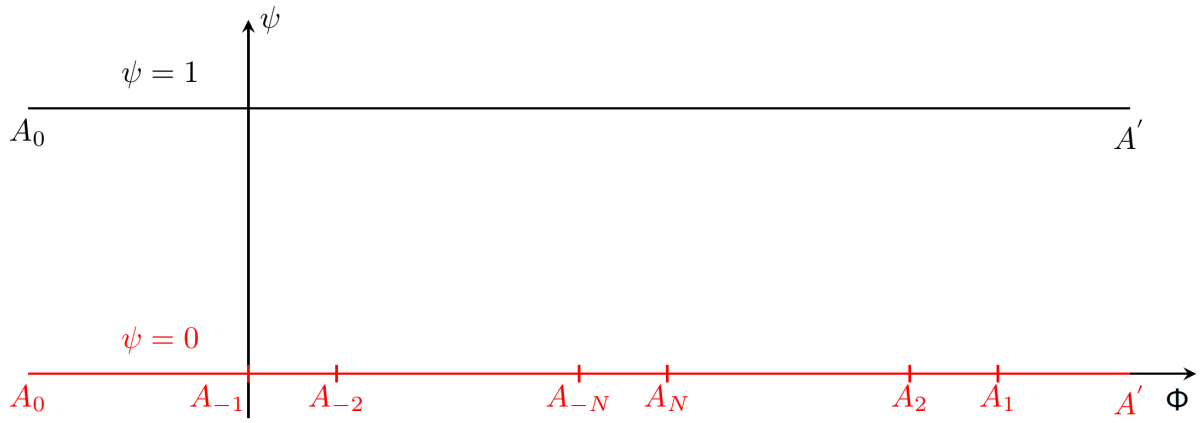

Figure 5.2: The potential f plane

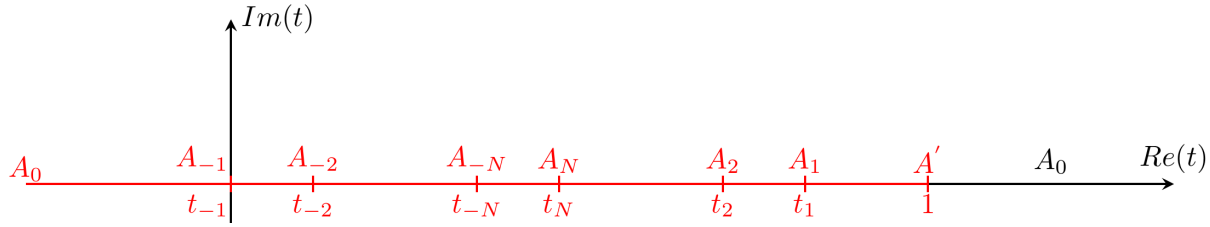

Figure 5.3: The auxiliary t plane

Using the Schwartz-Christoffel transformation, we map the potential plane f as seen in Figure 5.2 onto

the upper half of an auxiliary t-plane see Figure 5.3.

The tranformation used is:

$$f(t) = -\frac{1}{\pi}\ln(1-t). \tag{5.8}$$

5.1.1 The Hilbert method

In order to express κ as the single variable t function, we need to use the Hilbert method for the obtained mixed problem of the new plane. Hence, the solution for an analytic function $\chi(t)$ in the upper half-plane (see [43]) is given by

$$\chi(t) = \frac{1}{\pi} p.v. \int_{-\infty}^{+\infty} \frac{Im[\chi(s)]}{s-t} ds + \sum_{j=0}^{\infty} B_j t^j. \tag{5.9}$$

Where B_j are real constants and $p.v.$ is the principal value of the integral.
The real and imaginary parts of $\kappa(t)$ are given by

$$\begin{aligned} Im[\kappa(t)] &= -\theta(t). \\ Re[\kappa(t)] &= \ln q(t). \end{aligned} \tag{5.10}$$

Where

$$\theta(t) = \begin{cases} 0, & t < 0 = t_1, \\ \alpha_i, & t_i < t < t_{i-1}, \quad i = -N+1, \ldots, -1, \\ -\alpha_i, & t_{i+1} < t < t_i, i = 1, \ldots, N-1, \\ 0, & t_N < t < 1, \\ \theta(t), & t > 1. \end{cases} \tag{5.11}$$

To switch the function $\kappa(t)$ to $\chi(t)$, we use an auxiliary function $H(t)$

$$H(t) = \begin{cases} \sqrt{1-t}, & t < 1, \\ -i\sqrt{t-1}, & t > 1. \end{cases} \tag{5.12}$$

Using (5.10) and (5.12), with $\chi(t) = \kappa(t)/H(t)$, we get

$$\chi(t) = \left\{ \begin{array}{ll} \frac{\ln q(t) - i\theta(t)}{\sqrt{1-t}}, & t < 1, \\ \frac{\ln q(t) - i\theta(t)}{-i\sqrt{t-1}}, & t > 1. \end{array} \right\} = U(t) + iV(t). \tag{5.13}$$

Examining the upstream condition, we have

$$B_j = 0, j = 0, 1, 2, \ldots.$$

and hence

$$\chi(t) = \frac{1}{\pi} p.v. \int_{-\infty}^{+\infty} \frac{Im[\chi(s)]}{s-t} ds. \tag{5.14}$$

Smith and Lim [41] used an equivalent form for (5.14), we obtain

$$U(t) = \frac{1}{\pi} p.v. \int_{-\infty}^{+\infty} \frac{V(s)}{s-t} ds. \tag{5.15}$$

$$V(t) = -\frac{1}{\pi} p.v. \int_{-\infty}^{+\infty} \frac{U(s)}{s-t} ds. \tag{5.16}$$

Along the real axis of the upper half-plane $Im(t) = 0$ (see fig 5.3), the distribution of both real and imaginary parts of $\chi(t)$ can be recapitulated; check Table 5.1. Therefore, q_0 is defined in $t < 0$ and q_∞ is defined in $t_N < t < 1$.

Using (5.15), (5.16) and Table 5.1 , we obtain the following systems of the nonlinear integral equations:

Table 5.1: Distribution of the flow quantities along $Im(t) = 0$

t	$U(t)$	$V(t)$
$t < 0 = t_{-1}$	$\frac{\ln q_0(t)}{\sqrt{1-t}}$	0
$t_i < t < t_{i-1}; i = -N+1, \ldots, -1$	$\frac{\ln q_i(t)}{\sqrt{1-t}}$	$\frac{-\alpha_i}{\sqrt{1-t}}$
$t_{i+1} < t < t_i; i = 1, \ldots, N-1$	$\frac{\ln q_i(t)}{\sqrt{1-t}}$	$\frac{\alpha_i}{\sqrt{1-t}}$
$t_N < t < 1$	$\frac{\ln q_\infty(t)}{\sqrt{1-t}}$	0
$t > 1$	$\frac{\theta(t)}{\sqrt{t-1}}$	$\frac{\ln q(t)}{\sqrt{t-1}}$

$$\begin{aligned} \theta(t) &= \frac{\sqrt{t-1}}{\pi} p.v. \int_1^{+\infty} \frac{\ln q(s)}{(s-t)\sqrt{s-1}} ds + \sum_{i=-N+1}^{-1} \frac{2\alpha_i}{\pi} \tan^{-1}\left(\frac{(m_i - m_{i-1})\sqrt{t-1}}{t-1+m_i m_{i-1}}\right) \\ &- \sum_{i=1}^{N-1} \frac{2\alpha_i}{\pi} \tan^{-1}\left(\frac{(m_{i+1} - m_i)\sqrt{t-1}}{t-1+m_{i+1} m_i}\right), \qquad t > 1, \end{aligned} \tag{5.17}$$

where

$$m_i = \sqrt{1-t_i}. \tag{5.18}$$

And

$$\begin{aligned} \ln(q_j(t)) &= \frac{\sqrt{1-t}}{\pi} \left\{ p.v. \int_1^{+\infty} \frac{\ln q(s)}{(s-t)\sqrt{s-1}} ds + \sum_{i=-N+1}^{-1} \alpha_i \int_{t_i}^{t_{i-1}} \frac{ds}{(s-t)\sqrt{1-s}} \right. \\ &- \left. \sum_{i=1}^{N-1} \alpha_i \int_{t_{i+1}}^{t_i} \frac{ds}{(s-t)\sqrt{1-s}} \right\}, \end{aligned} \tag{5.19}$$

where $p.v.$ is the principal value of the integral and for $j = -N, ..., -1$, $q_j(t)$ being the flow speed in $t_j < t < t_{j-1}$, and for $j = 1, ..., N$, $q_j(t)$ being the flow speed in $t_{j+1} < t < t_j$.

Using (5.3) and (5.8), the coordinates of a point on the free-surface can be obtained as follows:

$$z(t) = z_\infty - \frac{1}{\pi} \int_t^{+\infty} \frac{e^{i\theta(s)}}{(1-s)q(s)} ds, \quad t > 1. \tag{5.20}$$

By separating the real and imaginary parts, we get:

$$x(t) = x_\infty - \frac{1}{\pi}\int_t^{+\infty} \frac{\cos\theta(s)}{(1-s)q(s)}ds, \quad t > 1, \tag{5.21}$$

$$y(t) = 1 - \frac{1}{\pi}\int_t^{+\infty} \frac{\sin\theta(s)}{(1-s)q(s)}ds, \quad t > 1. \tag{5.22}$$

5.2 The approximate equations

In this section, we approximate the nonlinear integral equations (5.6), (5.17), (5.21) and (5.22), when Weber number is large.

Using the first-order Taylor development with respect to $\frac{1}{We}\left|\frac{\partial\theta}{\partial\phi}\right|$, we can give the solution to the Bernoulli equation as follows:

$$q(t) \approx 1 - \frac{1}{We}\left|\frac{\partial\theta}{\partial\phi}\right|. \tag{5.23}$$

Using the relation (5.8), we obtain:

$$\frac{\partial\theta}{\partial\phi} = \frac{\partial\theta}{\partial t}\frac{\partial t}{\partial\phi} = \pi(t-1)\frac{\partial\theta}{\partial t}, \quad t > 1. \tag{5.24}$$

Consequently, for $t > 1$ the flow speed is approximated by

$$q(t) \approx 1 - \frac{\pi}{We}(t-1)\frac{\partial\theta}{\partial t}(t), \tag{5.25}$$

which yields

$$\ln q(t) \approx -\frac{\pi}{We}(t-1)\frac{\partial\theta}{\partial t}(t), \quad \text{and} \quad \frac{1}{q(t)} \approx 1 + \frac{\pi}{We}(t-1)\frac{\partial\theta}{\partial t}(t). \tag{5.26}$$

For small angles α_i, the change in θ will be minor, thus, allowing us to approximate $\sin\theta$ by $\theta(t)$ and $\cos\theta$ by one.
Using (5.26), we can approximate the angle of the free surface with the horizontal (5.17) by

$$\begin{aligned}\theta(t) \;\approx\; & -\frac{\sqrt{t-1}}{We}p.v.\int_1^{+\infty}\frac{(s-1)\frac{\partial\theta}{\partial s}(s)}{(s-t)\sqrt{s-1}}ds + \sum_{i=-N+1}^{-1}\frac{2\alpha_i}{\pi}\tan^{-1}\left(\frac{(m_i - m_{i-1})\sqrt{t-1}}{t-1+m_i m_{i-1}}\right)\\ & - \sum_{i=1}^{N-1}\frac{2\alpha_i}{\pi}\tan^{-1}\left(\frac{(m_{i+1}-m_i)\sqrt{t-1}}{t-1+m_{i+1}m_i}\right), \qquad t > 1,\end{aligned} \tag{5.27}$$

substituting (5.26) into (5.21) and (5.22), and after simplification, the free surface equations take the form:

$$\begin{aligned} x(t) &\approx x_\infty - \frac{1}{\pi}\int_t^{+\infty} \frac{1}{(1-s)}\left[1+\frac{\pi}{We}(s-1)\frac{\partial\theta}{\partial s}(s)\right]ds \\ &\approx x_\infty - \frac{1}{\pi}\int_t^{+\infty} \frac{1}{(1-s)}ds + \frac{1}{We}\left[\lim_{s\longrightarrow\infty}\theta(s)-\theta(t)\right] \\ &\approx x_\infty - \frac{1}{\pi}\int_t^{+\infty} \frac{1}{(1-s)}ds - \frac{1}{We}\theta(t), \end{aligned} \tag{5.28}$$

and

$$\begin{aligned} y(t) &\approx 1 - \frac{1}{\pi}\int_t^{+\infty} \frac{\theta(s)}{(1-s)}\left[1+\frac{\pi}{We}(s-1)\frac{\partial\theta}{\partial s}(s)\right]ds \\ &\approx 1 - \frac{1}{\pi}\int_t^{+\infty} \frac{\theta(s)}{(1-s)}ds + \frac{1}{2We}\left[\lim_{s\longrightarrow\infty}\theta^2(s)-\theta(t)^2\right] \\ &\approx 1 - \frac{1}{\pi}\int_t^{+\infty} \frac{\theta(s)}{(1-s)}ds - \frac{\theta^2(t)}{2We}. \end{aligned} \tag{5.29}$$

To solve the system of the nonlinear integral equations (5.25), (5.27)-(5.29), we use the Perturbation technique.

5.3 Perturbation technique

We expand $X(t)$ in terms of the small parameters α_i

$$X(t) = \sum_{j=-N+1}^{N-1}\sum_{k=0}^{\infty}\alpha_j^k X_{k,\alpha_j}(t). \tag{5.30}$$

Where $X(t)$ stands for $q(t)$, $\theta(t)$, $\theta^{'}(t)$, $x(t)$ and $y(t)$.

5.3.1 Zero-order approximation

This case corresponds to the flow far upstream, which we consider as uniform. Then, the zero-order approximation of the nonlinear integral equations (5.25), (5.27)-(5.29) is presented by:

- The velocity of the flow

$$q_0(t) \approx 1 - \frac{\pi}{We}(t-1)\theta_0^{'}(t) \approx 1. \tag{5.31}$$

- The velocity direction relative to the horizontal

$$\theta_0(t) \approx -\frac{\sqrt{t-1}}{We} p.v. \int_1^{+\infty} \frac{(s-1)\theta_0'(s)}{(s-t)\sqrt{s-1}} ds \approx 0. \tag{5.32}$$

- The free streamline equations:

$$\begin{aligned} x_0(t) &\approx x_\infty - \frac{1}{\pi}\int_t^{+\infty} \frac{1}{(1-s)} ds - \frac{1}{We}\theta_0(t) \\ &\approx x_\infty - \frac{1}{\pi}\int_t^{+\infty} \frac{1}{(1-s)} ds, \end{aligned} \tag{5.33}$$

and

$$y_0(t) \approx 1 - \frac{1}{\pi}\int_t^{+\infty} \frac{\theta_0(s)}{(1-s)} ds - \frac{\theta_0^2(t)}{2We} \approx 1. \tag{5.34}$$

On the other hand, we have the formula:

$$x_\infty \approx \frac{1}{\pi} p.v. \int_0^{+\infty} \frac{1}{(1-s)} ds, \tag{5.35}$$

hence

$$x_0(t) \approx -\frac{1}{\pi}\ln(t-1). \tag{5.36}$$

5.3.2 First-order approximation

Now, we find the first-order approximation of the nonlinear integral equations (5.25), (5.27)-(5.29) by using development (5.30) and the zero-order approximation of the system.
Using the development (5.30), we can write

$$X_{1,\alpha_i}(t) \approx \frac{X(t) - X_0(t)}{\alpha_i}. \tag{5.37}$$

Substituting (5.25) and (5.31) into (5.37) yields

$$q_{1,\alpha_i}(t) \approx \frac{\pi}{We}(t-1)\theta_{1,\alpha_i}'(t). \tag{5.38}$$

From (5.27), (5.32) and (5.37) we get:

- for $i = -N+1, ..., -1$,

$$\theta_{1,\alpha_i}(t) \approx -\frac{\sqrt{t-1}}{We}\int_1^{+\infty} \frac{(s-1)\theta_{1,\alpha_i}'(s)}{(s-t)\sqrt{s-1}} ds + \sum_{i=-N+1}^{-1} \frac{2}{\pi}\tan^{-1}\left(\frac{(m_i - m_{i-1})\sqrt{t-1}}{t-1+m_i m_{i-1}}\right), \tag{5.39}$$

- for $i = 1, ..., N-1$,

$$\theta_{1,\alpha_i}(t) \approx -\frac{\sqrt{t-1}}{We}\int_1^{+\infty}\frac{(s-1)\theta'_{1,\alpha_i}(s)}{(s-t)\sqrt{s-1}}ds - \sum_{i=1}^{N-1}\frac{2}{\pi}\tan^{-1}\left(\frac{(m_{i+1}-m_i)\sqrt{t-1}}{t-1+m_{i+1}m_i}\right). \quad (5.40)$$

On the other hand, from (5.28), (5.29), (5.34), (5.36) and (5.37), we find:

$$x_{1,\alpha_i}(t) \approx -\frac{1}{We}\theta_{1,\alpha_i}(t), \quad (5.41)$$

and

$$y_{1,\alpha_i}(t) \approx -\frac{1}{\pi}\int_t^{+\infty}\frac{\theta_{1,\alpha_i}(s)}{(1-s)}ds. \quad (5.42)$$

From (5.39), (5.40), and for a very large value of the Weber number We, we may neglect the first term with respect to the second one. Thus, we get the first-order approximation of the velocity direction relative to the horizontal axis:

- for $i = -N+1, ..., -1$,

$$\theta_{1,\alpha_i}(t) \approx \frac{2}{\pi}\arctan\left(\frac{(m_i-m_{i-1})\sqrt{t-1}}{t-1+m_im_{i-1}}\right), \quad (5.43)$$

- for $i = 1, .., N-1$,

$$\theta_{1,\alpha_i}(t) \approx -\frac{2}{\pi}\arctan\left(\frac{(m_{i+1}-m_i)\sqrt{t-1}}{t-1+m_{i+1}m_i}\right). \quad (5.44)$$

Substituting (5.43), (5.44) into (5.41) and (5.42) and carrying out the integration, one finds

- for $i = -N+1, ..., -1$,

$$x_{1,\alpha_i}(t) \approx -\frac{2}{\pi We}\arctan\left(\frac{(m_i-m_{i-1})\sqrt{t-1}}{t-1+m_im_{i-1}}\right), \quad (5.45)$$

- for $i = 1, .., N-1$,

$$x_{1,\alpha_i}(t) \approx \frac{2}{\pi We}\arctan\left(\frac{(m_{i+1}-m_i)\sqrt{t-1}}{t-1+m_{i+1}m_i}\right), \quad (5.46)$$

and

- for $i = -N+1, ..., -1$,

$$y_{1,\alpha_i}(t) \approx \frac{4\,(m_i-m_{i-1})}{\pi^2\sqrt{m_im_{i-1}}}\arctan\left(\sqrt{\frac{m_im_{i-1}}{t-1}}\right), \quad (5.47)$$

- for $i = 1, .., N-1$,

$$y_{1,\alpha_i}(t) \approx -\frac{4\,(m_{i+1}-m_i)}{\pi^2\sqrt{m_{i+1}m_i}}\arctan\left(\sqrt{\frac{m_{i+1}m_i}{t-1}}\right), \quad i = 1, .., N-1. \quad (5.48)$$

Using results (5.34),(5.36), (5.45)-(5.48) and expanding (5.30) enables finding the approximate solutions of the free-surface flow:

$$\begin{aligned} x(t) &\approx -\frac{1}{\pi}\ln(t-1) - \sum_{i=-N+1}^{-1} \frac{2\alpha_i}{\pi We}\tan^{-1}\left(\frac{(m_i - m_{i-1})\sqrt{t-1}}{t-1+m_i m_{i-1}}\right) \\ &+ \sum_{i=1}^{N-1} \frac{2\alpha_i}{\pi We}\tan^{-1}\left(\frac{(m_{i+1} - m_i)\sqrt{t-1}}{t-1+m_{i+1} m_i}\right), \end{aligned} \tag{5.49}$$

and

$$\begin{aligned} y(t) &\approx 1 + \sum_{i=-N+1}^{-1} \frac{4\,(m_i - m_{i-1})\,\alpha_i}{\pi^2\sqrt{m_i m_{i-1}}}\tan^{-1}\left(\sqrt{\frac{m_i m_{i-1}}{t-1}}\right) \\ &- \sum_{i=1}^{N-1} \frac{4\,(m_{i+1} - m_i)\,\alpha_i}{\pi^2\sqrt{m_{i+1} m_i}}\tan^{-1}\left(\sqrt{\frac{m_{i+1} m_i}{t-1}}\right), \quad t > 1. \end{aligned} \tag{5.50}$$

5.4 Application example for $N = 2$ and $\alpha_{-2} = \alpha_2 = 0$

The previous approximate scheme is used to calculate the solutions and the free surface profiles for fixed values of flow with large Weber number are found throughout a range of different Weber number. The Figure 5.4 presented the variation of the free surface shape with respect to the Weber number, fixed the angles values $\alpha_{-1} = \alpha_1 = \pi/6$, $l_{-2} = l_2 = 1$, and the depth of the obstacle value $r_{-1} = 0.65$.

As presented in figure 5.4, the curvature of the free surface is decreased if the Weber number decreases, because this is an important characteristic property of the surface tension effects.

The free-surface profiles for four different depths r_{-1} are plotted in figure 5.5 at a fixed Weber number $We = 200$, $l_{-2} = l_2 = 1$,$\alpha_{-1} = \alpha_1 = \frac{\pi}{8}$, This clarifies that increasing the depth r_{-1} results in more deviation of the free surface from the horizontal one.

Figure 5.6 shows the free-surface profiles for different angles α_1 at a fixed $\alpha_{-1} = \pi/8$,$r_{-1} = 0.5$, and at a fixed Weber number $We = 200$. Figure 5.7 shows the free-surface profiles for four different angles α_{-1} at a fixed $\alpha_1 = \pi/6$, $r_{-1} = 0.5$ and at a fixed Weber number $We = 200$.

The two figures 5.6 and 5.7 evidently show that the deviation of the free-surface results from the change in angles.

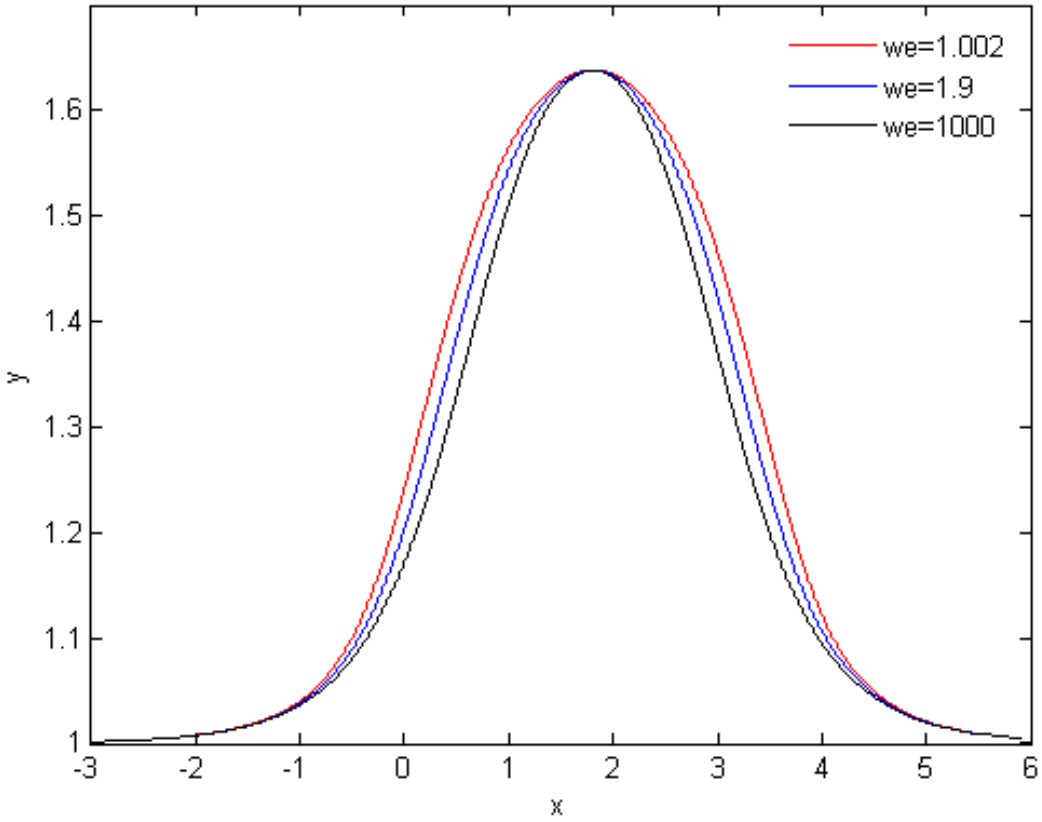

Figure 5.4: Effect of Weber number on the free-surface profile at a fixed the trapezoid depth $r_{-1} = 0.65$ and the angles $\alpha_{-1} = \pi/6$, $\alpha_1 = \pi/6$.

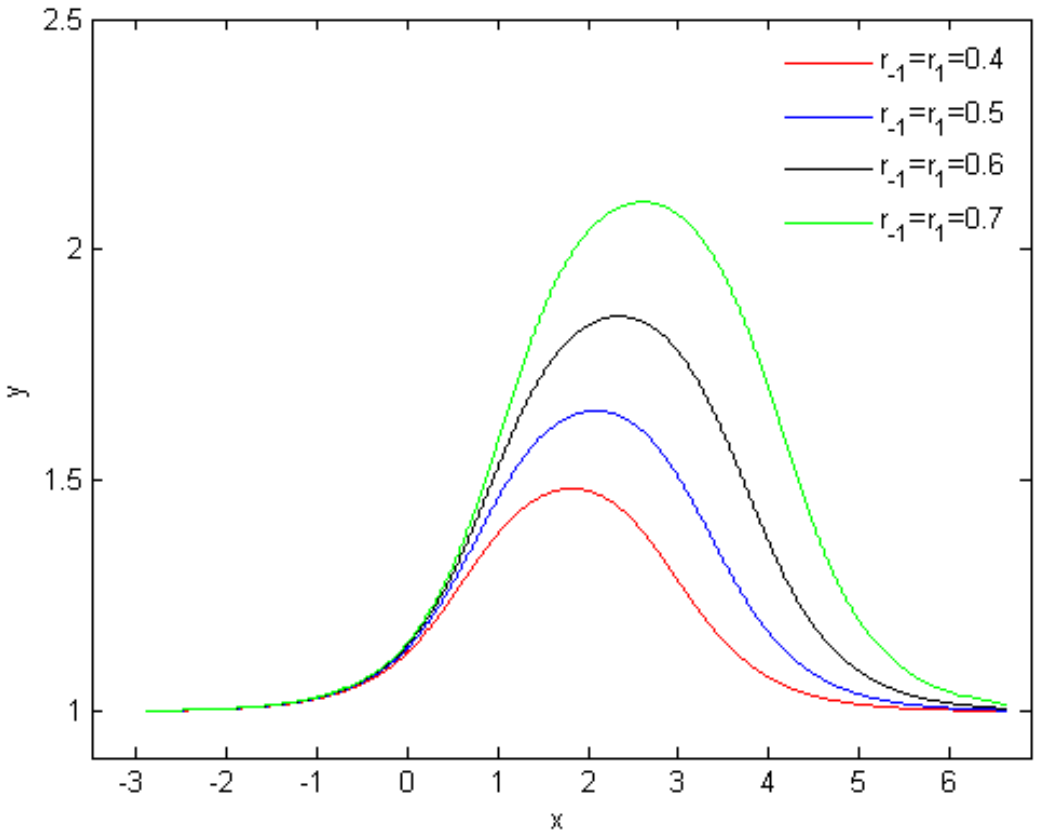

Figure 5.5: Effect of the trapezoid depth r_{-1} on the free-surface profile Weber number $We = 200$ and the angles $\alpha_{-1} = \alpha_1 = \pi/8$.

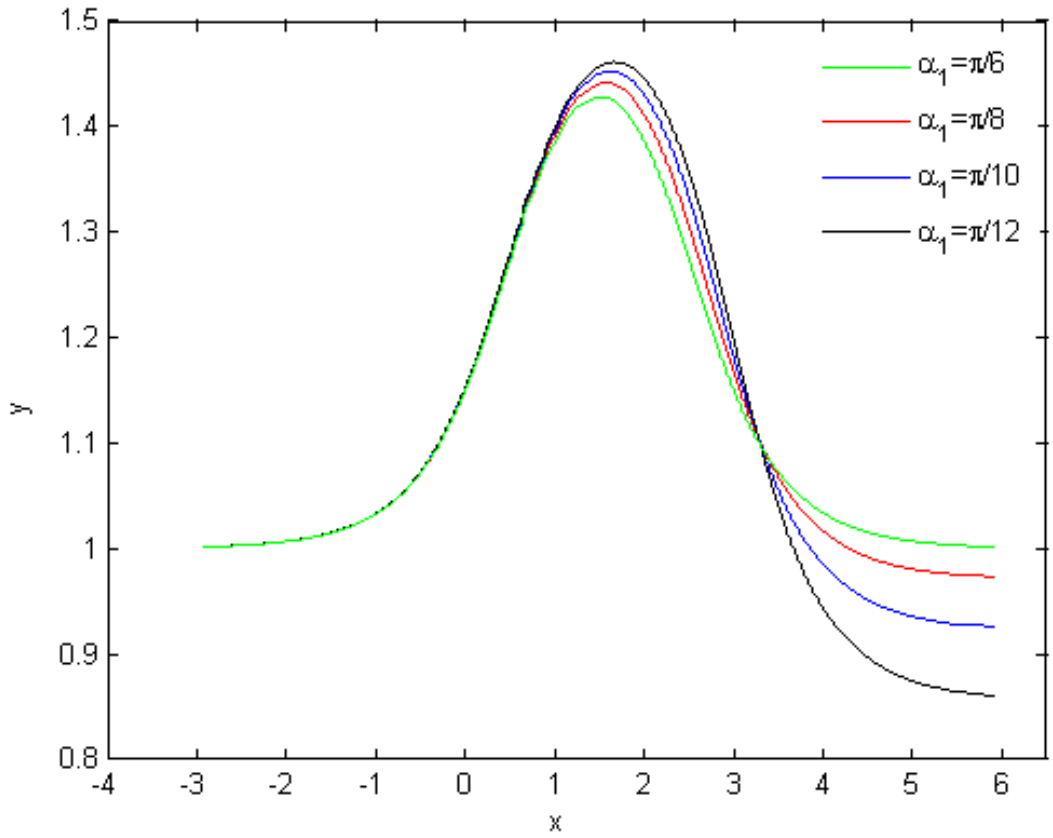

Figure 5.6: Effect of the angles α_1 on the free-surface profile Weber number $We = 200$, the angle $\alpha_{-1} = \pi/6$ and the trapezoid depth $r_{-1} = 0.5$

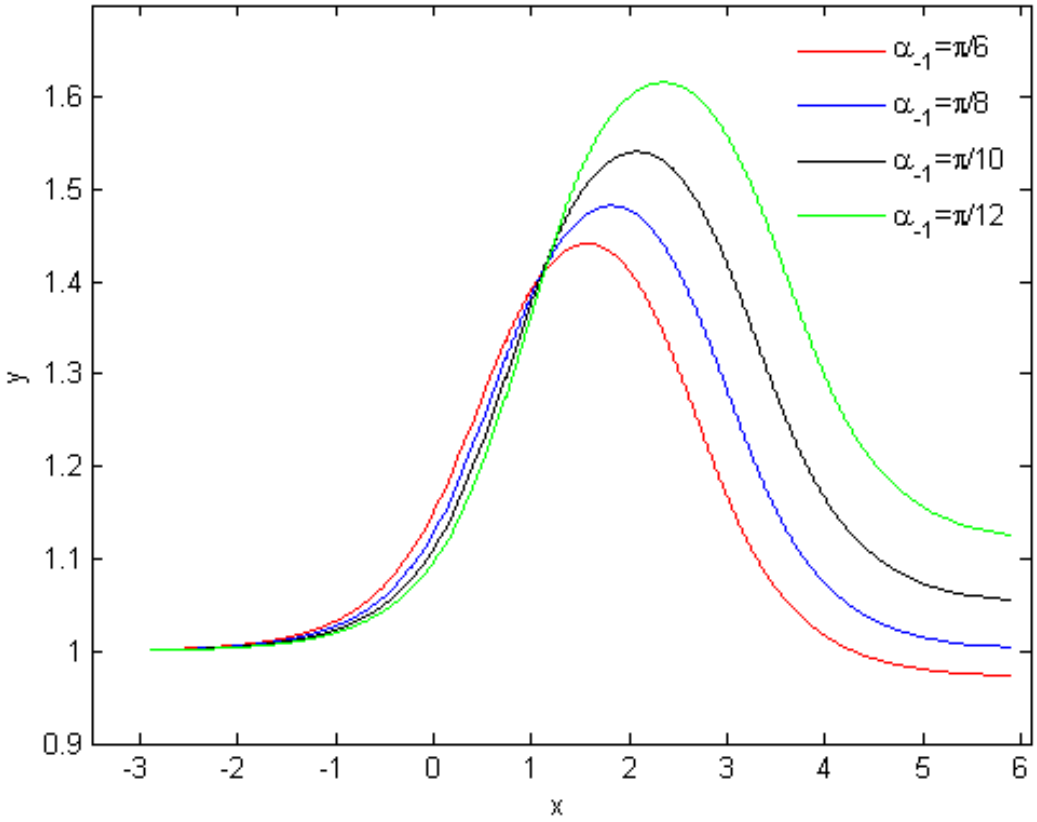

Figure 5.7: Effect of the angles α_{-1} on the free-surface profile Weber number $We = 200$, the angle $\alpha_1 = \pi/8$ and the trapezoid depth $r_{-1} = 0.5$

6

Application for some flow over a curved obstacle

In this chapter, we proposed two examples of the flow over a curved obstacle. The flow is assumed to be as steady and irrotational, the effect of the surface tension with smaller values is considered, but the gravity force is neglected, We apply the same steps as in the previous chapter (chapter 5) for obtaining the free surface profiles for different Weber number σ.

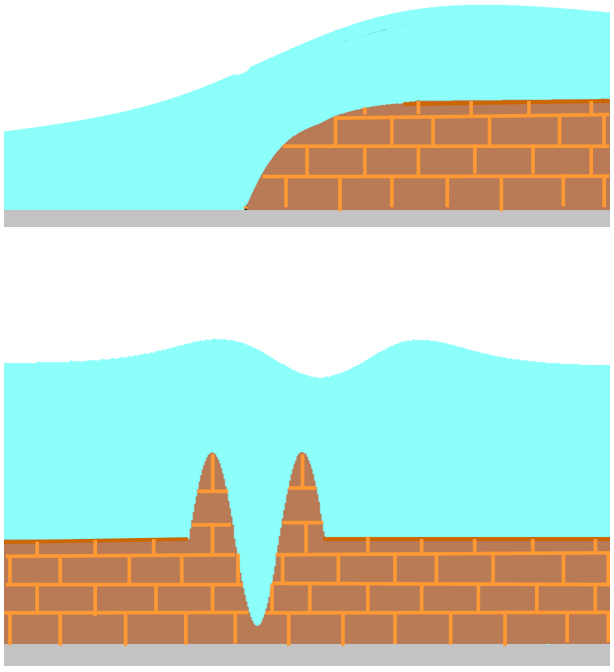

Contents in Brief

6.1 Free surface flow over a round obstacle

Example 6.1. This example treats the problem of determining the shape of the two dimensional free surface flow of inviscid and incompressible fluid over a round obstacle in channel. we seek the approximate solution of the proposed problem by using the results in chapter 5.

(i) Formulation of problem : Let us consider the motion of a two-dimensional flow of a fluid over a

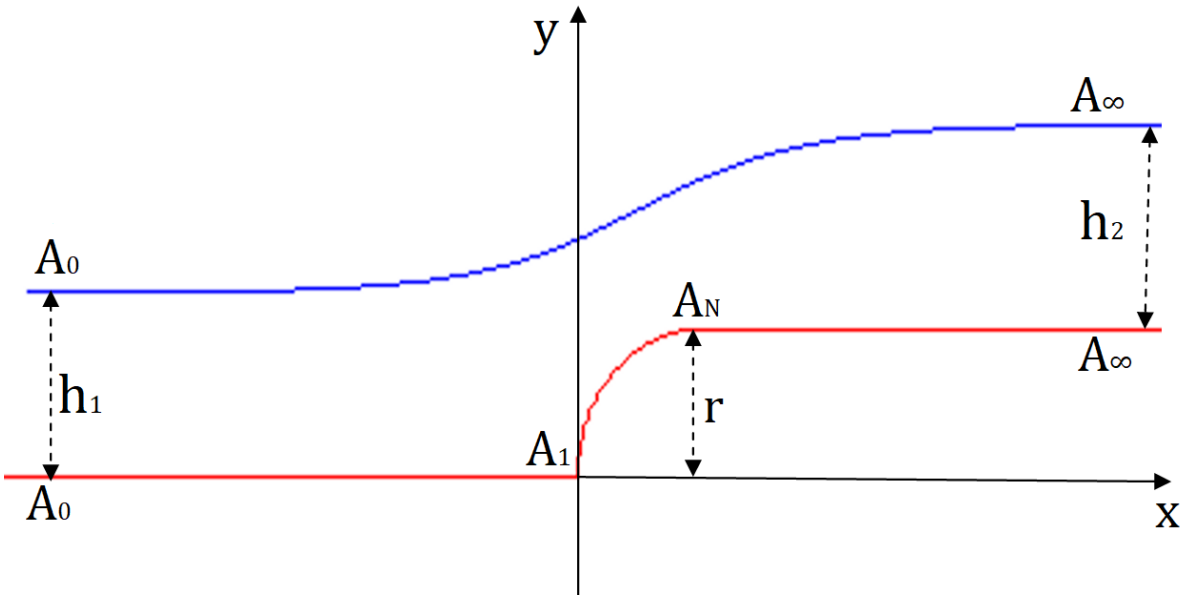

Figure 6.1: Sketch of the flow and of the coordinates.

round δ with the center being at the point $(r, 0)$ and the radius being r,

$$\delta = \left\{(x, y) : (x - r)^2 + y^2 = r^2, \quad -r \leq x \leq 0, \quad 0 \leq y \leq r\right\}.$$

The fluid is assumed to be incompressible, irrotational and inviscid. The effect of gravity is neglected but we take into account the superficial tension effect. Far upstream and downstream, the flow is proposed as uniform with a constant discharge $U_1 h_1 = U_2 h_2$, where $U_i, i = 1, 2$ design the velocities and $h_i, i = 1, 2$ the depths of the flow at upstream and downstream respectively, so that the bottom consists of a horizontal walls A_0A_1 and A_NA_∞, obstacle A_1A_N of a arc of the disk δ, we choose Cartesian coordinates with the origin in the point A_1(see Fig. 6.1). We divide the radius being r by the N horizontal lines where the lines intersect the curve of the round δ in the point $A_i, i = 1, 2, \ldots, N$ (sse figure 6.2), we note to the inclination angle between the wall A_iA_{i+1} and the horizontal plane by α_i,

$$\alpha_i = \arcsin\left(\frac{r}{Nl_i}\right), i = 1, 2, \ldots, N - 1,$$

where

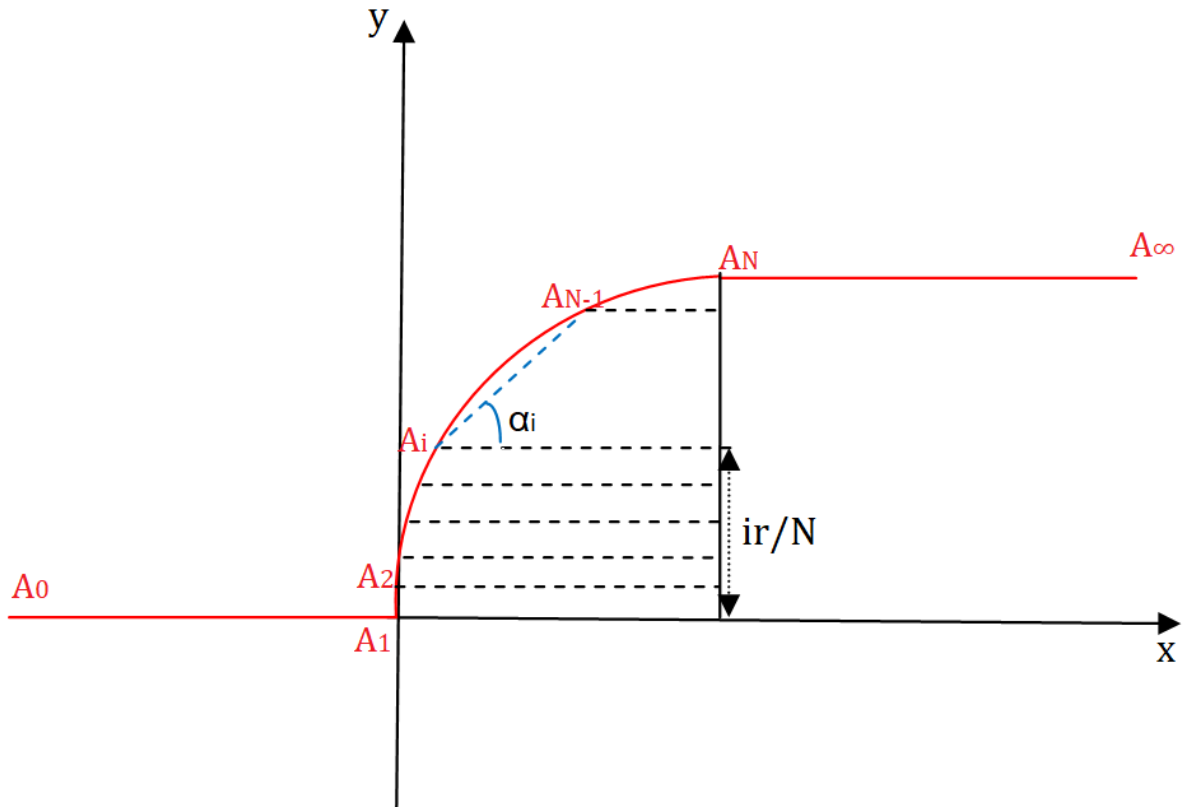

Figure 6.2: Discretzation of a a round obstacle.

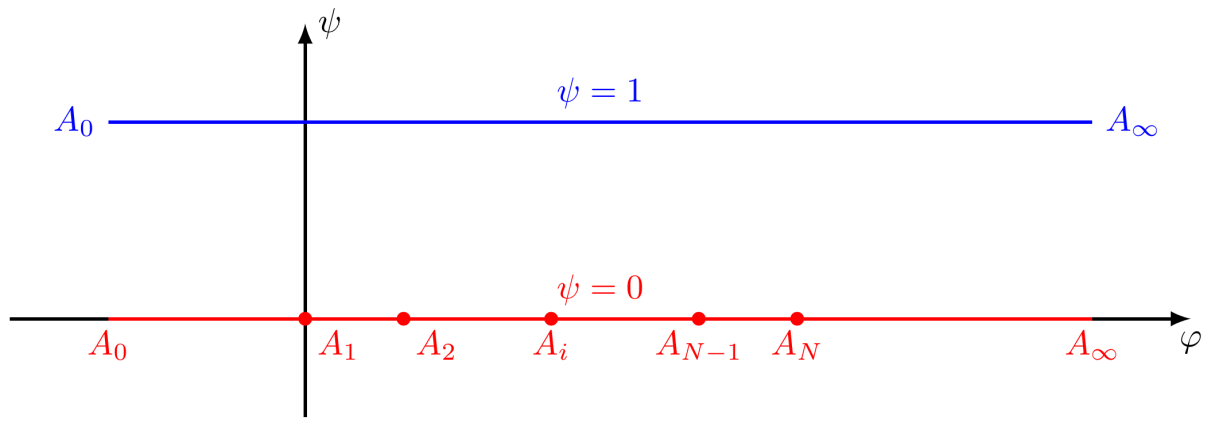

Figure 6.3: The potential f plane

$$l_i = |A_iA_{i+1}| = \sqrt{(x_{i+1} - x_i)^2 + \left(\frac{r}{N}\right)^2}, i = 1, 2, \ldots, N-1,$$

and

$$x_i = \sqrt{r^2 - \left(\frac{ir}{N}\right)^2} + r, i = 1, 2, \ldots, N.$$

Without loss of generality we choose $\phi = 0$ at pointA_1, $\psi = 1$ on the streamline A_0A_∞, and $\psi = 0$ on the streamline $A_0A_1A_2...A_NA_\infty$ (see Fig. 6.3).

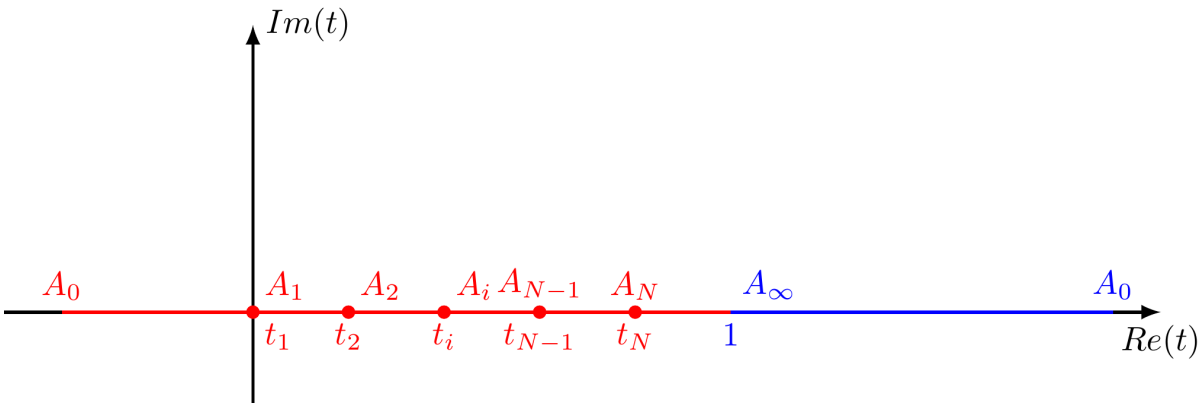

Figure 6.4: The auxiliary plane.

Using the Schwartz-Christoffel transformation, we map the potential plane f presented in Fig.6.3 onto the upper half of an auxiliary t-plane see Fig. 6.4.

(ii) Approximate results: For a large number of the discretization point N, and for all $i = 1, \ldots, N$, the segment A_iA_{i+1} approaches the tangent of the arc between A_iA_{i+1}. Additionally, we also use the previous approximate scheme (5.49), (5.50) to gets the approach solutions of the flow over a round obstacle:

$$x(t) = -\frac{1}{\pi}\ln(t-1) - \sum_{i=1}^{N-1} \frac{2\alpha_i}{\pi We} \tan^{-1}\left(\frac{(n_i - n_{i+1})\sqrt{t-1}}{t-1+n_in_{i+1}}\right),$$
$$y(t) = 1 + \sum_{i=1}^{N-1} \frac{4\alpha_i\,(n_i - n_{i+1})}{\pi^2\sqrt{n_in_{i+1}}} \tan^{-1}\left(\frac{\sqrt{n_in_{i+1}}}{\sqrt{t-1}}\right). \tag{6.1}$$

Approximate solutions for flows with large Weber number are found throughout a range of differentWeber number in figure 6.5 at a fixed the radius of the disk $r = 0.5$ and $N = 500$.

The free-surface profiles for four different the radius of the disk r are plotted in figure 6.6 at a fixed Weber number $We = 200$ and $N = 500$. The following table shows an inventory of l_i and t_i

Table 6.1: An inventory of l_i and t_i for the different of the radius of the disk r

r	$t_2 < t_i < t_N$	l_i
0.4	$0.0063 < t_i < 0.8602$	$0.0008 < l_i < 0.0253$
0.5	$0.0078 < t_i < 0.9145$	$0.0010 < l_i < 0.0316$
0.65	$0.0102 < t_i < 0.9591$	$0.0013 < l_i < 0.0411$
0.8	$0.0125 < t_i < 0.9805$	$0.0016 < l < 0.0506$

Figure 6.14 shows the free-surface profiles for four different of the number of divisions N at a fixed Weber number $We = 200$ and the radius of the disk $r = 0.5$. The following table shows an inventory of l_i and t_i for this case

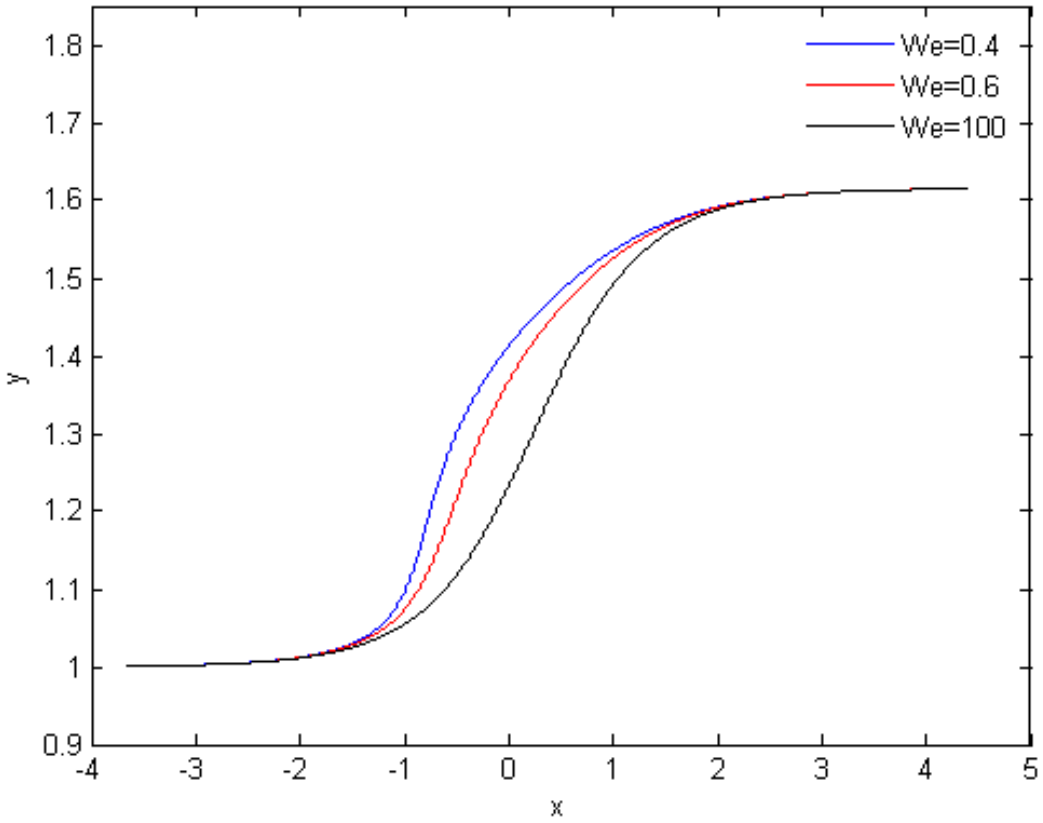

Figure 6.5: Effect of Weber number We on the free-surface profile.

Table 6.2: An inventory of l_i and t_i for the different of the number of divisions N

N	$t_2 < t_i < t_N$	l_i
5	$0.2807 < t_i < 0.8813$	$0.1049 < l_i < 0.3162$
20	$0.0757 < t_i < 0.9080$	$0.0251 < l_i < 0.1581$
50	$0.0309 < t_i < 0.9124$	$0.0100 < l_i < 0.1000$
100	$0.0156 < t_i < 0.9138$	$0.0050 < l_i < 0.0707$

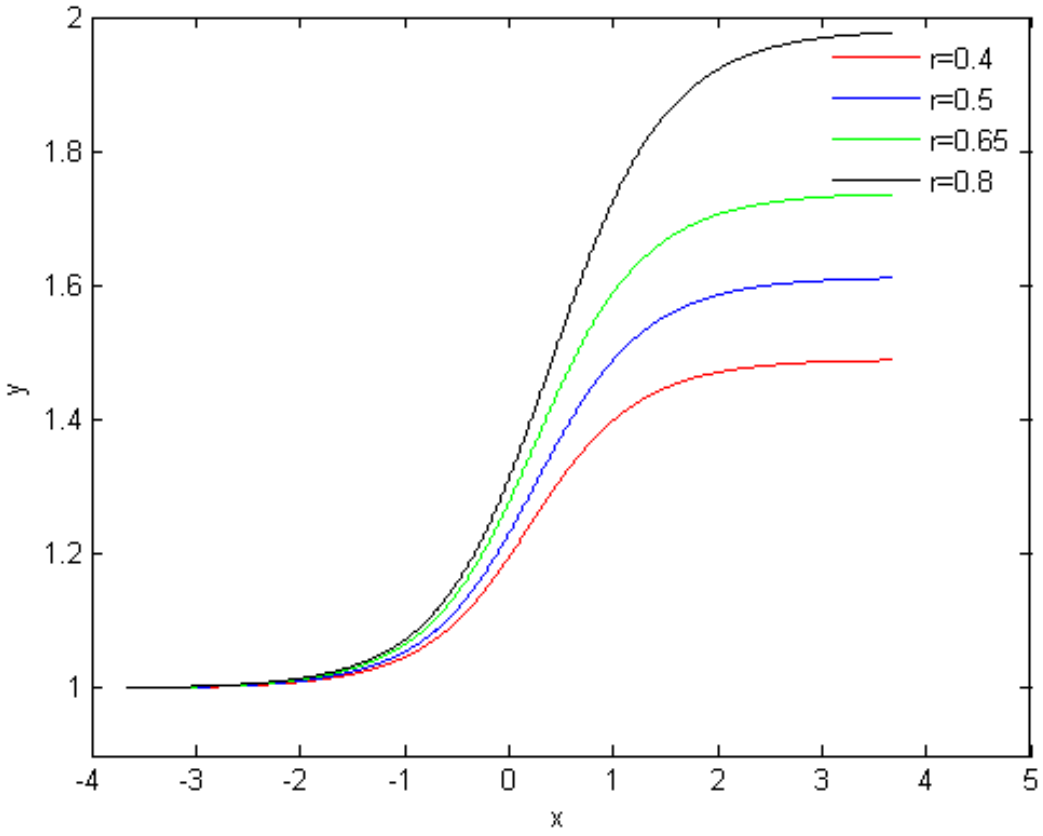

Figure 6.6: Effect of the radius of the disk r on the free-surface profile

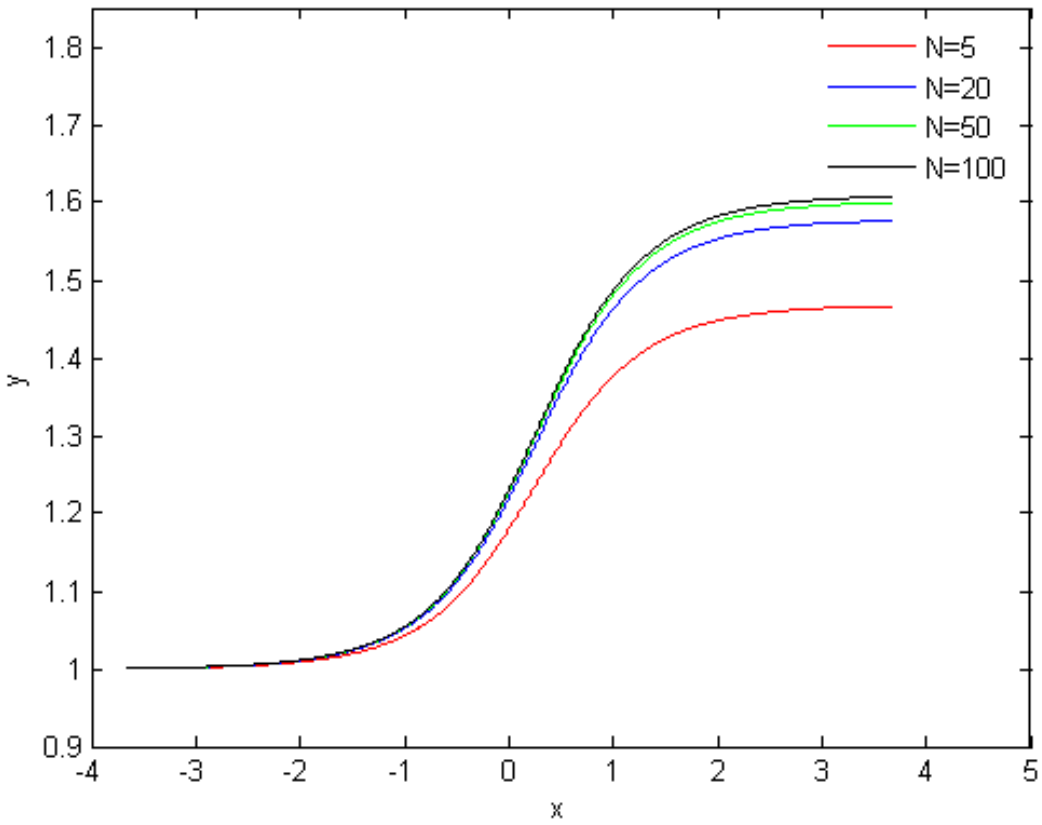

Figure 6.7: Effect of the number of divisions N on the free-surface profile.

6.2 Free surface flow over a sinusoidal bottom

Example 6.2. This example considers the problem of inviscid and incompressible flow with a free surface over a sinusoidal bottom. Applying the first order perturbation technique in conjunction with the Hilbert transformation, we provide an approximate solution to the boundary value problem with mixed boundary conditions arising from the flow problem. The unknown free-surface profiles are established for each large value of the Weber number. The obtained results reveal the simplicity of the used method; they also provide approximate solutions to these kinds of problems.

(i) Formulation of problem : Let us consider the motion of a two-dimensional flow over a sinusoidal bottom ($\delta(x) = \sin(ax)/b$). We assume that the fluid is imcompressible, irrotational and inviscid. We also consider the effect of the superficial tension while we neglect the effect of gravity. Far upstream

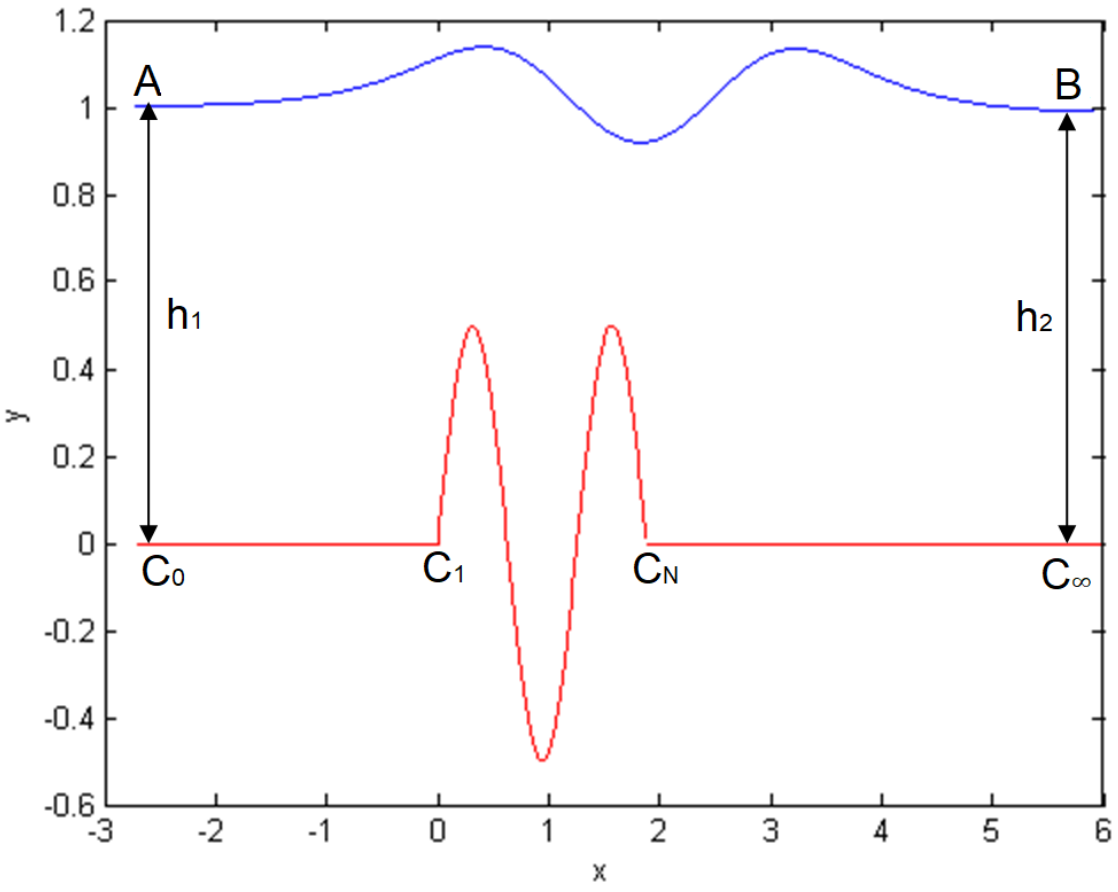

Figure 6.8: Sketch of the flow and of the coordinates. The figure is an actual computed surface profile for $\delta(x) = \sin(5x)/2$, the periodic $2n = 6$ and $N = 420$.

and downstream, the flow is proposed as uniform with a constant discharge $U_1 h_1 = U_2 h_2$, where ,

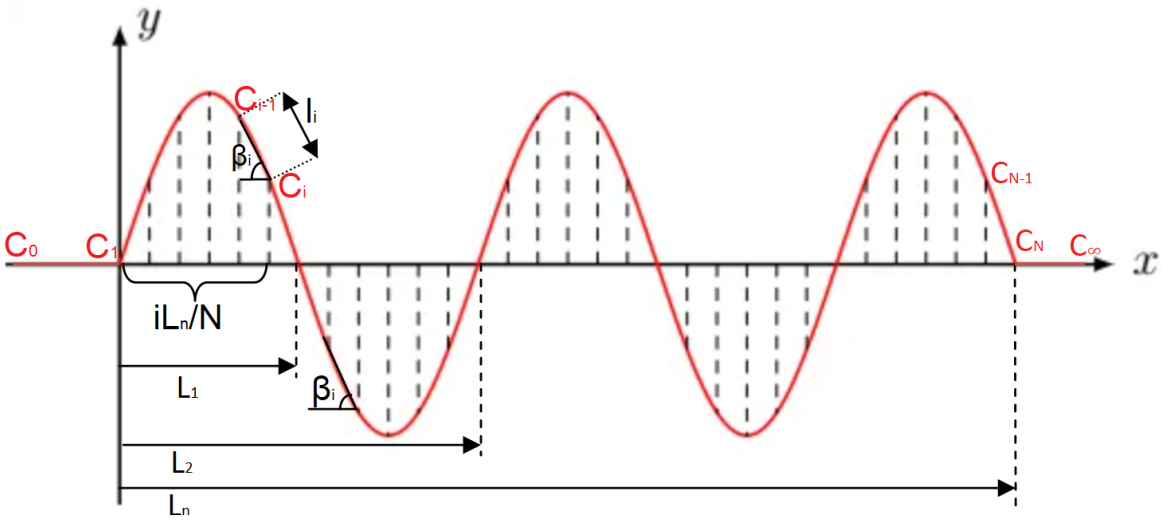

Figure 6.9: Discretzation of a sinusoidal bottom.

$U_i, i = 1, 2$ design the velocities and $h_i, i = 1, 2$ the depths of the flow at upstream and downstream respectively, what this denotes is that the sinusoidal bottom consists of a horizontal plane C_0C_1, an obstacle C_1C_N of a function curve $(\delta(x) = \sin(ax)/b)$ where $x \in [0, n\pi/a]\,, n = 1, 2, 3, \ldots$, and a horizontal plane C_NC_∞, where the bottom extends from $-\infty$ (point C_0) to $+\infty$ (point C_∞). Hence, we choose the point C_1 as the origin in the z-plane (see figure 6.8).
The length of the line segment $\|C_1C_N\|$:

$$\|C_1C_N\| = L_n = \frac{n\pi}{a}, n = 1, 2, 3, \ldots. \tag{6.2}$$

We discretize the length L_n by N perpendicular lines where the lines intersect the curve of the function $\delta(x)$ in the point $C_i, i = 1, 2, \ldots, N$ (sse figure 6.9). We note to the inclination angle between the wall C_iC_{i+1} and the horizontal plane by β_i,

$$\beta_i = \arccos\left(\frac{L_n}{Nl_i}\right); \quad i = 1, \ldots, N-1, \tag{6.3}$$

where

$$l_i = \|C_iC_{i+1}\| = \sqrt{\left(\frac{L_n}{N}\right)^2 + \left(\delta\left(\frac{(i+1)L_n}{N}\right) - \delta\left(\frac{iL_n}{N}\right)\right)^2}. \tag{6.4}$$

The dimensionless variables are defined by choosing U as the unit velocity and $h_1$as the unit length.

We choose $\phi = 0$ at a point C_1 and $\psi = 1$ on the streamline AB, $\psi = 0$ on the streamline $C_0C_1 \ldots C_NC_\infty$ (see figure 6.10).
Using the Schwartz-Christoffel transformation, we map the flow in the physical plane in f-plane (in figure 6.10) onto the upper half of an auxiliary τ-plane (in figure 6.11).

(ii) After applying the Hilbert method (section 5.1.1) in the new plane when the angle of the free surface

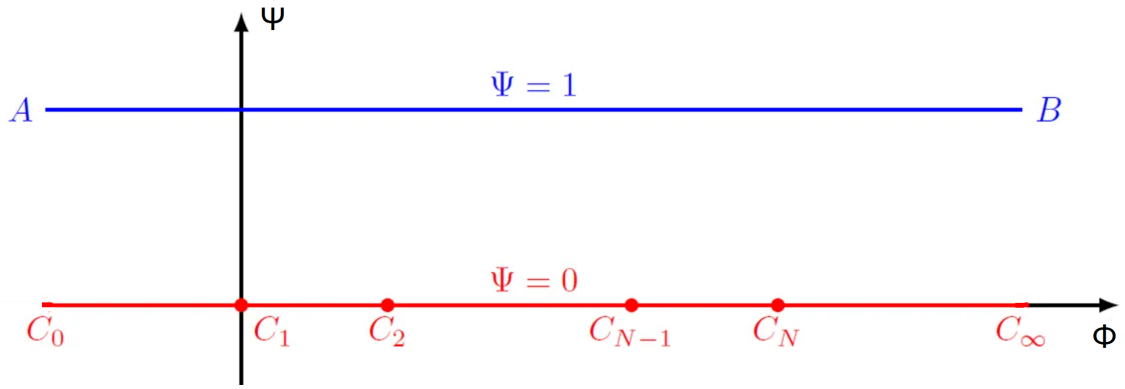

Figure 6.10: The potential f plane.

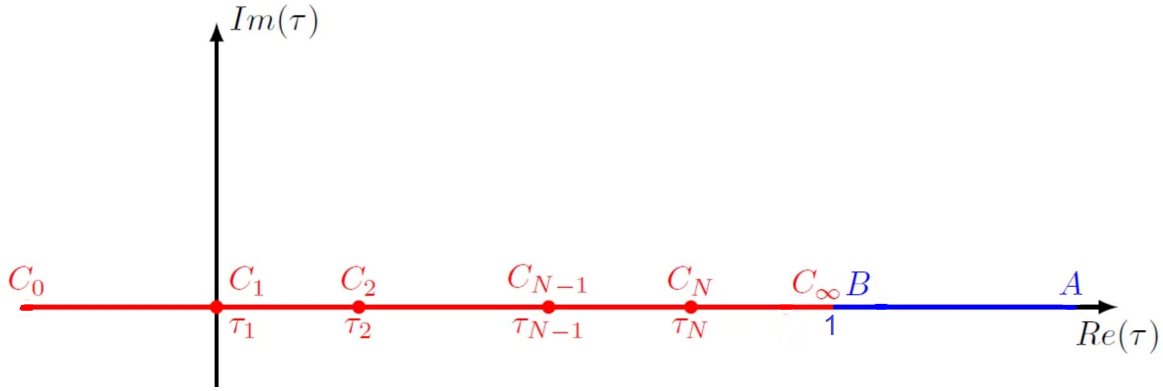

Figure 6.11: The auxiliary plane.

to the horizontal axis take the form :

$$\theta(\tau)=\begin{cases}0, & \tau<0=\tau_1,\\ \beta_i, & \tau_i<\tau<\tau_{i+1},\quad i=1,2,\ldots,N/2n,\\ -(-1)^k\beta_i, & \begin{cases}\tau_i<\tau<\tau_{i+1},\quad k=0,\ldots,n-1,\\ i=\frac{(2k+1)N}{2n},\ldots,\frac{(2k+3)N}{2n},\end{cases}\\ (-1)^n\beta_i, & \tau_i<\tau<\tau_{i+1}, i=\frac{(2n-1)N}{2n},\ldots,N,\\ 0, & \tau_N<\tau<1,\\ \theta(\tau), & \tau>1.\end{cases}\tag{6.5}$$

Along the real axis $Im(\tau)=0$ of the upper half-plane (see fig 6.11), the distribution of both real and imaginary parts of $\chi(\tau)$ can be recapitulated; check Table 6.3. From this, q_0 is defined in $\tau<0$, q_i is defined in $\tau_i<\tau<\tau_{i+1}$, q_∞ is defined in $\tau_N<\tau<1$.

Using (5.15), (5.16) and Table 6.3, we obtain the following systems of the nonlinear integral equations:

Table 6.3: Distribution of the flow quantities along $Im(\tau) = 0$

τ	$U(\tau)$	$V(\tau)$
$\tau < 0 = \tau_1$	$\frac{\ln q_0(\tau)}{\sqrt{1-\tau}}$	0
$\tau_i < \tau < \tau_{i+1}$ $i = 1, \ldots, N/2n$	$\frac{\ln q_i(\tau)}{\sqrt{1-\tau}}$	$\frac{-\beta_i}{\sqrt{1-\tau}}$
$\tau_i < \tau < \tau_{i+1}; K = 0, \ldots, n-1$ $i = \frac{(2k+1)N}{2n}, \ldots, \frac{(2k+3)N}{2n}$	$\frac{\ln q_i(\tau)}{\sqrt{1-\tau}}$	$\frac{(-1)^K \beta_i}{\sqrt{1-\tau}}$
$\tau_i < \tau < \tau_{i+1};$ $i = \frac{(2n-1)N}{2n}, \ldots, N-1$	$\frac{\ln q_i(\tau)}{\sqrt{1-\tau}}$	$\frac{-(-1)^n \beta_i}{\sqrt{1-\tau}}$
$\tau_N < \tau < 1$	$\frac{\ln q_\infty(\tau)}{\sqrt{1-\tau}}$	0
$\tau > 1$	$\frac{\theta(\tau)}{\sqrt{\tau-1}}$	$\frac{\ln q(\tau)}{\sqrt{\tau-1}}$

For $n = 1$, we have

$$\theta(\tau) = \frac{\sqrt{\tau-1}}{\pi} \left\{ p.v. \int_1^{+\infty} \frac{\ln q(s)}{(s-\tau)\sqrt{(s-1)}} ds \right\} + \sum_{i=1}^{N/2} I_i(\tau) - \sum_{i=N/2}^{N} I_i(\tau), \quad \tau > 1. \tag{6.6}$$

For $n = 2$, we have

$$\begin{aligned} \theta(\tau) = \frac{\sqrt{\tau-1}}{\pi} \left\{ p.v. \int_1^{+\infty} \frac{\ln q(s)}{(s-\tau)\sqrt{(s-1)}} ds \right\} + \sum_{i=1}^{N/4} I_i(\tau) - \sum_{i=N/4}^{3N/4} I_i(\tau) \\ + \sum_{i=3N/4}^{N} I_i(\tau), \quad \tau > 1. \end{aligned} \tag{6.7}$$

For $n = 3$, we have

$$\begin{aligned} \theta(\tau) = \frac{\sqrt{\tau-1}}{\pi} \left\{ p.v. \int_1^{+\infty} \frac{\ln q(s)}{(s-\tau)\sqrt{(s-1)}} ds \right\} + \sum_{i=1}^{N/6} I_i(\tau) - \sum_{i=N/6}^{3N/6} I_i(\tau) \\ + \sum_{i=3N/6}^{5N/6} I_i(\tau) - \sum_{i=5N/6}^{N} I_i(\tau), \quad \tau > 1. \end{aligned} \tag{6.8}$$

In general, $n = 1, 2, 3, \ldots$, we have

$$\begin{aligned} \theta(\tau) = \frac{\sqrt{\tau-1}}{\pi} \left\{ p.v. \int_1^{+\infty} \frac{\ln q(s)}{(s-\tau)\sqrt{(s-1)}} ds \right\} + \sum_{i=1}^{N/2n} I_i(\tau) - \sum_{k=0}^{n-1} (-1)^k \sum_{i=(2k+1)N/2n}^{(2k+3)N/2n} I_i(\tau) \\ + (-1)^n \sum_{i=(2n-1)N/2n}^{N-1} I_i(\tau), \quad \tau > 1. \end{aligned} \tag{6.9}$$

Where

$$\begin{aligned} I_i(\tau) &= -\frac{\sqrt{\tau-1}}{\pi}\int_{\tau_i}^{\tau_{i+1}} \frac{\beta_i}{(s-\tau)\sqrt{(1-s)}}ds, \quad i=1,2,\ldots,N-1, \\ &= \frac{2\beta_i}{\pi}\tan^{-1}\left(\frac{\left(\sqrt{1-\tau_i}-\sqrt{1-\tau_{i+1}}\right)\sqrt{(\tau-1)}}{\tau-1+\sqrt{(1-\tau_i)\,(1-\tau_{i+1})}}\right). \end{aligned} \tag{6.10}$$

(iii) Solution of the boundary-value problem and results: Using the same technique of the chapter 3, chapter 4, chapter 5, we get the free surface flow over a sinusoidal bottom as following:

$$\begin{aligned} x(\tau) \approx & -\frac{1}{\pi}\ln(\tau-1) - \frac{1}{\sigma}\sum_{i=1}^{N/2n}\arccos\left(\frac{L_n}{Nl_i}\right) I_i(\tau)\Upsilon_{k,i}(\tau) \\ & + \frac{1}{\sigma}\sum_{k=0}^{n-1}(-1)^k \sum_{i=(2k+1)N/2n}^{(2k+3)N/2n}\arccos\left(\frac{L_n}{Nl_i}\right) I_i(\tau)\Upsilon_{k,i}(\tau) \\ & - \frac{(-1)^n}{\sigma}\sum_{i=(2n-1)N/2n}^{N-1}\arccos\left(\frac{L_n}{Nl_i}\right) I_i(\tau)\Upsilon_{k,i}(\tau), \quad \tau>1. \end{aligned} \tag{6.11}$$

$$\begin{aligned} y(\tau) \approx & 1 + \sum_{i=1}^{N/2n}\arccos\left(\frac{L_n}{Nl_i}\right) J_i(\tau) - \sum_{k=0}^{n-1}(-1)^k \sum_{i=(2k+1)N/2n}^{(2k+3)N/2n}\arccos\left(\frac{L_n}{Nl_i}\right) J_i(\tau) \\ & + (-1)^n \sum_{i=(2n-1)N/2n}^{N-1}\arccos\left(\frac{L_n}{Nl_i}\right) J_i(\tau), \quad \tau>1. \end{aligned} \tag{6.12}$$

Where

$$J_i(\tau) = \frac{4\left(\sqrt{1-\tau_i}-\sqrt{1-\tau_{i+1}}\right)}{\pi^2\sqrt[4]{(1-\tau_i)\,(1-\tau_{i+1})}}\tan^{-1}\left(\frac{\sqrt[4]{(1-\tau_i)\,(1-\tau_{i+1})}}{\sqrt{\tau-1}}\right), \tag{6.13}$$

and

$$\Upsilon_{k,i} = \begin{cases} \dfrac{1}{\beta_i}; & 1<i<N/2n \\ -\dfrac{(-1)^K}{\beta_i}; & \dfrac{(2k+1)N}{2n}<i<\dfrac{(2k+3)N}{2n}, 0<k<n-1, \\ \dfrac{(-1)^n}{\beta_i}; & \dfrac{(2n-1)N}{2n}<i<N-1. \end{cases} \tag{6.14}$$

Along C_jC_{j+1} where $q=q_j$, $z_j=l_je^{-i\beta^*}, j=1,\ldots,N$, we have

$$\theta=\beta^*=\begin{cases} \beta_j, & \tau_j<\tau<\tau_{j+1}, \quad j=1,2,\ldots,N/2n, \\ -(-1)^K\beta_j, & \begin{cases}\tau_j<\tau<\tau_{j+1}, \quad k=0,\ldots,n-1, \\ j=\frac{(2k+1)N}{2n},\ldots,\frac{(2k+3)N}{2n},\end{cases} \\ (-1)^n\beta_j, & \tau_j<\tau<\tau_{j+1}, j=\frac{(2n-1)N}{2n},\ldots,N. \end{cases} \tag{6.15}$$

On the other hand

$$z_j - z_\infty = -\frac{1}{\pi}\int_{\tau_j}^{\tau_{j+1}}\frac{e^{i\beta^*}}{(1-s)q_j(s)}ds = l_je^{-i\beta^*}, \tag{6.16}$$

therefore:

$$l_j = -\frac{1}{\pi}\int_{\tau_j}^{\tau_{j+1}} \frac{1}{(1-s)q_j(s)}ds. \tag{6.17}$$

Along the solid boundaries, we can approximate q_j by one and for (6.17), we could obtain:

$$l_j \approx -\frac{1}{\pi}\ln\left(\frac{1-\tau_j}{1-\tau_{j+1}}\right). \tag{6.18}$$

Consequently,

$$\tau_j \approx 1 - e^{-\pi\sum_{k=1}^{j} l_k}. \tag{6.19}$$

For a large number of the discretization point N, and for all $i = 1, \ldots, N$, the segment $c_i c_{i+1}$ approaches the tangent of the arc between $c_i c_{i+1}$. Additionally, we also use the previous approximate scheme to calculate the solutions and the free surface profiles for a fixed $\delta(x) = \sin(5x)/2$, $n = 2$ and $N = 1000$ and different values of Weber numberσ.

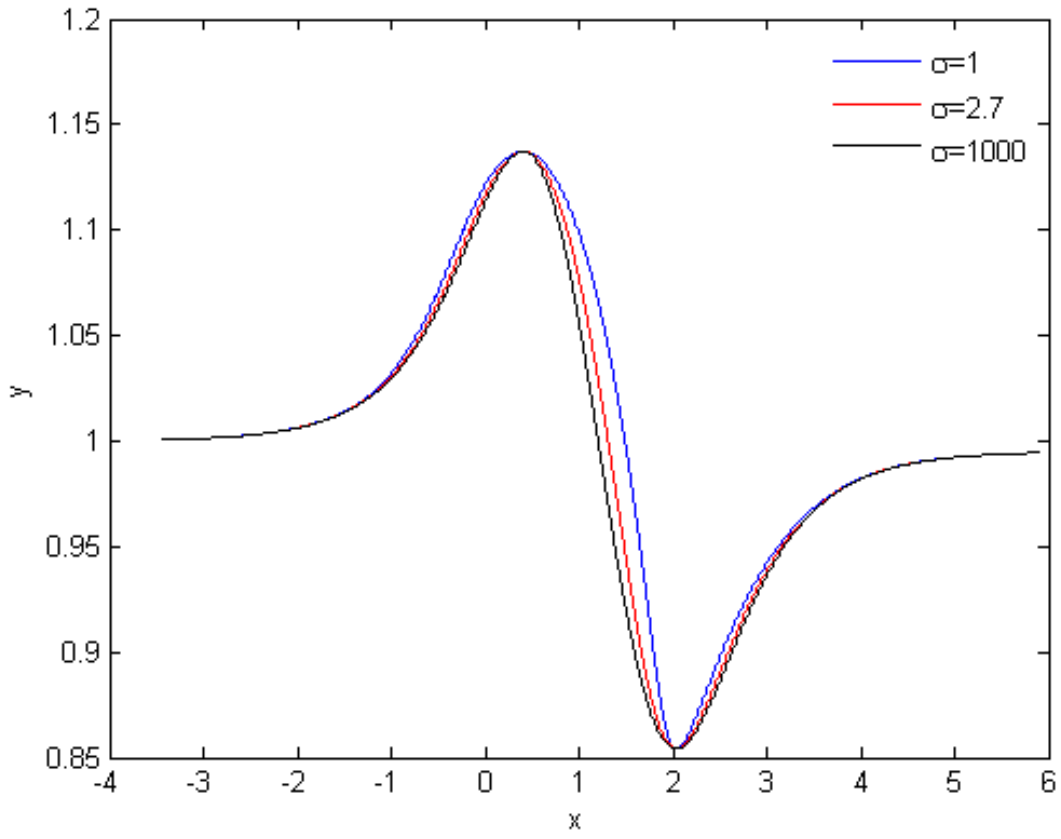

Figure 6.12: The effect of Weber number σ on the free-surface profile at a fixed $(\delta(x) = \sin(5x)/2$,$n = 2$ and $N = 1000$.

Figure 6.12 presents the variation of the free surface shape with respect to the Weber number. According to this figure, if the Weber number decreases, the curvature of the free surface decreases

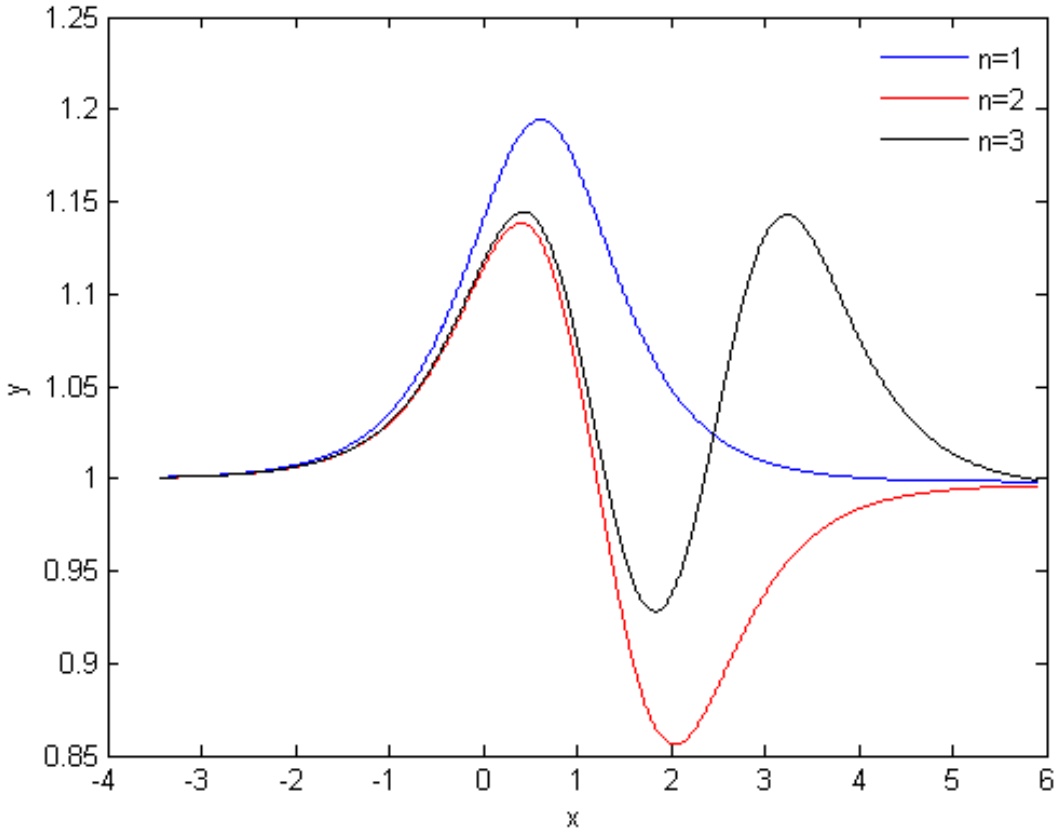

Figure 6.13: Effect of the bottom shape on the free-surface profile for different n values and at a fixed $\delta(x) = \sin(5x)/2$, $\sigma = 1000$ and $N = 1000$.

accordingly; the reason is because this is a characteristic property of the surface tension effects.

The free surface profiles for different number of discretization N are plotted in figure 6.14. The free-surface profile for different n values and at a fixed $\delta(x) = \sin(5x)/2$, $\sigma = 1000$ and $N = 1000$ are plotted in figure 6.13.

The present example provided an attempt to solve a steady free-surface flow over a sinusoidal bottom's nonlinear problem using a numerical method. As a result, mapping the flow domain of the physical plane onto an upper half-plane is done using Schwartz-Christoffel transformation. Using the Hilbert method for a mixed boundary value problem results in obtaining a nonlinear integral equation's system. Moreover, the perturbation technique is employed in order to reach an approximate solution of the problem for a large Weber number.

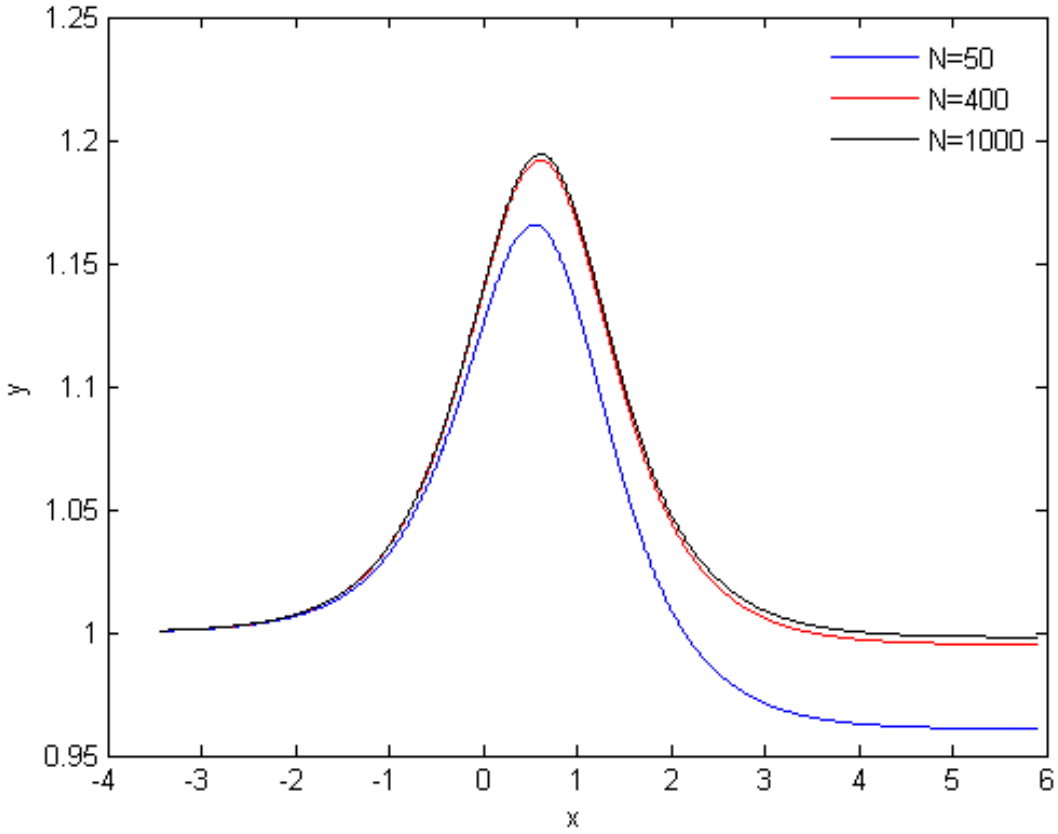

Figure 6.14: Effect of number of discretisation point N on the free-surface profile at a fixed $\delta(x) = \sin(5x)/2$, $\sigma = 1000$ and $n = 1$.

General conclusions and future research

In this work, we assign an analytical and an approximate studies of a two-dimensional problems of free surface flow issued from an opening and flow over an obstacle of any shape placed in bottom, in the case where the effect of the surface tension is taken into consideration, due to this cause the problem becomes very difficult because of the non-linear condition on the free boundary of the flow domain. To treat this this problem we used analytical and numerical methods based on the theory of complex variable, we think that the following set of results are reached:

- ☆ The first was to give a mathematical formulation of the considered problems, using the aspects theory of functions of a complex variables.
- ☆ The second result is to use the theory of the hodograph method, which bases on the conformal transformations, to find the analytical solution of the problem in the case where the effect of the surface tension is neglected and the results obtained are the subject of an article appearing in a renowned journal [12].
- ☆ Thus, using the Hilbert transformation and the perturbation technique; the results are calculated for a large values of the Weber number. These results demonstrate that the used method is easily implemented, as this studies has been published in an international journals [13], [14] and [15].
- ☆ Finally, the generalization of the problem for different wall configurations, for example in the case of or curved wall, the results obtained are the subject of a two articles appearing in a renowned journal [16] and [27].

The application of the Hilbert method which also results from the use of conformal transformations and Cauchy's theorem. This method has shown its effectiveness in finding the approximate solution of the problem. These two methods return very important simplifications on the treatment of this type of problem, in our case they make it possible to reduce the the difficulty of the problem, and to transform the two-dimensional problem considered to another onedimensional one. An approximation solutions of some problems for a large Weber number are attained through the perturbation technique.
We observe that the results found by these used methods are easily implemented, and provides respectivelly analytical and approximate solutions to these kinds of problems.

Following this work and as perspectives, several ideas appeared. First, seems interesting to consider the problem in the three-dimensional case. Finally, it is necessary to use other numerical methods such as the finite element method or the finite volume method to solve this kind of problems.

Bibliography

[1] M.B. Abd-el-Malek, S.Z. Masoud, (1988), Linearized solution of a flow over a ramp, *Appl. Math. Model.*, 124, 406—410.

[2] M.B. Abd-el-Malek, S.N. Hanna, (1989), Approximate solution of a flow over a ramp for large Froude number. *J. Comput.Appl.Math*, 28, 105–117.

[3] M.B. Abd-el-Malek, S.N. Hanna and M.T. Kamel, (1991), Approximate solution of gravity flow from a uniform channel over triangular bottom for large Froude number, *Appl. Math. Model.*, 15(1), 25–32.

[4] M.B. Abd-el-Malek, (1991), Approximate solution of gravity-affected flow from planar sluice gate at high Froude number, *J. Comput. Appl. Math.*, 35, 83-97.

[5] R.C. Ackerberg, Ta-Jo. Liu ,(1987), The effects of capillarity on the contraction coefficient of a jet emanating from a slot, *Phys. Fluids*, 30, 289–296.

[6] A. Amara , A.Gasmi, (2018). The effect of surface tension on the jet flow in U-shaped channel. *Int. J. Pure Appl. Math.*, 118(3), 625–635.

[7] J. Asavanat, J-M. Vanden-Broeck, (1996), Nonlinear free-surface flow emerging from vessels and flows under sluice gate, *J. Austral. Mat. Soc.*, B 38, 63-86.

[8] G. K. Batchelor, (1967), An introduction to fluid dynamics, Cambridge: Cambridge University Press.

[9] G. Birkoff, E.H. Zarantonello, (1957), Jet, Wakes and Cavities academic, New York.

[10] B. Bouderah, H. Serguine and A. Gasmi, (2007), The Free-Surface Flow due to a Jet Against an Infinite Vertical Plate in Presence of Surface Tension, *Appl. Math. Sci.*, 1(43), 2119–2128.

[11] B. Bouderah, A. Gasmi and H. Serguine, (2007), Zero Gravity of Free-Surface Jet Flow, *Int. Math. Forum*, 2(66), 3273–3277.

[12] M.M. Bounif, A. Gasmi, (2022), The Application of the Hodograph method to free surface flow problem, Article submitted for publication.

[13] M.M. Bounif, A. Gasmi, (2021), First order perturbation approach for the free surface flow over a step with large Weber number, *INCAS Bulletin*, 13(2), 11–19.

[14] M.M. Bounif, A. Gasmi, (2022), An approximate solution technique for the flow past an obstacle with a large Weber number, *Int. J. Appl. Comput. Math*, 8(1), 1–12.

[15] M.M. Bounif, A. Gasmi, (2022), Perturbation approach for a flow over a trapezoidal obstacle, *Journal of Siberian Federal University. Mathematics & Physics*,15(3), 1–12.

[16] M.M. Bounif, A. Gasmi, (2022), Two dimensional free surface flow over a round obstacle with surface tension effect, Article submitted for publication.

[17] M.J. Cooker, (1999), Potential flow for a steady jet in a wedge, *Q. J. Mech. appl. Math*, 52, 127-140.

[18] G. D. Crapper, (1984), Introduction to Water Waves, Ellis Horwood Limited.

[19] F. Dias, J.B. Keller, J-M.Vanden-Broeck, (1988), Flows over rectangular weirs, *Phys. Fluids*, 31(8), 2071–2076.

[20] F. Dias, Kharif, (1999), Nonlinear gravity and capillary-gravity waves, *Ann. Rev. Fluid Mech*, 31, 301-346.

[21] L.K. Forbes, L.W. Schwartz, (1982), Free-surface flow over a semicircular obstruction. *J. Fluid Mech.*, 114, 299–314.

[22] A. Gasmi, H. Mekias, (2003), The effect of surface tension on the contraction coefficient of a jet, *J.Phys. A: Math. Gen*, 36, 851-862.

[23] A. Gasmi, H. Mekias, (2007), A jet from container and flow past a vertical flat plate in a channel with the surface tension effects, *Appl. Math. Sci.*, 54(1), 26-87.

[24] A, Gasmi, A. Amara, (2018), Free-surface profile of a jet flow in U-shaped channel without gravity effects, *ASCM (Kyungshang)*, 118(3), 393–400.

[25] A. Gasmi, (2014), Two-dimensional cavitating flow past an oblique plate in a channel, *J. Comput. Appl. Math.*, 259, 851-862.

[26] A. Gasmi, (2014), Numerical Study of Two-Dimensional Jet Flow Issuing from a Funnel, *Adv. Appl. Math.*, 87, 161-169.

[27] A. Gasmi, M.M. Bounif, (2022) An approximate solution for the flow over a sinusoidal bottom with large Weber number effect, Article submitted for publication.

[28] J. Hureau, R. Weber, (1998), Impinging free jets of ideal fluid, *J. Fluid Mech*, 372, 357-374.

[29] V. V. Klokov, D. E. Sergeev, (2012), Simulation of the stationary electrochemical surface treatment by two asymmetric cathode plates, *J. Appl. Mech. Tech. Phys.*, 53, 6, 961-965.

[30] J. Lighthill, (1986), An Informal Introduction to Theoretical Fluid Mechanics, *Clarendon Press: Oxford*.

[31] L. D. Landau, E. M. Lifshits, (1959), Fluid mechanics, *Pergamon Press Oxford, UK.*

[32] R. Matiur, (2011), Mechanics of real fluids, *WIT Press*.

[33] S. G. E. Mikhlin, (1947), NI Muskhelishvili, Singular integral equations, *Uspekhi Matematicheskikh Nauk*, 2(2), 235-237.

[34] L.M. Milne-Thomson, (1968), Theoretical Hydrodynamics, 5th edition Macmillan, *New York*.

[35] W. Peng, D. F. Parker, (1997), An ideal fluid jet impinging on an uneven wall, *J. Fluid Mech*, 333, 231-255.

[36] D.E. Rutherford, (1959), Fluid Dynamics, Oliver & Boyd.

[37] Y. A. Semenov, G. X. Wu, (2013), Asymmetric impact between liquid and solid wedges, *Proc. R. Soc. A*, 469, 1.

[38] Y. A. Semenov, G. X. Wu, A. A. Korobkin, (2015), Impact of liquids with different densities,*J. Fluid Mech.*, 766, 5-27.

[39] Y. A. Semenov , G. X. Wu, J. M. Oliver, (2013), Splash jet generated by collision of two liquid wedges, *J. Fluid Mech.*, 737, 132-145.

[40] B.K. Shivamoggi, (1998), Theoretical Fluid Dynamics, 2nd Edition-Wiley-Interscience.

[41] A.C. Smith, TH.Lim, (1980), The steady water wave: A numerical solution using the Riemann-Hilbert method, *Int J Eng Sci*, 18(1), 139–152.

[42] A.C. Smith, M.B. Abd-el-Malek, (1983), Hilbert's methods for numerical solution of flow from a uniform channel over a shelf, *J. Engrg. Math.*, 17, 27-39.

[43] C.S. Song, (1963), A Quasi-linear and Linear Theory for Non-Separated and Separated Two-Dimensional, Incompressible Irrotational Flow About-Lifting Bodies, *St. Anthony Falls Lab*, Series B, 63.

[44] M.R. Spiegel, S. Lipschutz, J.J. Schiller and D. Spellman, (2009), Schaum's outline of Complex Variables,*McGraw Hill Professional*.

[45] M.R. Spiegel, S. Lipschutz,J.J. Schiller and D. Spellman, (2015), Complex variables: With an introduction to conformal mapping and its applications, *McGraw-Hill*.

[46] J-M. Vanden-Broeck, (1987), Free-surface flow over an obstruction in a channel, *Phys. Fluids*, 30(8), 2315–2317.

[47] J-M. Vanden-Broeck, (1986), flow under a gate, *Phys. Fluids*, 29(10), 3148–3151.

[48] J-M. Vanden-Broeck, (1987), Free-surface flow over an obstruction in a channel, *Phys. Fluids*, 30(8), 2315–2317.

[49] J-M. Vanden-Broeck, (1986), Flow under a gate, *Phys. Fluids*, 29, 3148-3151.

[50] J-M. Vanden-Broeck, (1997), Numerical calculations of the free-surface flow under a sluice gate, *J. Fluid Mech*, 330, 339-347.

[51] L.H. Wiryanto, (2020), Zero gravity of free-surface flow under a sluice gate,*J. Phys. Conf. Ser.*, IOP Publishing.

ملخص

نهتم في هذه الرسالة بإيجاد الحل الدقيق والتقريبي لمسالة ثنائية الأبعاد لتدفق سائل من تحت حاجز وكذلك لجريان سائل فوق عائق ذو شكل كيفي، نعتبر ان السائل غير قابل للانضغاط وغير لزج كما أن تأثيرات الجاذبية مهملة. تتميز هذه المسالة بالشرط غير الخطي المعطى بمعادلة برنولي على السطح الحر وكذلك الشكل المجهول لهذا الجريان، عند إهمال تأثير التوتر السطحي، يمكن الحصول على الحل الدقيق باستخدام طريقة الهودوجراف. ولكن إذا أدخلنا تأثير التوتر السطحي فانه من الصعب ايجاد الحل الدقيق للمسالة، لذلك نلجأ الى استخدام طريقة تقريبية لإيجاد الحل التقريبي، وتعتمد كلتا الطريقتين على نظرية التحويلات المتطابقة، كما ان هاتان الطريقتان تعطيان تبسيطات مهمة للغاية في معالجة هذا النوع من المشاكل، ففي كلتا الحالتين المعالجتين خفضتا من صعوبة المسألة، وحولتها من مسألة ثنائية البعد إلى مسألة ذات بعد واحد.

الكلمات المفتاحية : جريان ذو سطح حر، سائل غير قابل للانضغاط، توتر سطحي، التحويلات المتطابقة، طريقة الهودوجراف، طريقة هيلبرت، تقنية الاضطراب.

Abstract

In this thesis, we are interested in finding the analytical and the approximate solution to a twodimensional problem of a fluid flow under a gate, as well as a fluid flow over any obstacle, we consider that the fluid is incompressible and inviscid, and the effects of gravity are neglected. This problem is characterized by the nonlinear condition given by Bernoulli's equation on the free surface as well as the unknown shape of this flow. When the surface tension effect is neglected, the exact solution can be obtained using the Hodograph method's. But if we introduce the effect of surface tension, it becomes difficult to find the exact solution to this problem, so we resort to using an approximate method to find the approximate solution, and both methods based on the conformal transformations theory, these two methods demonstrate that there are easily implemented give very important simplifications to this type of problem. In the two cases the problem difficulty is reduced, and transformed it from a two-dimensional problem to a one-dimensional problem.

Keywords: Free surface flows, Incompressible, Surface tension, Conformal transformations, Hodograph method, Hilbert method, Perturbation technique.

Résumé

Dans cette thèse, nous intéressons à trouver la solution analytique et approchée d'un problème bidimensionnel d'écoulement de fluide sous un barrage et aussi un écoulement au-dessus d'un obstacle quelconque, on considère que le fluide est incompressible et non visqueux, et les effets de la gravité sont négligés. Ce problème est caractérisé par la condition non linéaire donnée par l'équation de Bernoulli sur la surface libre ainsi que par la forme inconnue de cet écoulement. Lorsque l'effet de tension de surface est négligé, la solution exacte peut être obtenue en utilisant la méthode Hodographe. Mais si nous introduisons l'effet de la tension de surface, il devient difficile de trouver la solution exacte à ce problème, nous avons donc recours à une méthode approchée pour trouver la solution approchée, et les deux méthodes basées sur la théorie des transformations conformes, ces deux méthodes démontrent qu'il y ait des facilités de mise en œuvre et donnent des simplifications très importantes à ce type de problème. Dans les deux cas, la difficulté du problème est réduite et transformée d'un problème bidimensionnel à un problème unidimensionnel.

Mots clés: Ecoulements à surface libre, Incompressible, Surface tension, Transformations conformes, Méthode hodographe, Méthode de Hilbert, Technique de Perturbation.